AD-A154 352 SAND DISPERSION FROM AN EPHEMERAL RIVER DELTA ON THE WAVE-DOMINATED CENTRAL CALIFORNIA COAST(U) CALIFORNIA UNIV SANTA CRUZ D M HICKS MAR 85 N00014-80-C-0440 1/3

UNCLASSIFIED F/G 8/3 NL

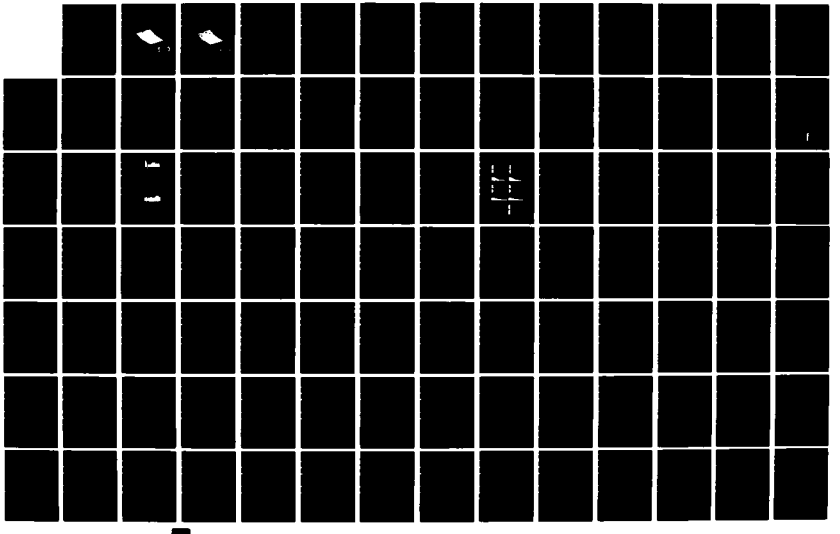

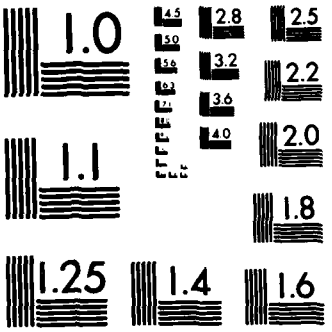

(12)

SAND DISPERSION FROM AN EPHEMERAL RIVER DELTA ON THE WAVE-DOMINATED CENTRAL CALIFORNIA COAST

Contract N00014-80-C-0440
University of California, Santa Cruz

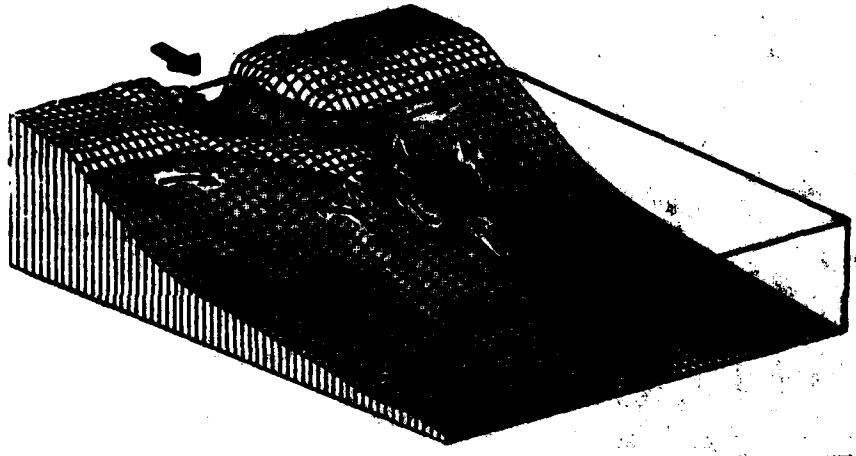

D. MURRAY HICKS

1985

SAND DISPERSION FROM AN EPHEMERAL RIVER DELTA ON THE WAVE-DOMINATED CENTRAL CALIFORNIA COAST

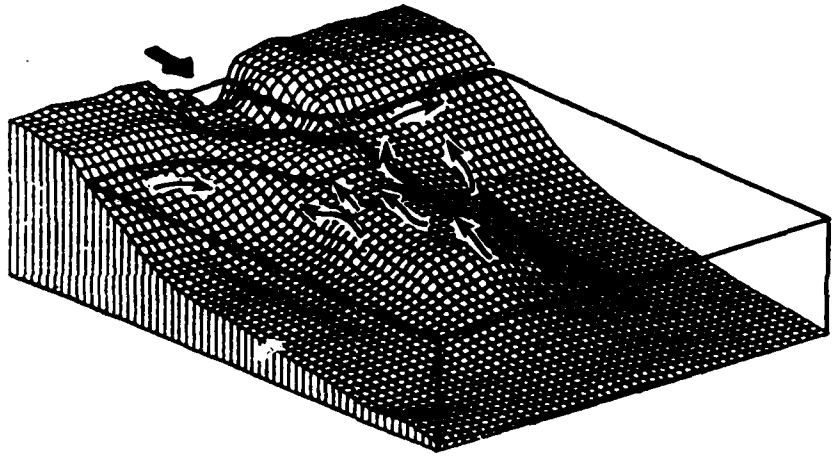

D. MURRAY HICKS

1985

UNIVERSITY OF CALIFORNIA

SANTA CRUZ

SAND DISPERSION FROM AN EPHEMERAL RIVER DELTA ON THE WAVE-DOMINATED CENTRAL CALIFORNIA COAST

A Dissertation Submitted in partial satisfaction of the requirements for the degree of

DOCTOR OF PHILOSOPHY

in

EARTH SCIENCES

by

Darryl Murray Hicks

March 1985

The dissertation of Darryl Murray Hicks is approved:

Douglas S. Inman, Co-chairman

Gary B. Griggs, Co-chairman

Stanley A. Ivins

Maseng Moore

Dean of the Graduate Division

To Sandy, Katie, and Charlotte

TABLE OF CONTENTS

TABLE OF CONTENTS

TABLE OF CONTENTS

TABLE OF CONTENTS

LIST OF SYMBOLS

Symbols from the Roman alphabet		Dimensions
C_n	wave group velocity	LT^{-1}
c_{rb}	surf similarity parameter	0
E	wave energy per unit area	MT^{-2}
g	gravitational acceleration	LT^{-2}
h	water depth	L
H	root-mean-square wave height	L
H_s	significant wave height	L
I_l	immersed weight longshore transport rate	MLT^{-3}
K, K", K"'	dimensionless proportionality coefficients	0
K'	dimensional proportionality coefficient	$L^2T^2M^{-1}$
km	kilometers	L
L	wavelength in deep water	L
m	meters	L
n	ratio of wave group velocity to wave celerity	0
S_{xy}	longshore component of the radiation stress	MT^{-2}
Q_l	"at rest" volume longshore transport rate	L^3T^{-1}
u_m	maximum horizontal wave orbital velocity	LT^{-1}
v_l	average longshore current	LT^{-1}
x	horizontal coordinate	L
y	horizontal coordinate	L

Symbols from the Greek Alphabet		
α	angle between wave crest and shoreline	0
β	beach slope angle	0
ρ	density of sea water	ML^{-3}

Subscripts

∞	in deep water
a	at the wave array
b	at the wave break-point
l	denotes longshore direction
s	denotes a significant wave parameter

Abbreviations

CDIP	Coastal Data Information Program
CERC	Coastal Engineering Research Center
MLLW	Mean Lower Low Water level
MSL	Mean Sea Level
USACE	United States Army Corps of Engineers
USGS	United States Geological Survey

LIST OF FIGURES

LIST OF FIGURES

LIST OF FIGURES

LIST OF TABLES

ACKNOWLEDGEMENTS

This research was carried out under the supervision of Professors D. L. Inman at Scripps Institution of Oceanography and G. B. Griggs at the University of California, Santa Cruz. I thank them for their support and guidance.

I am indebted to Professor Inman and the staff and students at the Center for Coastal Studies for making my time at Scripps so rewarding. Thanks also to Dr. Hany El Wany for sharing the task of predicting longshore transport divergence.

I am deeply indebted to the many people who helped with the field work. Paul Boisson, Marty Garrison, and Keith Watts turned out time and again - my hat goes off to this special breed of friend.

My appreciation to John Dingler, of the U.S. Geological Survey, who loaned his hydrographic surveying equipment.

Sandy, my wife, typed the manuscript. Harry Grow lent me his printer and his time. Mike Clark, Fred Crowe, Guy Tapper, and Rene Wagemakers helped with the figures. My good friends Tom White, Jim Zampol, Russ Johnson, and Vivian McKenna helped get things together at the end. Thank you all.

The research was supported, in turn, by the Institute for Marine Resources, the Santa Cruz Harbor Board, the Marine Studies Board at U.C. Santa Cruz, and the Office of Naval Research under contract with Scripps Institution of Oceanography. I was supported by a study award from the

Ministry of Works and Development, New Zealand. My visit to Scripps was funded by the Institute for Marine Resources.

VITA

Born:	12 June 1954 - Invercargill, New Zealand
1975	B.Sc. Honours, First Class in Geology, University of Otago, Dunedin, New Zealand
1977	B.E., Civil Engineering, with First Class Honours, University of Canterbury, Christchurch, New Zealand
1978-1980	Research Scientist, Water and Soil Division, Ministry of Works and Development, Christchurch, New Zealand
1980-1985	Fulbright Fellow, Ministry of Works and Development Post-graduate Study Fellow

PUBLICATIONS

Carter, R.M., D.M. Hicks, R.J. Norris, and I.M. Turnbull, 1978, "Sedimentation patterns in an ancient arc-trench-ocean basin complex: Carboniferous to Jurassic Rangitata Orogen, New Zealand", in "Sedimentation in submarine canyons, fans, and trenches", D. J. Stanley and G. Kelling, eds., Dowden, Hutchison and Ross, Strousberg, pp. 340-361.

Griffiths, G.A. and D. M. Hicks, 1980, "Comment on 'Clutha Flood of October 1978' by I. G. Jowett", Journal of Hydrology (N.Z.), vol. 19(1), pp. 75-77.

Griffiths, G.A. and D.M. Hicks, 1981, "Transport of sediment in mountain streams: performance of a measurement system during a two year storm", Journal of Hydrology (N.Z.), vol. 20(1), pp. 131-136.

Hicks, D.M., 1981, "Deep-sea fan sediments in the Torlesse Zone, Lake Ohau, South Canterbury, New Zealand", New Zealand Journal of Geology and Geophysics, vol. 24(2), pp. 209-230.

Hicks, D.M. and P.S. Bright, 1981, "An integrated system for automatic collection of flow and suspended sediment data", Journal of Hydrology (N.Z.), vol. 20(2), pp. 147-151.

Hicks, D.M. and D.L. Inman, 1985, "Bedload stresses and Bagnold's bedload transport theory - a comment", submitted to Sedimentology.

Inman, D.L., S.A. Jenkins, and D.M. Hicks, 1984, "Oscillatory bursting", Transactions, American Geophysical Union, vol 65, no. 45, p. 955.

Jowett, I.G. and D.M. Hicks, 1981, "Surface sampling of suspended sediment, Clutha River System", Journal of Hydrology (N.Z.), vol. 20(2), pp. 121-130.

Waldorf, B.W., R.E. Flick, and D.M. Hicks, 1983, "Beach sand level measurements, Oceanside and Carlsbad, California", Scripps Inst. Oceanography Reference Series report no. 83-6, 37p.

FIELDS OF STUDY

At University of California, Santa Cruz

Studies in Earth Sciences
Professors G.B. Griggs, S.J. Dreiss, J.C. Moore, O.T. Tobisch, K. Cameron, and E.A. Silver

Studies in Marine Geology
Dr. W.R. Normark

At University of California, Berkeley

Studies in Fluvial Geomorphology
Professor L.B. Leopold

At Scripps Institution of Oceanography

Studies in Nearshore Processes
Professors D.L. Inman and R.T. Guza

Studies in Physical Oceanography
Professors W.H. Munk, C.S. Cox, M.L. Hendershott, and J.L. Reid

Studies in Fluid Mechanics
Professor C.D. Winant

Studies in Coastal Marine Geochemistry
Professor E.D. Goldberg

ABSTRACT OF THE DISSERTATION

Sand Dispersion from an Ephemeral River Delta
on the Wave-dominated Central California Coast

by

Darryl Murray Hicks

Doctor of Philosophy in Earth Sciences

University of California, Santa Cruz, 1985

Professor Douglas L. Inman, Co-chairman

Professor Gary B. Griggs, Co-chairman

A flood delta on the wave-dominated Central California coast was studied to determine the time scale and mechanisms by which river sand was incorporated into the longshore transport regime. The results are pertinent to sediment management on coasts with Mediterranean type climates and drainages. On such coasts, generally, rivers supply most of the littoral sand yet the bulk of this supply accompanies large infrequent floods. In contrast, the nearshore transport processes operate with much greater continuity and regularity.

The delta studied was built by a 30-year return period flood at the mouth of the San Lorenzo River. The peak discharge at the river mouth during this flood was about 1,100 m^3/sec. The river drains an area of 357 km^2 on the northern shore of Monterey Bay. There, most wave energy arrives as swell from the northwest and, except during brief flood periods, it dominates the river outflow. As a result, the San Lorenzo delta is an ephemeral feature. The study extended two years: in both years the river's supply of sand and gravel was about 300,000 m^3, ten times its mean annual supply and equivalent to almost twice the mean annual net longshore transport past the mouth.

Methods of investigation included: surveys of nearshore topography, estimates of the river's littoral sediment yield using river flow data and river channel surveys, and estimates of the longshore variation in longshore-transport potential using a wave refraction program. The surveyed sand level changes provided a means of tracing bulk sand movements. The longshore transport predictions were used to confirm the direction of sand movement.

Compared size distributions of littoral and river sediment suggested that essentially all river sediment finer than 0.18 mm was quickly lost from the shore zone. Estimates of the river's littoral sediment yield based on riverflow data and this "cut-off" grainsize agreed well with the accretion observed on the delta through the first year of the study, when probably little sediment was moved far from the river mouth.

The accretion and erosion predicted by the divergence of the longshore transport potential generally agreed qualitatively, but not

quantitatively, with the survey results. The observed sand volume changes were smaller than those predicted. The delta interrupted the continuity of the longshore transport of sand past the river mouth. Significant accretion occurred on the upcoast flank of the delta as sand accumulated in a transport convergence zone; for a period, some beaches downcoast lost sand.

Initially, the bulk of the delta sediment was deposited seaward of the surfzone. Only about one quarter of the winter flood deposits were returned shoreward each summer - the rate of return was regulated by the onshore transport potential. Most of the sand moving shoreward did so under one large bar feature. Lesser volumes of sand migrated shoreward as series of small longshore bars. Sand level changes showed that cross-shore movements played an integral role in the longshore dispersion of the river sand: directly, through longshore components to the seasonal cross-shore migrations; and indirectly, through the return of sand from offshore to the surfzone "littoral river of sand".

The overall pattern of longshore sand dispersion from the river mouth, shown by net longshore volume changes, was that of a low-amplitude sandwave which migrated and dispersed gradually alongshore in the direction of the dominant longshore transport. The longshore transport divergence necessary to propagate the sandwave appeared to combine longshore variations both in the cross-shore sediment fluxes, which have longshore components, and in the surfzone longshore transport.

Similar river sand dispersion mechanisms appear to have operated at other, larger, flood deltas observed on the Southern California coast.

1. INTRODUCTION

Rivers are an important source of California's littoral sand. This has been demonstrated by many studies that compute the time-averaged littoral sediment budget of individual coastal cells (e.g Inman and Frautschy, 1966; Inman and Brush, 1973). However, little attention has been given to the fact that the most important events supplying river sand, i.e. large floods, are very irregular, infrequent, and peaky. In contrast, the waves and currents that move the sand operate with much greater regularity and frequency.

What is the significance of this? How, and at what rate, is sand from the transitory delta deposited at the river mouth during a flood incorporated into the littoral pathway? Is it gradually eroded; translated alongshore as a sandwave; smeared along and offshore by storms and transport direction reversals; or, returned to the river estuary by wave and tidal action? These details are important to coastal engineering and management which must be concerned with not only the local short-term shoreline stability around the river mouth, but also the routing of littoral sand through the entire littoral cell.

While each California open-coast river mouth is unique, those of the central and southern coast at least are generally similar in terms of their intermittent sand supplies, overall wave dominance, and a net southerly longshore sand transport. Their deltas, built during temporary periods of river dominance, are ephemeral features. The longshore sand dispersion is apparently rapid, yet its mechanism is not well understood.

1.1 River Sand Supplies to the California Coast

Many studies have shown rivers to be the dominant sand sources for the California Coast. Estimates of the river contribution to the total sand supply of individual littoral cells range from 60% for the Monterey Littoral Cell (Arnal et al, 1973) to about 85% for the Pismo Beach - Santa Barbara (Bowen and Inman, 1966) and Oceanside (Inman and Jenkins, 1983) littoral cells.

The infrequent delivery of this sand is demonstrated in Fig. 1, which shows the annual suspended sediment yield of three California coastal rivers. The data in this plot are based on USGS streamflow and sediment measurements made at sites near the coast. While the portion of the total river load that is trapped in the nearshore zone is less than the river's suspended load (analysis in a later section suggests that the volume equivalent of about 28% of the suspended load is trapped), the suspended load record is nonetheless a fair indicator of the relative magnitudes and frequencies of littoral sediment supply events. Since sediment transport rate in rivers is a power function of water discharge, the bulk of the sand yield over a period of time has accompanied the largest floods.

Short estuaries, of the order of 1 km in length, are found at the mouths of many Californian coastal rivers. Often, these estuaries trap the sand yield of smaller floods and are flushed only by the larger floods. They therefore enhance the episodicity of the coastal sand supply. Observations through this century show little estuarine aggradation, evidence that sand is eventually flushed from these small temporary traps.

Figure 1. Annual suspended sediment yields of three California coastal rivers.

a. SANTA CLARA RIVER at MONTALVO
(BROWNLIE and TAYLOR, 1981, and
USGS, WATER RESOURCES DIVISION)

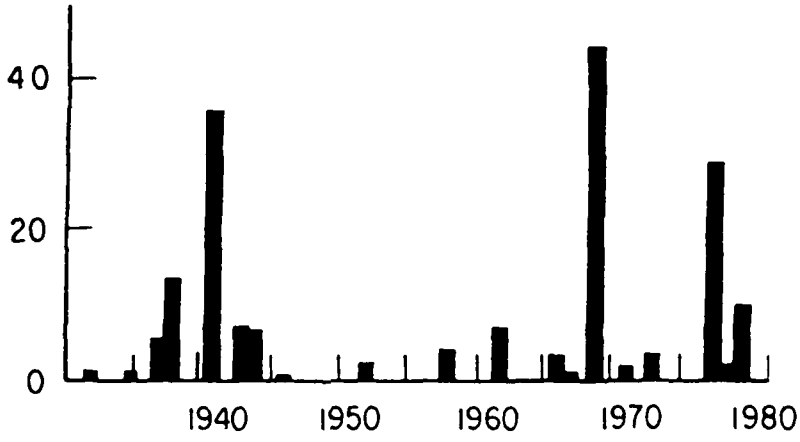

b. SALINAS RIVER at SPRECKLES
(USGS, WATER RESOURCES DIVISION)

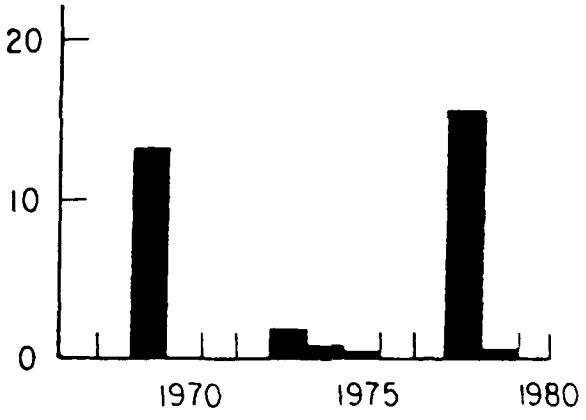

C. SAN LORENZO RIVER at BIG TREES
(USGS, WATER RESOURCES DIVISION)

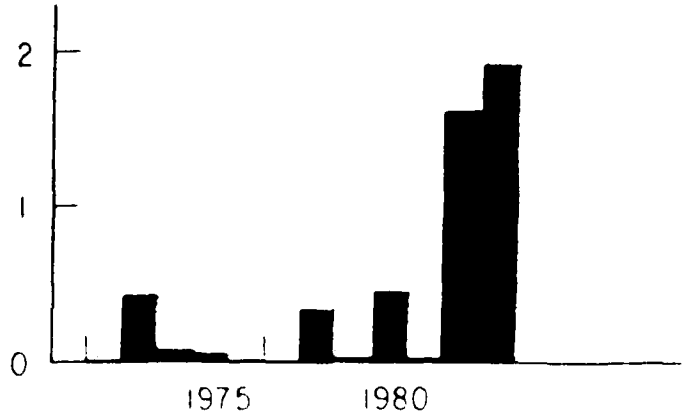

SUSPENDED SEDIMENT YIELD, millions tons

YEAR

1.2 Sand Transport along the California Coast

Compared to river floods, the significant sand transport events along the coast of California occur much more often and regularly. The largest variations in longshore transport appear at less than annual time scales. When these are averaged over a year or two, the transport appears fairly steady.

Seymour and Castel (1985) investigated the short-term episodicity of the longshore transport potential using directional wave data from seven sites along the California Coast. They found that in a given year the transport potential was very episodic, with almost half of the annual transport occurring during 10% of the time in a few mainly wintertime events.

The longer-term episodicity of longshore transport can be observed in the accumulation rates at littoral drift traps. Fig. 2 shows the variation in annual drift accumulation at two California harbors. At Santa Cruz, the data include rates of sediment impoundment upcoast of the harbor and sediment dredging from the entrance channel (Fig. 2a). While some sand naturally by-passes this harbor and so escapes being trapped, Inman (1976) and Walker and Williams (1980) indicate there is a reasonable correlation between the volume trapped and the total volume in transport. The harbor at Santa Barbara is a complete trap of littoral drift; the data plotted for there are based on accretion surveys and dredgings at the harbor entrance (Fig. 2b). At both locations, the variation in the annual transport rate is small, particularly when compared to the annual variations in river sediment yield indicated in Fig. 1.

Figure 2. Annual littoral drift entrapment at Santa Cruz and Santa Barbara harbors. (a) At Santa Cruz, the total littoral drift includes that trapped upcoast on Seabright Beach and that trapped in the harbor entrance. (Data from Walker and Williams, 1980). (b) At Santa Barbara, the littoral drift is trapped on a shoal inside the breakwater. (Data from Wiegel, 1959).

a. SANTA CRUZ HARBOR

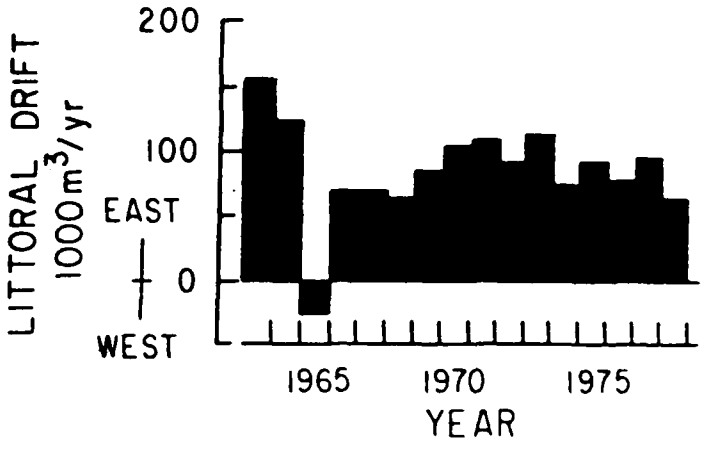

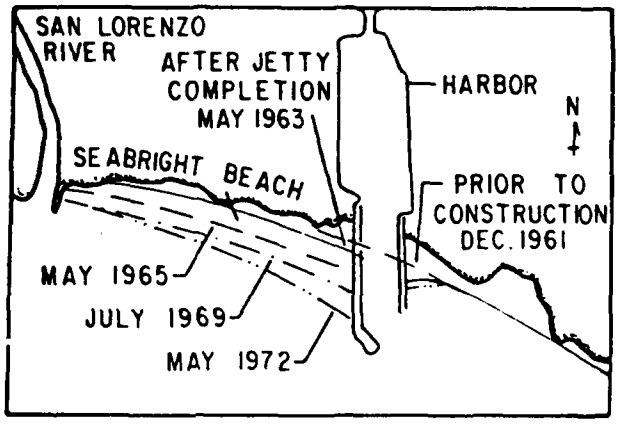

b. SANTA BARBARA HARBOR

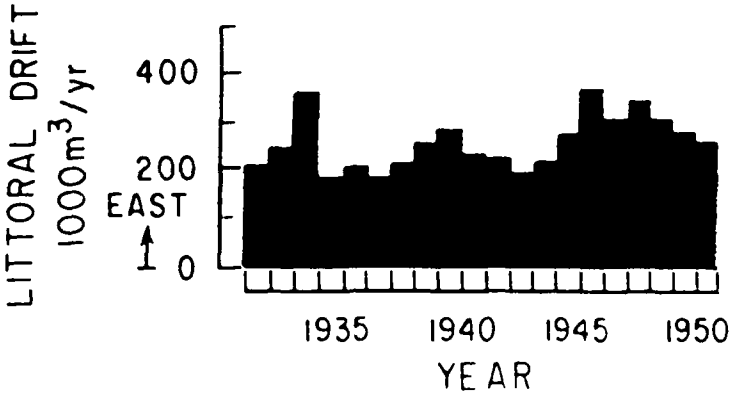

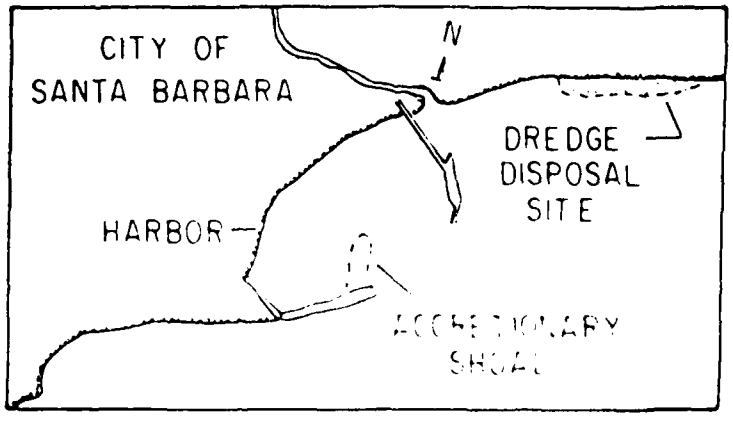

1.3 Characteristics of Coastal Deltas

In general, when a river enters the ocean its momentum and sediment carrying capacity are dissipated and it deposits its sediment load as a delta. On meso- and microtidal coasts (with tidal ranges less than 4m) the delta's form, both in plan and in cross-section, is controlled by the interplay between river and wave power (Bates, 1959; Coleman and Wright, 1975; Coleman, 1981). Where rivers dominate, i.e., where sediment is supplied at a rate faster than the waves can redistribute it alongshore, a delta builds seaward; the new shoreline extends at a high angle to the old shoreline and the profile of the delta-front is convex-up. Where waves dominate, the river sediment is efficiently sorted into coarse and fine fractions: sand and coarser material is moved alongshore and moulded into wave-built shoreline-parallel features such as beaches, barriers, and spits; finer material is spread widely offshore. The wave-built profiles are concave-up.

Wright and Coleman (1973) use the "discharge effectiveness index" to quantify, in a relative sense, the river/wave dominance. This index equals the ratio of river discharge per unit width of river mouth to wave power per unit length of shoreline.

The river mouths of the central and southern California coast are typically wave-dominated, as demonstrated by their extremely low time-averaged discharge effectiveness indices, linear shoreline features, concave-up profiles, and well sorted coastal sediments. The discharge effectiveness indices of several California rivers are compared in Table I with those of rivers having a range of delta morphologies. The principal reasons for the wave dominance are: the

Table I. Relative dominance of river flow over wave power at coastal deltas.

Delta	Mean Nearshore Wave Power (watt/m)	Mean River Discharge (m^3/s)	Mean Discharge Effectiveness Index	Relative Supremacy
				RIVER
Worldwide:				
Mississippi+	0.13	17,700	$1x10^2$	
Danube+	0.13	6,290	$2x10^1$	
Ebro+	0.49	552	$6x10^0$	
Niger+	6.6	10,900	$9x10^{-2}$	
Sao Francisco+	100	3,110	$3x10^{-2}$	
Senegal+	380	770	$6x10^{-3}$	
Shoalhaven•	1,500	57	$1x10^{-3}$	
Nile#	2,500	2,730	$1x10^{-3}$	
California:				
San Lorenzo*	4,500	3.8	$4x10^{-5}$	
Santa Clara°	2,200	4.1	$6x10^{-6}$	
Ventura°	2,200	2.0	$6x10^{-6}$	
Santa Maria-	6,300	0.8	$4x10^{-6}$	
				WAVE

Data Sources:

+ Wright and Coleman (1973) - Note that Wright and Coleman's published data on wave power appear to be about a factor of 100 too small. Consequently, their D.E.I.'s are probably about a factor of 100 too large.

• Wright (1976)

Inman (1984)

* USGS, Water Resources Division (1982) - for river data
Walker et al (1978) - for wave data

° USGS, Water Resources Division (1982) - for river data
USACE, L.A. District (1980) - for wave data

- Bowen and Inman (1966)

exposure to many long fetches of a large ocean, the semi-arid climate, and the generally small size of coastal drainage basins.

As a result of the consistently high wave power and erratic sediment supplies, the deltas at these California river mouths tend to be ephemeral features, small in size, and mostly subaqueous. They are built rapidly during floods, or flood periods, when the river temporarily dominates over the waves; then follows a transitional period when the delta deposit is reworked by wave action. Finally, essentially complete wave dominance occurs; the shoreline is again straight and the river mouth is often closed off. For smaller rivers and floods, the river may never dominate over wave action since, along coastal California, rainstorms are frequently associated with coastal storms.

Thus a typical California coastal delta's history can be summarized as one of rapid construction, fairly rapid or concurrent reworking and destruction, and often prolonged non-existence.

1.4 Theoretical Review and Previous Studies

The detailed mechanisms by which river sand is moved alongshore from these wave-dominated river mouths are only vaguely understood. Any general notion that river sand entering the ocean is swept directly alongshore (e.g. Shephard, 1963) ignores the possibility that much of the sand may be deposited initially seaward of the surfzone, beyond the "littoral river of sand" (Inman and Brush, 1973). Also, the delta modifies the nearshore processes and conditions by changing the shore

profile and planform, and by redirecting and redistributing the incident wave energy by refraction and diffraction.

The problem can be investigated on two scales: detailed study of river mouths during the period of delta deposition and reworking; and larger scale studies concerned with routing the river sand inputs along the coastlines of littoral cells.

Previous studies focussing on individual river mouths have been descriptive investigations of detailed processes: the flow patterns, the resultant sediment movements, and the evolving morphologic features - the "morphodynamics". Coleman (1981) reviews the significant river mouth processes and forcing functions. We will summarise these in the context of a flood debouching onto an originally straight coastline. The geometry of the sediment deposit at the river mouth reflects the interaction between riverflow, friction across the seabed at the river mouth, buoyancy effects, and tidal and wave effects. Figs 3a-e summarise conditions when one or two of these controls dominate.

In the absence of significant tides and waves, high-velocity hypopycnal flood flows diffuse offshore as a turbulent plane-jet and deposit a thick, elongate-offshore, river mouth bar (Fig. 3a). With less density contrast between the effluent and ocean water, the effluent spreads, mixes, and decelerates more rapidly and a more circular bar is deposited (Fig. 3b).

With a shallow nearshore slope, bottom friction becomes an important factor in decelerating and spreading the river effluent. A feedback loop operates as deposition proceeds: the growing river mouth bar further decelerates and chokes the outflow, diverting it laterally.

Figure 3. River mouth depositional patterns showing the effects of dominance by riverflow inertia and buoyancy, friction, and waves.

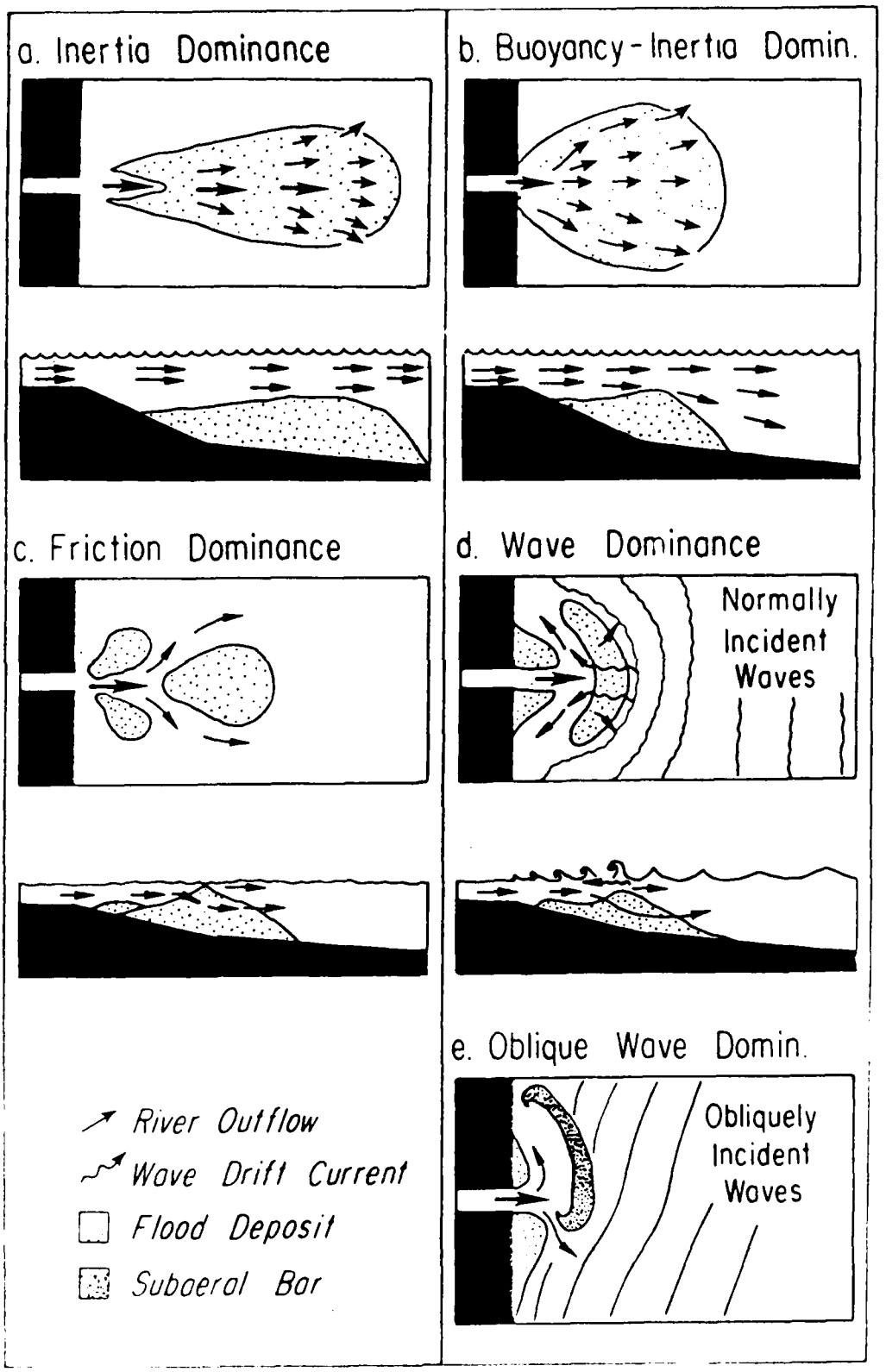
a. Inertia Dominance
b. Buoyancy - Inertia Domin.
c. Friction Dominance
d. Wave Dominance
Normally
Incident
Waves
e. Oblique Wave Domin.
Obliquely
Incident
Waves
River Outflow
Wave Drift Current
Flood Deposit
Subaeral Bar

Levees are built on the shoreward side of the new outflow channels. The result is a wide central bar fronting a bifurcating channel (Fig. 3c).

In the case of high energy waves, the transport and dispersion of sediment resulting from the intense water motion, strong drift currents, and turbulence of breaking waves dominate the effects of effluent inertia and buoyancy. The waves also sort the river's sediment load. The result is a lunate sand bar located close to the river mouth (Fig. 3d).

Clearly, the geometry and morphology of the river mouth should evolve following, or even during, a flood period in response to a change from inertia-buoyancy dominance to wave-friction dominance. During the flood, the dominant depositional feature may be a seaward-elongated bar. Relatively quickly however, this will be reworked and the river mouth should be characterised by a broad crescentic bar located closer to the river mouth, broad shallow subaqueous levees, and a constricted outlet. Eventually, the shoreward migrating bar will weld to the shoreline and may plug the outlet channel. Wright (1976) describes such a morphological evolution at the wave-dominated Shoalhaven River mouth in Australia.

Oblique wave approach may lead to a range of effects. Mild wave-induced longshore transport during and after the flood may deflect the outlet channel alongshore, build spits off the river mouth bar, and return the sediment from offshore further down the coast (Fig. 3e). Strong longshore transport during the flood may sweep much of the river sediment alongshore immediately.

Hence there are two mechanisms for moving the river sediment alongshore from the river mouth under the influence of obliquely-incident waves: comparatively rapid longshore transport within the surfzone, and a longshore component of cross-shore migration. If much of the river sediment is deposited beyond the surfzone during a flood, its return to the "littoral river of sand" will be regulated by the onshore transport potential. It may well take several seasons of swell waves to rework and return a given deposit of river sand to the shore and to re-establish an equilibrium profile off the river mouth.

Previous studies of California coastal deltas are few and have not been reported in detail. In the year following the record floods of January-February 1969, the deltas of the Santa Clara and Santa Ana Rivers, and of San Juan Creek were surveyed repeatedly (U.S. Army Corps of Engineers, L.A. District, 1970). Likewise in 1978, the Santa Clara and Ventura River deltas were surveyed (USACE, L.A. District, 1980). All of these deltas underwent a similar morphologic evolution. Their form soon after construction resembled that depicted in Fig. 3e. Waves reworked the river sand into a bar opposite the river mouth. With time, this bar grew in height, migrated landward, and was extended downcoast. After several months, the bar merged with the downcoast beach, which then widened considerably. The beach immediately upcoast of the river mouth also widened as it became a temporary convergence zone for littoral drift.

The transport processes by which periodic river sand inputs travel through littoral cells has never been addressed directly. The central issue at this scale concerns whether the sand is eroded gradually from

the river mouth, or whether it is translated alongshore as a kinematic accretionary sandwave that leaves its signature in the shoreline planform. There is some observational and theoretical justification that the latter should occur, at least in some situations.

Longshore-progressive accretionary sandwaves, initiated by sudden sand inputs to the nearshore, have been described frequently in the coastal engineering literature. They have been variously termed sand "humps", "bumps", "pulses", or "slugs". The sand sources include a tidal-inlet delta (Bakker, 1968), a beach fill (Everts et al, 1974; Chapman, 1978), or various natural sand by-passing events around headlands (Chapman and Smith, 1981) and across tidal inlets (Brunn, 1966; Everts et al, 1980). Conversely, the sand "input" event may be a negative one: for example, when the littoral sand supply is trapped by an artificial structure. In this case, an erosion wave propagates downcoast (Inman and Jenkins, 1983).

At Santa Barbara, California, both accretionary and erosive sand waves have been observed. The harbor breakwater there traps sediment transported alongshore from the west (Fig. 2b). Periodically, this sediment is dredged and released to the beaches east of the harbor (Wiegel, 1959). Hunter (1946) found that high accretion rates in the harbor lagged 3 to 4 years behind high rainfall events in the watersheds of coastal streams upcoast from the harbor. This suggests that the periodically-high river sediment inputs were translated alongshore as sandwaves. Bailard and Jenkins (1982) found that temporal shoreline variations for 30 km downcoast from the harbor could be explained by

progressions of accretion and erosion waves stemming from periods of dredging and non-dredging at the harbor.

The mechanism for propagating accretionary sandwaves must be associated with longshore divergence in the longshore transport rate. This divergence may be induced by changes in the transport potential, the sand supply, or both. Supply effects should be important where sand is input to a generally barren, sand-starved, bedrock coastline.

Variation in the longshore transport potential can accompany changes in both the planform and profile of the shore created by a sand excess. This becomes clearer after considering the currently popular Scripps/Corps of Engineers longshore transport relation

$$I_l = K\,(E\,Cn\,\sin\alpha\cos\alpha)_b \qquad (1)$$

where I_l is the immersed-weight longshore transport rate in the surfzone, K is a dimensionless coefficient, evaluated by Komar and Inman (1970) as 0.77, $E = {}^1/_8\,\rho g\,H^2$ is the wave energy per unit surface area, H is the root-mean-square wave height, Cn is the wave group velocity, and α is the angle the incident wave crests make with the shoreline. The subscript b indicates that the parameters are evaluated at the breaker line. Inman (1978) discusses the source and derivation of equation (1).

For a given deep-water wave condition, the three-dimensional configuration of the nearshore influences, by refraction, the breaker angle and wave height at any point along the shore. The shore profile also influences the breaker type and hence also the value of the coefficient K (Inman and Jenkins, 1983; White and Inman, 1985).

Mathematical models for simulating progressive sandwaves have been developed around this relation, or its precursors, and have been applied successfully to prototype sandwaves over appropriate time and length scales. For example, Bakker (1968) modelled sandwaves initiated by the periodic shoaling of a tidal-inlet delta located at the upcoast end of Vlieland Island on the German Coast. Typically, the modelled sandwaves have wavelengths of the order of 10 km and celerities of the order of 1 km/yr; they attenuate exponentially alongshore and the model time scale is of the order of 10 years.

Similar techniques have been used to model river delta growth (e.g. Pelnard-Considere, 1954; Grijm, 1960 and 1964; Bakker and Edelman, 1964; and Komar, 1973). Bakker and Edelman (1964) modelled delta planform evolution on a shoreline subject to obliquely-incident waves. They predicted the growth of a spit downcoast from the river mouth, erosion of the original shoreline in the lee of the spit, and accretion on the upcoast side of the delta - all consequences of longshore transport divergence around the modified shoreline. This result was first hypothesized by Inman and Bagnold (1963).

Generally, however, such models are too simple to apply to at least the depositional phase of the California coastal deltas. This is because they simulate the long-term growth of a delta experiencing a steady wave regime and sediment supply sustained over time scales of many years. Models of small ephemeral California-type deltas must simulate delta growth and "morphodynamics" over time scales of a few days. To do so they need to be an order of magnitude more complex. They must simulate: the net fluid motions driven by rapid variation in

riverflow, tide, and waves; the fluid-sediment interactions; and the resultant three-dimensional morphologic evolution. Since each of these tasks remains a topic of fundamental research, any present attempt at an integrated deterministic model must be premature.

1.5 The Dissertation Study

The present study is a descriptive one. It focusses on the detailed sand dispersion from one California river mouth - that of the San Lorenzo River at Santa Cruz on the central coast. In early January 1982, the San Lorenzo flooded with a magnitude estimated to have a 30-year return period, building a 0.3 km^2 delta off its mouth. By late summer, the delta had apparently disappeared. During the subsequent winter, larger than average floods rebuilt the delta, but again by late summer, the visible signs of a delta were gone.

The objectives of the 21-month study were threefold: to trace sediment movements in the vicinity of the river mouth and hence to elucidate the time scale and mechanisms by which the river sand was incorporated in the littoral "river of sand"; to determine the volume of the river's sand yield and so its importance to the local short-term littoral sediment budget; and to assess the impact of the river delta on the progress of littoral drift from upcoast and on the stability and "health" of the surrounding beaches. Also, the study is pertinent to the maintenance of an artificial harbor, located less than 1 km downcoast of the river mouth.

The bathymetry of a control cell containing the river mouth constituted the principal data collected. Spatial and temporal volume

changes were used to trace the sand migration. River flow and sediment records provided an independent estimate of river sediment supply, while a wave array monitored the nearshore forcing function.

The analysis was aimed at deriving a conceptual model for the river sand dispersion: a prerequisite for any further studies of a deterministic nature.

2. THE STUDY AREA AND ENVIRONMENT

2.1 Choice of Site

The San Lorenzo River mouth at Santa Cruz, California, was chosen for study mainly because a large flood occurred there at the right time. However, other advantages of the site included an active flow-recording and sediment station on the river only 11 km upstream of the mouth, an active slope-array-type wave recorder installed 800 m alongshore from the river mouth, a partial littoral drift trap 900 m downcoast from the river mouth in the form of the Santa Cruz small craft harbor, a reasonable state of knowledge on the local nearshore processes and sediment budget, and reasonable logistics.

2.2 Coastal Features

Santa Cruz is located on the northern shore of Monterey Bay, some 110 km south of San Francisco (Fig. 4). The area is flanked by the Santa Cruz Mountains which consist of a plutonic and metamorphic core overlain and lapped by Tertiary sediments. These mountains are drained by a number of small, steep-gradient, coastal streams, the largest of which is the San Lorenzo River.

The locality occurs within a littoral cell which begins probably south of Halfmoon Bay and terminates at the Monterey submarine canyon (Fig. 4). The cell boundaries have been established mainly on the basis of heavy-mineral and grainshape studies of littoral sands (Yancey and Lee, 1972; Clark and Osborne, 1982). Sand is moved southward through the cell by the predominant northwest swell.

Figure 4. Location maps of study area.

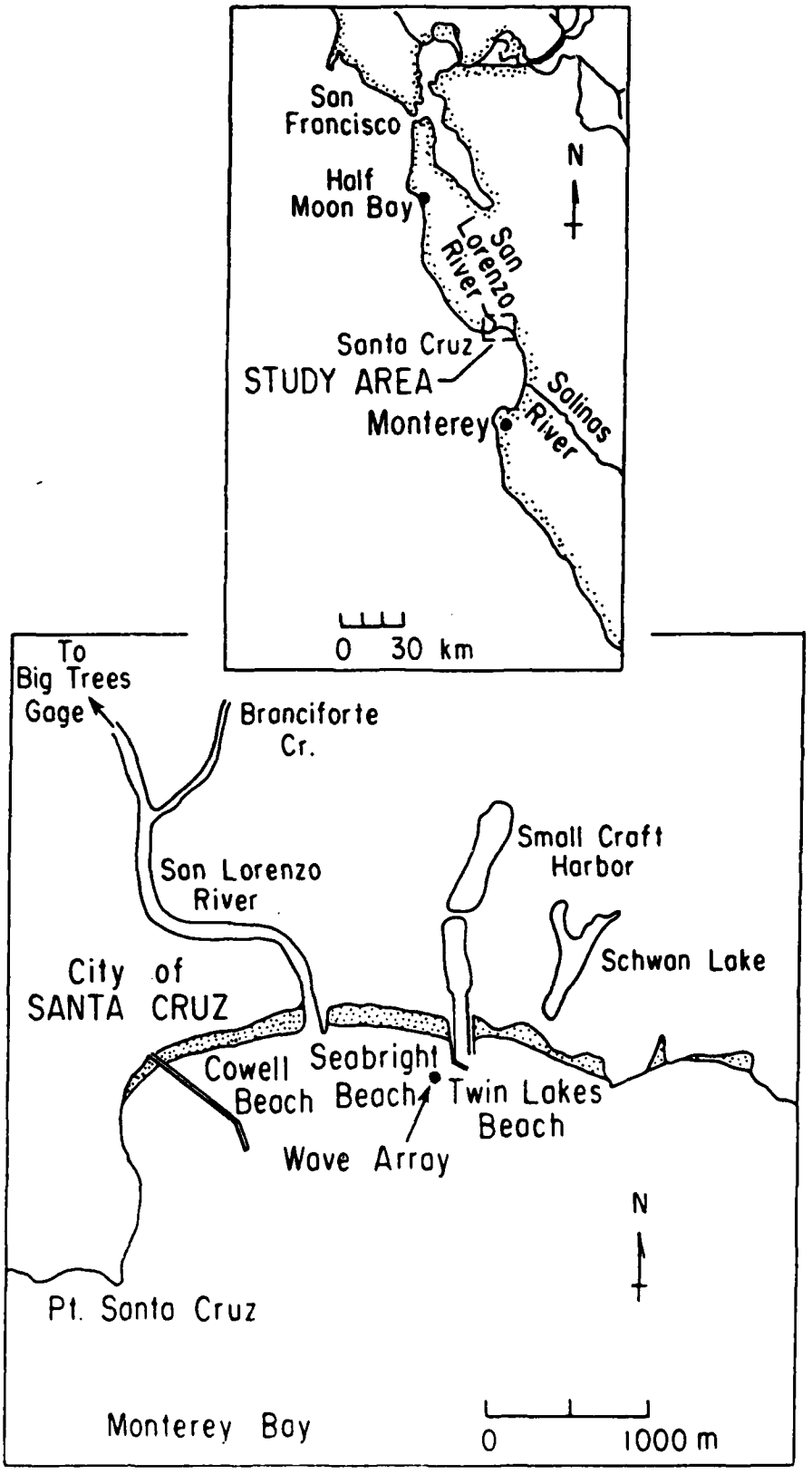
San
Francisco
N
Half
Moon Bay
San
Lorenzo
River
Santa Cruz
STUDY AREA
Salinas
River
Monterey
0 30 km
To
Big Trees
Gage
Branciforte
Cr.
Small Craft
Harbor
San Lorenzo
River
Schwan Lake
City of
SANTA CRUZ
Cowell
Beach
Seabright
Beach
Twin Lakes
Beach
Wave Array
N
Pt. Santa Cruz
Monterey Bay
0 1000 m

Northwest of Point Santa Cruz, the shoreline comprises sea cliffs, cut into uplifted marine terraces, and small pocket beaches which are found mostly at the mouths of the coastal creeks. Littoral sediment sources are the coastal creeks and eroding marine terraces. No deltas are found at the mouths of these streams: a reflection of their small drainage areas and the vigorous wave climate.

Southeast of Point Santa Cruz, sandy beaches are more prominent. These beaches undergo typical seasonal changes in profile. In winter, storm waves erode and flatten the beach face. In summer, swell waves return the sand and build a high wide berm. The beach material is medium-fine sand. The beaches slope steeply, with a concave-up profile, to the 6 m isobath, then a 16 km wide continental shelf slopes very gently to the southwest. This shelf drops off into Monterey Canyon in the middle of Monterey Bay. The shelf bottom comprises bedrock partially overlain with unconsolidated sediment.

The San Lorenzo River debouches at the east end of Cowell Beach beside a small natural rock groin, as shown on Fig 4. Further east are Seabright and Twin Lakes Beaches, separated by the Santa Cruz small craft harbor. The construction of the harbor jetties in 1963 resulted in the growth of a 400,000 m^3 accretionary fillet on the upcoast side, Seabright Beach, and erosion of the downcoast beaches and cliffs (USACE, San Francisco District, 1969; Anderson, 1971; Moore, 1972; Inman, 1976; Griggs and Johnson, 1976). Sand began to by-pass the jetties as early as 1965. Each winter since then, the harbor mouth has been essentially closed by sand build-up, necessitating an annual spring dredging and more recently a phased dredging program (Walker and

Williams, 1980). The dredge spoil is pumped subaerially onto Twin Lakes Beach within 100 m of the eastern jetty.

2.3 Oceanographic Climate

The waves arriving at Santa Cruz can be divided into three categories according to origin: Northern Hemisphere swell, Southern Hemisphere swell, and seas generated by local winds (Marine Advisors, 1961). The tides are mixed, predominantly semidiurnal. The mean high water - mean low water range is 1.1 m; the mean higher high water - mean lower low water range is 1.6 m; the estimated extreme range is 3.2 m (Walker et al, 1978). Coastal ocean currents in the area are weak and change seasonally.

2.4 Local Littoral Sediment Budget

The longshore sand transport rate at Santa Cruz has been estimated from wave studies, both hindcast (Anderson, 1971; Walker et al, 1978) and directly measured (Seymour et al, 1980), and from the accretion rates at the harbor (Moore, 1970; Walker and Williams, 1980). It probably averages about 200,000 m^3/yr net to the east: a figure typical of Southern California littoral cells (Inman and Frautschy, 1965). However, the uncertainty in this figure may be up to a factor of 2.

The San Lorenzo River is the only significant local sediment source. During periods of high runoff a temporary delta often forms at its mouth. Estimates of the San Lorenzo's average yield of sand and coarser sediment cluster around 60,000 m^3/yr (Griggs and Johnson, 1976; Inman, 1976; Jones-Tillson et al, 1979). In section 3.4 it is

suggested that sand fractions finer than 0.18 mm are lost from the Santa Cruz nearshore zone. Correcting for this, the river's average yield of littoral sediment becomes about 30,000 m^3/yr. Therefore, on average, the San Lorenzo supplies something like 15% of the littoral drift passing the harbor. The remainder of the littoral drift must come from the open coast to the north. Sand influxes around Point Santa Cruz are often noted shortly after a winter storm or a period of strong northwesterly swells (Griggs and Johnson, 1976).

2.5 The San Lorenzo River

The San Lorenzo River drains a catchment area of 357 km^2. Within its basin, elevations range from sea level to 1000 m. The average annual rainfall is 120 cm, but varies from about 76 cm near the ocean to 152 cm in the higher mountain areas. Runoff is quick: the time to concentration at the San Lorenzo mouth is only 5-6 hours. The principal flow gage is the USGS station at Big Trees, 11 km upstream of the mouth. There, the mean annual flow is 3.8 m^3/sec, the mean annual flood is 233 m^3/sec, the 10-year flood is 525 m^3/sec, and the largest flood on record, the 30-year event, is 847 m^3/sec. The equivalent flows at the mouth can be estimated from these figures by applying the ratio of total basin drainage area to drainage area upstream of Big Trees (272 km^2).

The flow is seasonal: it averages less than 1 m^3/sec for the summer months, June to October, and swells to an average of more than 10 m^3/sec the rest of the year. Most flood flows have occurred in December-January. Since the sediment transport capacity increases

approximately with the square of the discharge (Jones-Tillson et al, 1979), sediment yield events are essentially ephemeral.

Five km upstream of its mouth, the San Lorenzo River emerges onto a narrow floodplain. From there on downstream, it is confined within an artificial channel about 80 m wide. The river mouth's behaviour is typified by seasonal cycles. During summer low-flow periods, waves move sand into the mouth, forming a berm and tending to close the channel. During winter, high waves erode the berm, high flows scour the channel bed, and an offshore sand bar is deposited. Because of the floodplain channel's narrow width and relatively steep slopes, the tidal prism is small and tidal currents are relatively inefficient in moving sediment into or out of the mouth. The main tidal effect is on the backwater levels during flood flows.

2.6 Conditions During Study Period

The study period extended from January 1982 through September 1983, and essentially covered two winter-summer streamflow and beach cycles. The 1982 winter was marked by a phenomenal hydrological event in the San Lorenzo watershed. In contrast, the concurrent coastal conditions at Santa Cruz were less extreme. The following winter again produced exceptionally high river flows, which this time were accompanied by intense coastal storms.

An indication of the relative sequences and magnitudes of the river and coastal events through the study period is given by Fig. 5. It shows the record of daily mean flow in the San Lorenzo River at the Big Trees gage and significant wave height at 7 m depth off the harbor. The

Figure 5. River flow and wave height at Santa Cruz during the study period.

DAILY MEAN RIVER FLOW : SAN LORENZO RIVER at BIG TREES SITE

(MEAN ANNUAL FLOW = 3.8 m^3/sec
BASED on a 32yr. RECORD PERIOD)

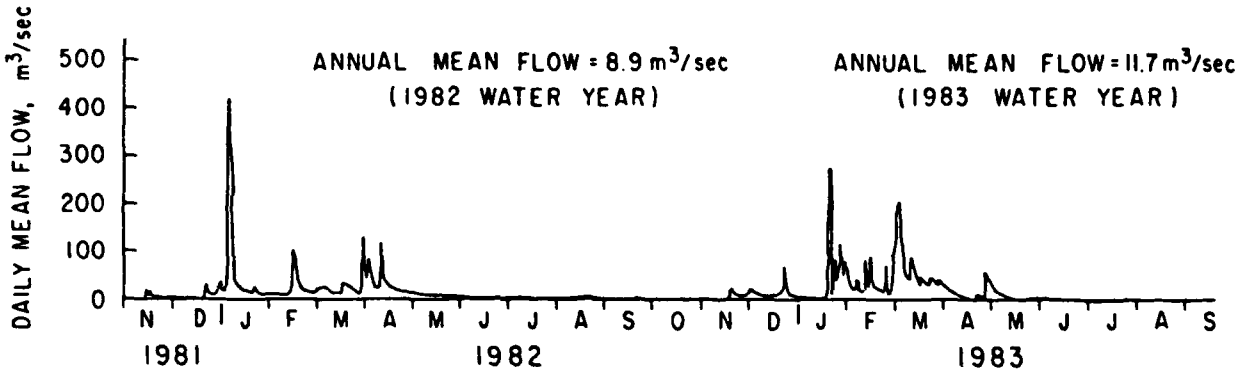

DAILY MEAN SIGNIFICANT WAVE HEIGHT : SANTA CRUZ HARBOR ARRAY

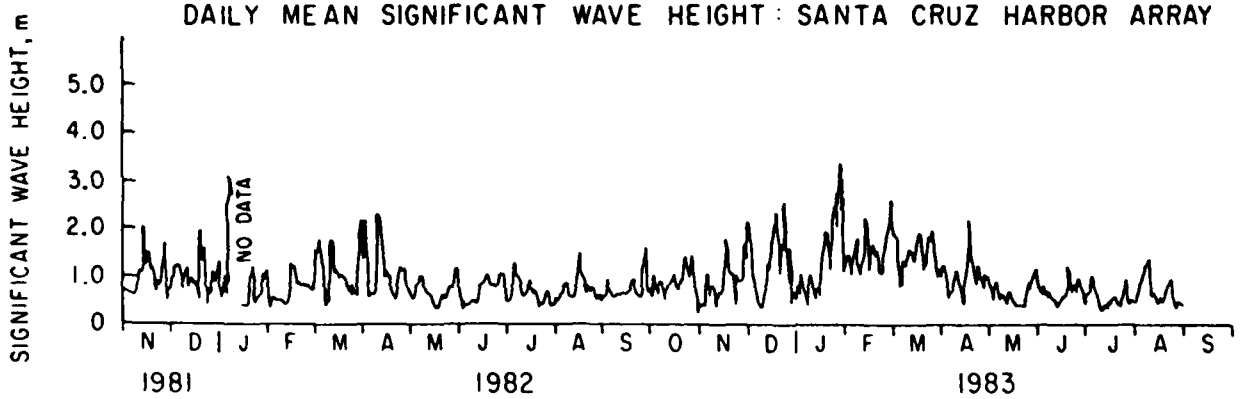

long-term representativeness of the study period can be gaged from Fig. 6. On this figure, the 1982 monthly means of river discharge, wave power, and discharge effectiveness index are compared with long-term average values.

Further details of the study area - its littoral sediment budget, wave climate, and the conditions during the study period - are included in Appendix A.

Figure 6. Monthly mean river flow, wave power, and Discharge Effectiveness Index through 1982 compared to the long-term average conditions. q_r is the river flow per unit width of river mouth in $m^3/sec/m$. p is the wave power per unit length of breaker crest in Nm/sec/m. In (a), q_r and p are normalized in terms of their maximum values. In (b), the ratio q_r/p equals the Discharge Effectiveness Index (DEI).

a. MONTHLY MEAN RIVER DISCHARGE AND WAVE POWER
SAN LORENZO RIVER MOUTH

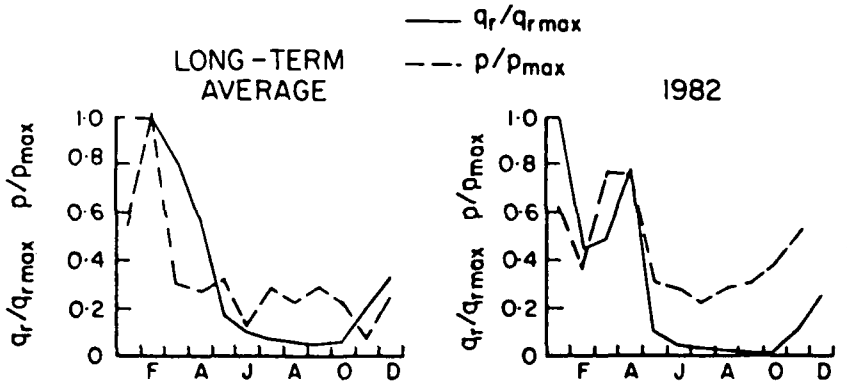

b. DISCHARGE — EFFECTIVENESS INDEX

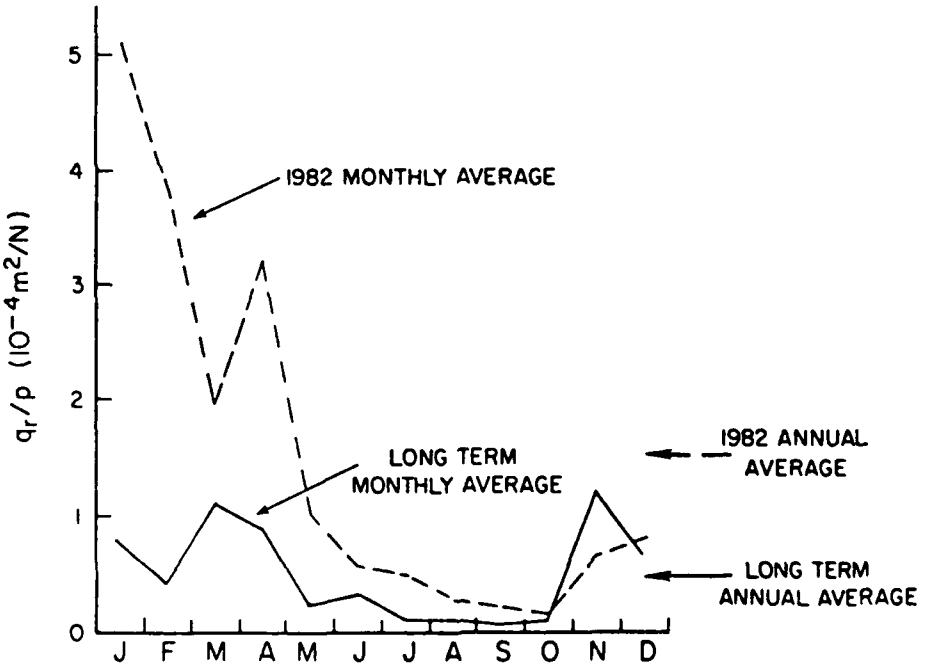

3. METHODS AND PROCEDURES

3.1 Study Objectives and Approach

As mentioned in the introduction, the study objectives were threefold: to quantify the river sediment supply to the littoral cell; to trace sand movements at and away from the river mouth; and to observe the impact of the temporary river delta on the local beaches and on littoral drift arriving from upcoast. The approach adopted to meet these objectives involved monitoring the sand volume and distribution within a control cell while keeping track of sand fluxes into and through the cell.

The control cell extended 1825 m alongshore and offshore to about 8-10 m depth, enclosing the river mouth and the harbor. The essential features of its sediment budget are shown in Fig. 7. Two independent estimates of the river sediment supply were derived: one from flow records and bed volume changes in the river channel, and the other from accumulation volumes at the river mouth. Sand level changes (i.e. volume per unit area and per unit beach length) provided a bulk means of tracing sand movements. Wave data were used to predict, in relative terms, the potential rates and directions of longshore transport into and through the cell. The sand trapping and dredging history of the harbor provided a lower limit to the transport rate immediately upcoast of the harbor. The longshore transport predictions and overall volume changes were not expected to be sufficiently accurate to balance the sediment budget of the control cell. A summary description of data collection procedures and analysis follows. Further details are given in Appendices B - E.

Figure 7. The sediment budget of the control cell. Sand sources are the river, dredge spoil from the harbor, longshore transport, and possibly onshore transport. Sand sinks are the harbor entrance, longshore transport, and offshore transport. The river sediment derives from the bed of the floodplain channel, the main stem upstream of the floodplain, and the tributary Branciforte Creek.

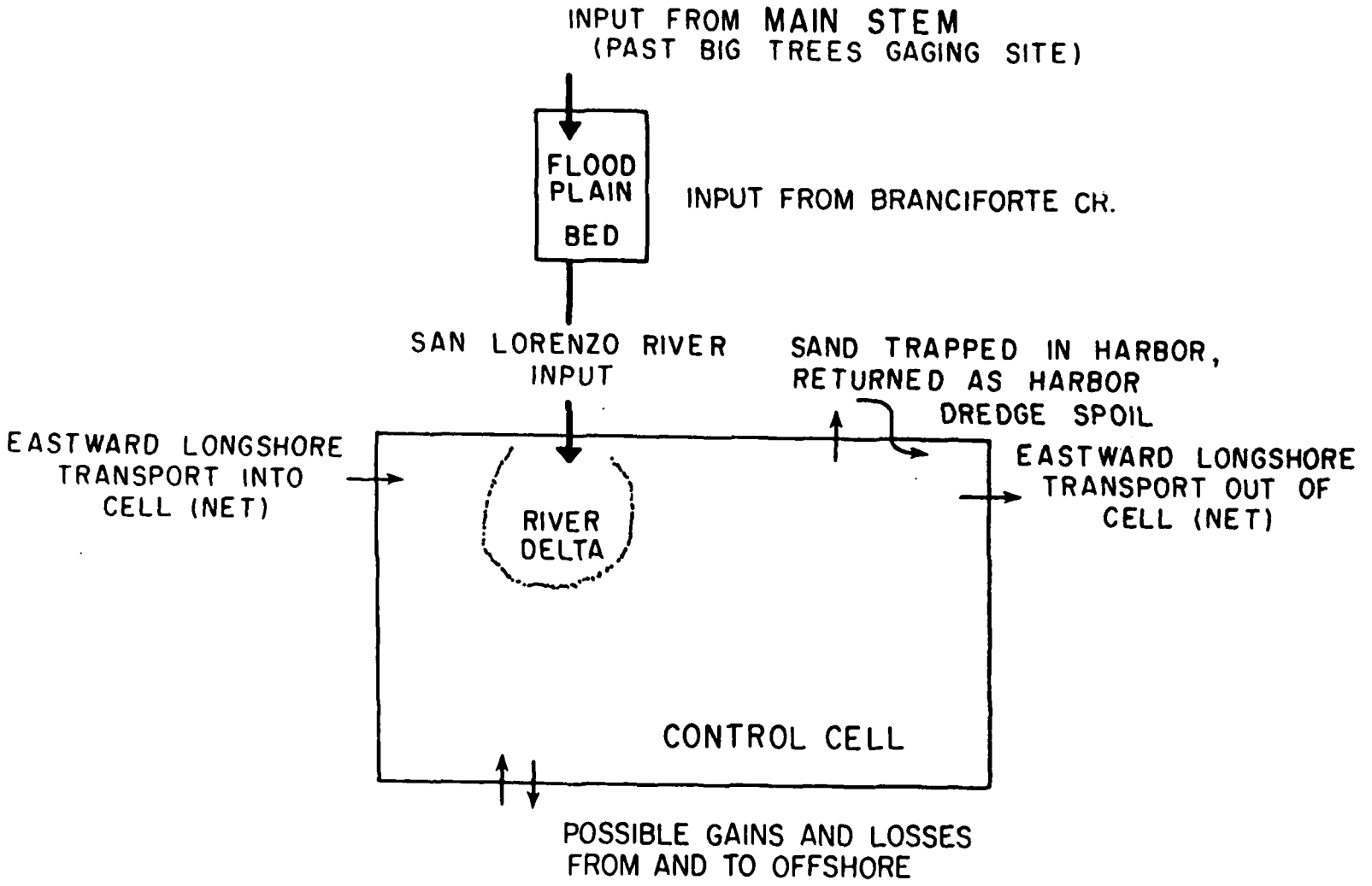
INPUT FROM MAIN STEM
(PAST BIG TREES GAGING SITE)
FLOOD PLAIN
BED
INPUT FROM BRANCIFORTE CR.
SAN LORENZO RIVER INPUT
SAND TRAPPED IN HARBOR, RETURNED AS HARBOR DREDGE SPOIL
EASTWARD LONGSHORE TRANSPORT INTO CELL (NET)
RIVER DELTA
EASTWARD LONGSHORE TRANSPORT OUT OF CELL (NET)
CONTROL CELL
POSSIBLE GAINS AND LOSSES FROM AND TO OFFSHORE

3.2 Nearshore Topographic Surveys

The total sand volume and sand distribution within the control cell were monitored by repeat surveys of 9 rangelines that extended from the back-beach area offshore to about 8 m depth. The rangelines are located in Fig. 8. Survey methods were similar to those of Nordstrom and Inman (1975). These rangeline surveys were supplemented with surveys of the harbor entrance channel and with photographs. The topographic and bathymetric data obtained were worked up into several formats. Initially, beach profiles were plotted. Contour maps were then drawn for each survey; these were differenced to form isopach maps that showed sites of between-survey accretion or erosion. Volume changes per unit shore length were found by integrating elevation changes in the cross-shore direction from the isopach maps. Summing these changes in volume alongshore showed total volume changes within segments of the control cell, for example at the river mouth, and overall.

The uncertainty in measurements of bottom elevation is estimated as +/- 12 cm. Thus changes in bottom elevation between surveys are accurate to +/- 24 cm. The uncertainty in the total volume change per meter length of beach under a rangeline is about +/- 42 m^3. This figure should probably be doubled to account for errors induced by interpolating alongshore between rangelines. The uncertainty in estimates of total volume change, integrated along the 1825 m length of the control cell, then becomes +/- 150,000 m^3. Since the uncertainties in volume change estimates grow in proportion to the area of integration, the control cell shoreline length and offshore extent were delimited to ensure that the overall volume changes were significant.

Figure 8. Rangeline locations and the boundaries of the control volume in the harbor entrance.

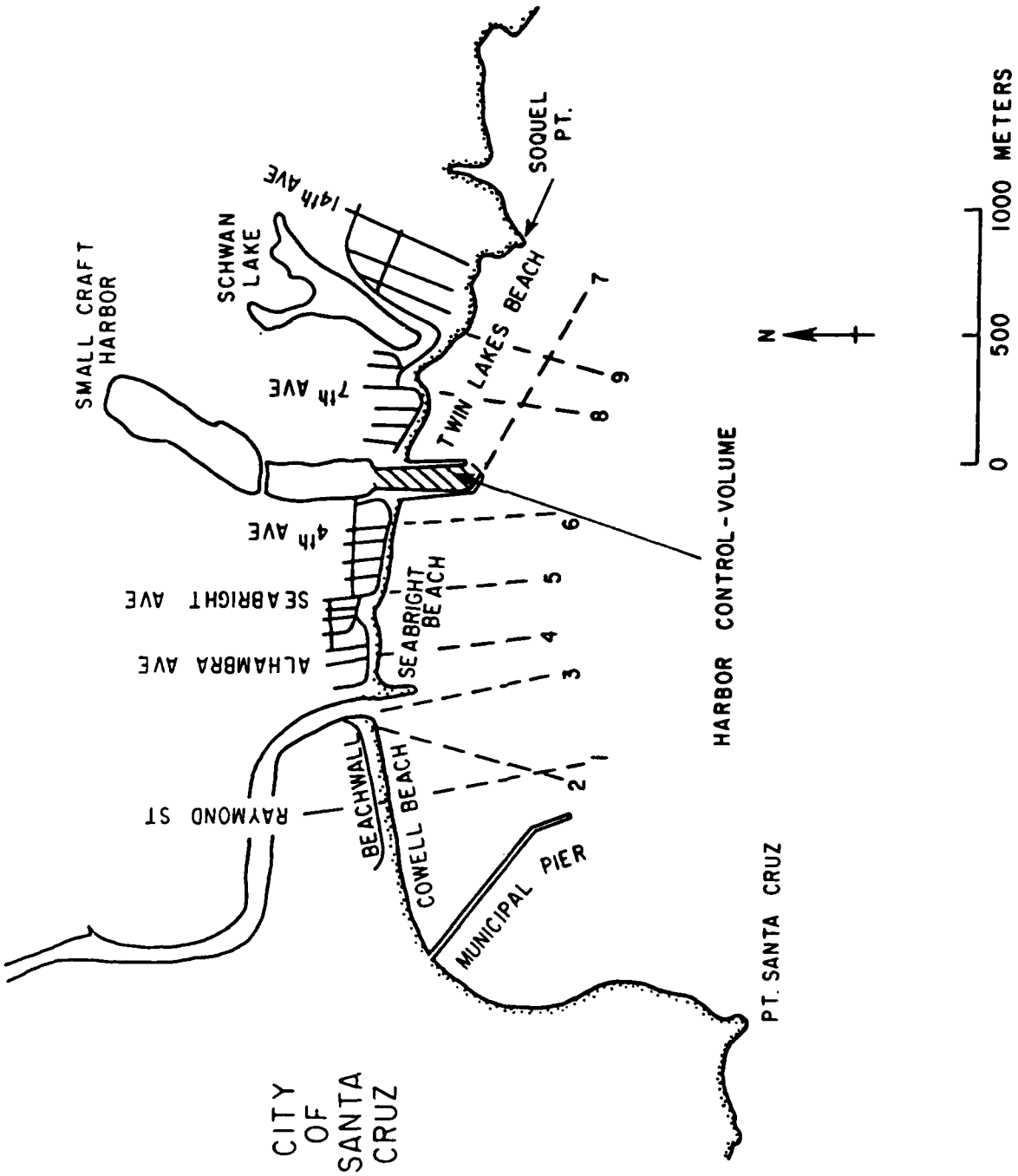
SMALL CRAFT HARBOR
SCHWAN LAKE
14th AVE
SOQUEL PT.
7th AVE
TWIN LAKES BEACH
7
8
9
4th AVE
6
SEABRIGHT AVE
5
ALHAMBRA AVE
SEABRIGHT BEACH
4
3
RAYMOND ST
BEACHWALL
COWELL BEACH
2
MUNICIPAL PIER
HARBOR CONTROL-VOLUME
PT. SANTA CRUZ
CITY OF SANTA CRUZ
N
0
500
1000 METERS

The surveys began on 28 January 1982, 24 days after the San Lorenzo River's record flood. The pre-flood topography at the river mouth was estimated, essentially, by assuming that the contours on the beaches to either side had continued straight across the river mouth. Surveys were repeated at approximately 2-month intervals until September 1983.

Appendix B details rangeline benchmark locations, field methods, analysis procedures, uncertainty estimates, and the method of estimating the river mouth topography before the January 1982 flood.

3.3 Harbor Sedimentation Surveys and Dredgings

The Santa Cruz harbor entrance channel is a partial trap to sediment by-passing the harbor jetties. Therefore, the volume of sediment trapped in the harbor must be accounted for in the sediment budget of the control cell. Also, the accumulation rate gives a lower limit to the eastward longshore transport past the western jetty.

The harbor mouth sedimentation was estimated from bathymetric surveys and dredging logs. The surveys were eade by the Santa Cruz Harbor Board who regularly monitor the configuration of the entrance channel. The Harbor Board's sounding charts were first contoured, then the areas associated with each contour were measured with a planimeter in order to determine volumes by the end-area method. The control volume boundaries for the computations are shown in Fig 8.

Generally, the uncertainty in the volume estimate was +/- 5000 m^3, based on comparison surveys made only a few days apart. Some surveys extended only part way up the entrance channel: the volume beyond there had to be interpolated from post and previous surveys. However, the

error arising from this interpolation was recovered in the next full survey.

The entrance channel was "phase-dredged" in the winter-spring of both 1982 and 1983. Dredged volumes derive directly from the operators' logs. Their accuracy is assumed reasonable.

3.4 River Supply of Littoral Sediment - from River Data

Quantifying the San Lorenzo River's supply of littoral sediment into the control cell involves determining the river's total sediment yield, and then estimating how much of it is likely to be transported as littoral drift in the local littoral cell. The latter requires size-distributions representative of the river's load and of the local littoral sediment, in order to determine a "littoral cut-off" size. All river sediment finer than this is expected to be swept out of the nearshore zone.

3.4.1 The "Littoral Cut-off" Grainsize

One way to obtain a representative size distribution of the littoral sediment is from the average of many samples collected systematically across the shore zone. However, there are easier, if more approximate, ways. One way relies on the fact that the bulk of the dynamic prism of sand under the beach profile is exchanged seasonally between the subaerial beach face (i.e. the berm) and an offshore bar. Therefore, summertime samples of the accreting beach face are representative of the dynamic prism volume as a whole (Inman, 1953). Another way is to determine the size distribution of the sediment moved

alongshore as littoral drift. This can be done by sampling littoral drift traps. The latter approaches were used in this study.

Size distributions for beach face samples collected during the summer surveys, for samples of sediment trapped in the harbor entrance channel, and for a sample of the harbor dredge spoil are shown in Fig. 9. All of these size distributions are very similar in terms of size range, approximately log-normal shape, good overall sorting, and a small well-sorted fine tail. The average of these is taken as the representative littoral sand size-distribution and is also plotted in Fig. 9, along with representative size distributions of suspended load and bedload from the San Lorenzo River. The river's bedload is similar to the beach sand while the river's suspended load is much finer and poorly sorted.

The "minimum significant size" on the littoral sand distribution is taken as the beginning size of the fine tail, which is 0.18 mm or 2.5 phi units. A statistical interpretation can be placed on this definition. Since, on average, 16% of the littoral samples are finer than this size, and the distribution is approximately log-normal, the significant size corresponds to one standard deviation finer than the mean. A more basic interpretation says that sediment finer than this size comprises an insignificant portion of the littoral material. The error induced in the littoral sediment yield estimate using this approach involves an underestimate of 16% at most. As shown in Fig. 9, essentially all (96%) of the river bedload, but only 21% of the suspended load, is coarser than 0.18 mm.

Figure 9. Size distributions of sand from the beach face, harbor bed, and harbor dredge spoil and of suspended load and bedload from the San Lorenzo river. The "minimum significant size" of littoral sand is taken as 0.18 mm. On average, 16% of the littoral sand is finer than 0.18 mm while 21% of the river's suspended load and 96% of the river's bedload are coarser than 0.18 mm.

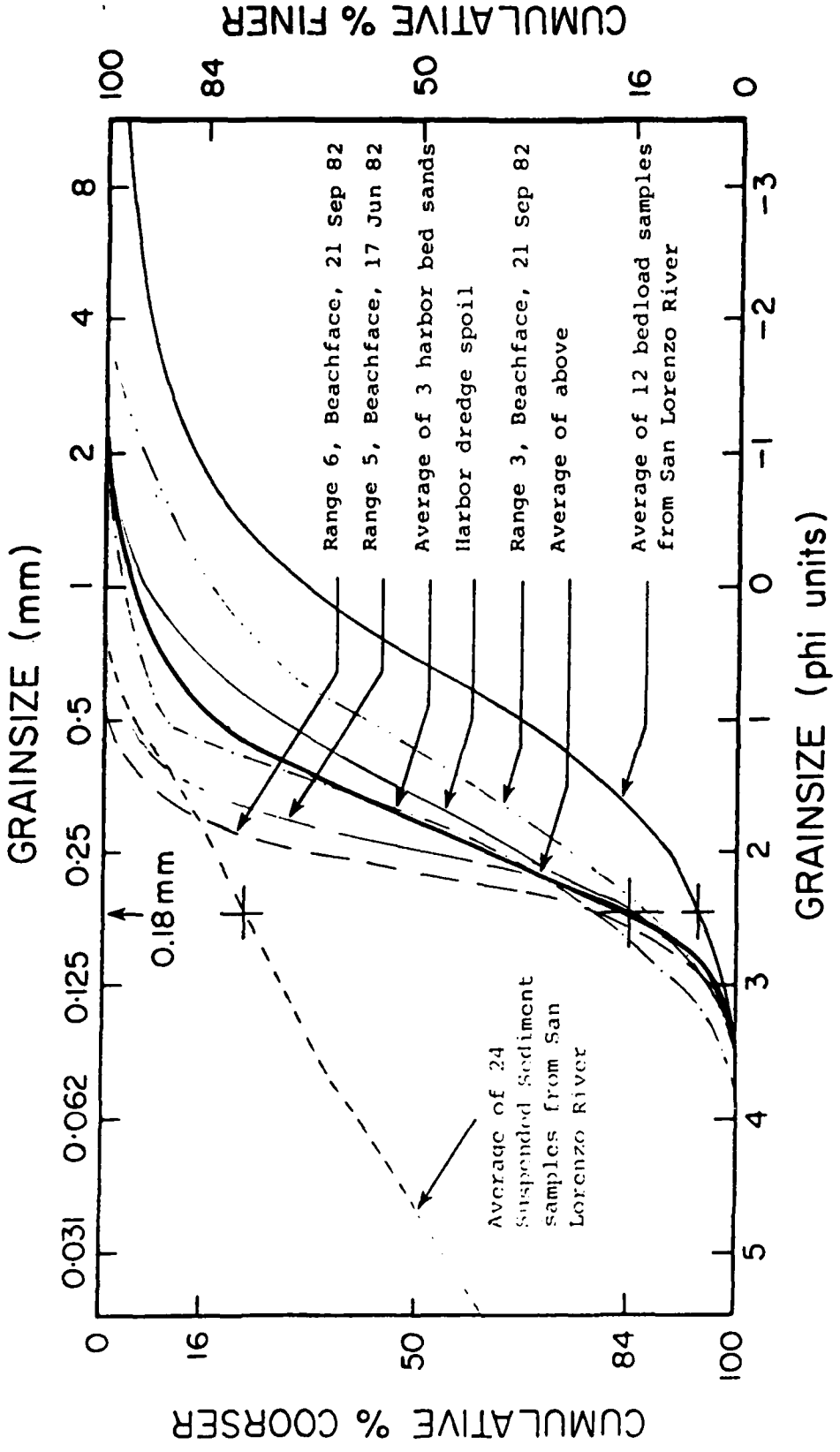
CUMULATIVE % FINER
100
84
50
16
0
GRAINSIZE (mm)
8
4
2
1
0·5
0·25
0·125
0·062
0·031
0.18 mm
Range 6, Beachface, 21 Sep 82
Range 5, Beachface, 17 Jun 82
Average of 3 harbor bed sands
Harbor dredge spoil
Range 3, Beachface, 21 Sep 82
Average of above
Average of 12 bedload samples from San Lorenzo River
Average of 24 suspended sediment samples from San Lorenzo River
GRAINSIZE (phi units)
-3
-2
-1
0
1
2
3
4
5
CUMULATIVE % COARSER

3.4.2 River Sediment Yield

The principal gage on the sediment yield of the San Lorenzo watershed is the USGS station at Big Trees, located approximately 11 km upstream of the mouth. Sediment sources downstream from there which contribute significantly to the yield at the mouth are the tributary Branciforte Creek and the bed of the San Lorenzo's floodplain channel.

San Lorenzo at Big Trees Gaging Site

The sediment yield of the San Lorenzo River past the Big Trees gaging site for the period January through September 1982 derives from the USGS Water Resources Division estimates of suspended load and bedload (Water Resources Division, 1984). Because of funding cuts, the USGS sediment record at Big Trees was terminated in October 1982. From then until September 1983, both suspended load and bedload yields were estimated using ratings of daily sediment load to daily mean water discharge, in combination with the record of daily mean flow.

The river's littoral sediment yield at Big Trees was taken as the sum of its bedload and 21% of its suspended load. On average, this littoral load turns out to be equivalent to 28% of the total suspended load.

Details of the methods for estimating sediment yield and of the particle size analyses are contained in Appendix C.

Branciforte Creek

Branciforte Creek, draining an area of 82 km^2, joins the San Lorenzo main stem about 1 km upstream from the river mouth. Since it is

ungaged, its sediment yield was scaled from that of the San Lorenzo at Big Trees in proportion to catchment area.

Floodplain

The scour/fill record of the San Lorenzo floodplain channel through the study period was estimated from four cross-sectional surveys done by the City of Santa Cruz. The surveys included fourteen cross sections located along the length of the floodplain between the Highway 1 bridge and the river mouth. Volume changes were calculated by the end-area method.

On average, 97% of the floodplain bed-material is coarser than 0.18 mm. Thus all sediment scoured from the floodplain channel is assumed to remain in the shore zone. Particle size plots and further details of the floodplain yield estimate are included in Appendix C.

3.5 LONGSHORE TRANSPORT OF SAND

Three approaches were used to estimate the longshore transport rate of sand. A lower bound on the eastward transport past the western harbor jetty could be found from the sedimentation rates in the harbor entrance channel. The transport potential at the east end of Seabright Beach, beside the harbor, was computed from wave data collected by a nearby slope array. This wave data was also used to estimate the transport potential and divergence along the entire shoreline of the control cell. Unfortunately, the transport computations were possible only until late January 1983, when the slope array malfunctioned and lost its ability to resolve wave direction.

3.5.1 Wave Measurements

A continuously operating directional wave measurement slope-array is located at a depth of 7 m approximately 100 m west of the harbor jetties. Details of the system are given by Seymour et al (1980). The wave data is collected and analysed by the Nearshore Research Group at Scripps Institution of Oceanography under contract with the U.S. Army Corps of Engineers. It is published monthly in reports of the Coastal Data Information Program (CDIP). These reports list 6-hourly samplings of the energy and directional spectra, plus the total energy, total longshore component of radiation stress (S_{xy}), significant height, and significant angle. The total energy, summed over all frequencies, is reported as the water surface variance. The significant height is 4 times the water surface standard deviation. The significant angle is the incident angle that would produce the same total S_{xy} if all of the wave energy arrived from one direction; it approximately equals the energy-weighted direction averaged across all period bands. The determination of S_{xy} is based on the cross-spectral analysis method of Longuet-Higgins et al (1963), as described by Seymour and Higgins (1978).

The computed S_{xy} and also the directional spectra are sensitive to the assumed bottom contour orientations in the vicinity of the array. For this reason, all directional data published in the 1982 CDIP reports were rejected when it was discovered from the bathymetric surveys that the beach normal assumed in the CDIP computations, 25 degrees east of north, was incorrect by more than 10 degrees. This beach normal orientation had been determined from a survey in 1977. The

direction-dependent data were recalculated based on shore-normal trends of 15 degrees east of north for January-October 1982 and 13 degrees east of north from November on.

3.5.2 Longshore Transport Potential Near Wave Array

The recalculated CDIP wave data was used with the method of Seymour and Higgins (1978) to compute the potential for longshore transport shoreward of the array. Seymour and Higgins' formula relates the transport rate in the surfzone to S_{xy} and significant wave height at the array. This involves two assumptions: the shoreline contours are straight and parallel so that S_{xy} is conserved between the array and the breakpoint (after Longuet-Higgins, 1970); and the depth at breaking, h_b, can be approximated by 1.65 times H_s at the array. The relation used in this study is

$$Q_l = 980\ S_{xy}\ (H_s)^{0.5} \qquad (2)$$

where Q_l is the "at rest" volume transport rate of sand in m^3/yr, S_{xy} and H_s at the array are expressed in their CDIP reported units of cm^2 and cm respectively, and the proportionality coefficient, 980, has units $m^3/yr.cm^{2.5}$. Equation (2) differs from Seymour and Higgins' relation only in the value of the proportionality coefficient, as discussed in Appendix D.

Equation (2) was used to compute the longshore transport rate every 6 hours through the 13-month record period. The results are considered accurate to within a factor of 2 at best. This uncertainty is due to the assumptions and approximations in the transport relation's

derivation, the oversimplicity of the transport model, and uncertainties in the input wave data. These points are discussed in detail in Appendix D.

3.5.3 Longshore Variation in Longshore-transport

A computer-run back-refraction procedure was employed to predict, from the wave data recorded at the array, the variation in wave conditions and hence the longshore transport rate and divergence along the shoreline of the control cell. The main objectives of this were to confirm and resolve ambiguities in the longshore sand migrations deduced from the bathymetric surveys. While the magnitudes of the transport rates and divergences were not expected to be particularly accurate, it was hoped that the time-averaged trends and directions would be valid and useful.

Each 6-hourly spectral record at the wave array was collapsed to a representative wave and back-refracted offshore, using a numerical refraction technique based on that of Dobson (1967), until deep-water conditions were encountered. A large number of parallel deep-water wave rays were then refracted shoreward until a breaking criterion was passed. The wave parameters at the break point were used to compute the longshore transport rate from an equivalent version of equation (1). Since the arrival points of the returned rays varied for each record, the transport rates at fixed locations spaced evenly alongshore were interpolated. The longshore rate-of-change in transport rate between the fixed stations determined the transport divergence.

Subroutines were employed to ensure that there was a sufficient concentration of rays returned to the delta area and to remove unnatural caustics induced by the numerical refraction procedure. The digitized nearshore bathymetry was changed periodically in accordance with the surveyed changes. Also, each refraction run was repeated across a hypothetical "no-delta" bathymetry in order to assess the impact of the river delta on the "background" sand transport past the river mouth.

Details of the wave data, bathymetry, refraction procedure, longshore transport computation, and the inherent assumptions, approximations, and uncertainties are given in Appendix E, along with some example results.

4. RESULTS AND DISCUSSION

The principal result of the study concerns the movement of sand by nearshore processes at and away from the river mouth. Primarily, the sand migrations are traced from the nearshore topographic surveys by looking at differential volume changes across the control cell through the study period. However, before such bulk sand movements can be interpreted unambiguously, the river sand supply-rate and the direction and magnitude of the longshore transport potential must be considered. Therefore, in this section, the first results to be presented and discussed concern the river yield and the longshore transport potential. Then, sequential morphologic changes, sand volume shifts, and overall changes in the control cell volume are described and summarised. The effects of the river delta on the local beaches and on the "background" longshore transport regime are considered. Finally, a conceptual model is synthesized for the longshore-migration mechanism of the river mouth deposit.

4.1 River Yield of Littoral Sediment

Two independent estimates of the littoral sediment yield from the San Lorenzo River are compared in Fig. 10. The first estimate, based on the river-measured data and shown in Table II, combines the littoral sediment yields of the Big Trees gaging station, Branciforte Creek, and the floodplain channel. The second estimate is based on the surveyed volume increases off the river mouth and within the control cell.

Each estimate is subject to uncertainties. The river data is subject to the assumptions made regarding the littoral cut-off

Figure 10. Sediment volume gains within longshore segments of the control cell compared with the littoral sediment yield of the San Lorenzo River. The volume changes and river yield are cumulative since 1 January 1982.

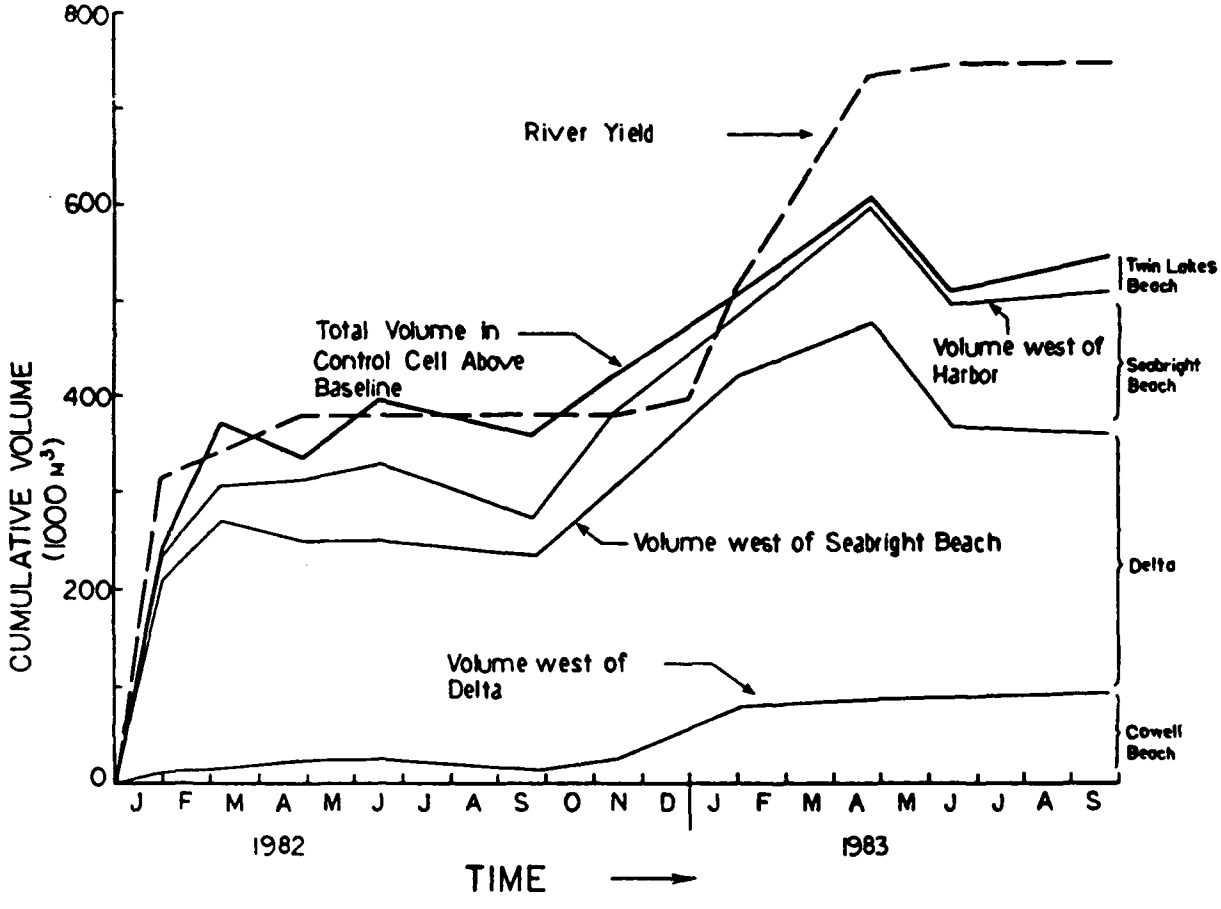
800
600
400
200
0
CUMULATIVE VOLUME (1000 M³)
River Yield
Total Volume in Control Cell Above Baseline
Volume west of Harbor
Volume west of Seabright Beach
Volume west of Delta
Twin Lakes Beach
Seabright Beach
Delta
Cowell Beach
J F M A M J J A S O N D J F M A M J J A S
1982
1983
TIME

Table II. San Lorenzo sediment yield at mouth

Date	Cumulative Suspended Load● (1000 Tonnes)	Cumulative Littoral Susp. Load + (1000 Tonnes)	Cumulative Bedload● (1000 Tonnes)	Total Littoral Load x 1.23Δ (1000 Tonnes)	Littoral Load in Period (1000 Tonnes)	Flood Plain Scour in Period (1000 Tonnes)	Littoral Load in Period (1000 Tonnes)	Littoral Load in Period (1000 m^3)*	Cumulative Littoral Load (1000 m^3)
1 Jan 82	0	0	0	0					0
30 Jan 82	960	202	32	287	287	217	504	315	315
7 Mar 82	1156	243	50	360	73	-30	43	27	342
26 Apr 82	1491	313	96	503	143	-80	63	39	381
16 Jun 82	1492	313	99	507	4	-5	-1	-1	380
21 Sept 82	1492	313	99	507	0	0	0	0	380
12 Nov 82	1492	313	99	508	0	0	0	0	380
1 Jan 83	1598	336	117	550	42	-13	29	18	398
31 Jan 83	2277	478	140	761	211	-20	191	119	517
25 Apr 83	3424	719	237	1176	415	-70	345	216	733
14 Jun 83	3488	732	252	1211	35	-10	25	16	749
23 Sept 83	3488	733	253	1212	1	0	1	1	750

+ Based on a littoral load "cut-off" size = 0.18 mm

* Littoral load bulk density assumed equal to 1.6 Tonnes/m^3

● Bedload and suspended load determined as detailed in Appendix C

Δ 1.23 equals ratio total drainage agea/drainage area upstream of Big Trees

Ratios: $\frac{\text{Littoral Load}}{\text{Suspended Load}} = 0.28$

$\frac{\text{Littoral Load}}{\text{Total Load}} = 0.26$

grainsize, representative size distribution of river sediment, sediment rating curves, bedload prediction formulae, and floodplain scour history. The river mouth accretion rates are made uncertain by survey inaccuracies, by the boundaries assumed for the deposition area, and by sand gains and losses due to longshore transport. As discussed previously, the uncertainty in volume change between surveys is about 80 m^3 per m shore length while the estimate of pre-flood bathymetry off the river mouth introduces a total error of about 50,000 m^3 when it is used as the baseline.

As seen in Fig 10, through 1982, the sediment yield predicted by the river data exceeds by about 30% the accretion in a 300 m wide sub-cell surrounding the river mouth. However, it agrees well with the total volume gain within the control cell. This is consistent with a relatively small fraction of the river sand being dispersed eastwards away from the river mouth during 1982. Through November-December 1982, a period of low river sediment yield, the cumulative river yield since January dipped below the total cell accretion. This can be traced to accretion west of the river mouth on Cowell Beach, caused by the delta's ponding of littoral drift from the west.

Overall for 1982, the agreement between the two estimates of river littoral sediment supply is good, and justifies the assumptions and approaches used. The supply for the year can be placed between a conservative estimate of 260,000 m^3, the net accretion off the river mouth, and 410,000 m^3, the net accretion off and east of the river mouth and also the yield predicted from the river data. The absolute minimum

yield for the January '82 flood must be 144,000 m^3, the volume scoured from the floodplain channel.

Through 1983, the yield predicted by the river data exceeds even the total cell accretion by a factor of 2. There are two probable reasons for this: a net loss of sediment from the control cell due to transport alongshore and perhaps offshore, and a gross overestimate of the yield predicted from the river data. Fig. 10 clearly shows a net loss due to eastward transport after April 1983. The sand volume lost from off the river mouth during this period does not reappear as accretion on the beaches to the east or in the harbor trap.

The high river yields predicted for January-April 1983 may be due to inaccuracies in the rating technique employed. As detailed in Appendix C, the suspended sediment yields for the 1983 water-year were based on a daily rating curve prepared from 1982 data. It is unlikely that the same rating applied for both seasons. One would expect the 1983 flows to contain less sediment than the 1982 flows due to the "flushing effect" of the 1982 flood. This flood "shocked" the watershed - it was a 30-year river event born of a 100-year rainfall, and it arrived after a period of relative drought. A large amount of sediment was stored in the channel and was available for transport. Conversely, the 1983 winter rain fell on a watershed that was essentially saturated and flushed of sediment.

A conservative estimate of the river yield for the period January-September 1983, based on the accretion at and east of the river mouth, is 160,000 m^3. The actual yield is probably somewhere between this value and the 320,000 m^3 estimated from the river data.

It is interesting how the "bedload" yield of the San Lorenzo at Big Trees over the study period almost exactly equalled the volume that accreted in the floodplain channel after the 3 January 1982 flood (Fig. 11). It appears, superficially at least, that none of the bedload passing the Big Trees site during and after this flood reached the ocean. Rather, it filled the large flood-scoured hole in the floodplain. By May 1983, the scour-hole had been filled and the river bed returned to its pre-January 1982 condition. Support for this conclusion is found in the similar size distributions of Big Trees bedload and floodplain bed-material (Fig. 12). It is likely that the flood flows of the 1982-83 winter scoured the floodplain channel to some extent. However, any scour-holes must have been refilled quickly.

Compared to the average annual sediment yield of the San Lorenzo River, the yields of 1982 and 1983 were exceptionally high. This is in terms of both total sediment yield and contribution to the littoral budget. Fig. 1c shows estimates of annual suspended load at Big Trees gaging station since the sediment record began in 1972. Estimates for all years except 1983 are derived from the USGS, Water Resources Division, annual data reports. The 1983 yield comes from this study and, as previously discussed, may be overestimated by up to 50%. Assuming that the littoral load is equivalent to 28% of the suspended load, some interesting figures emerge. Approximately 70% of the load totalled over the 11 year record period was delivered in 1982-83. The littoral load averaged only 28,000 m^3/yr up to 1981, 78,000 m^3/yr up to 1983, and 300,000 m^3/yr for 1982-83 alone. The 1982-83 average yield is 10 times the best estimate of the long-term average yield which is based on Jones-Tillson's (1979) flow-duration statistics for 32 years of flow

Figure 11. Bed-material volume changes in the San Lorenzo River floodplain channel compared with the river's bedload yield at the Big Trees gaging site. Volume changes and bedload are cumulative since 1 January 1982.

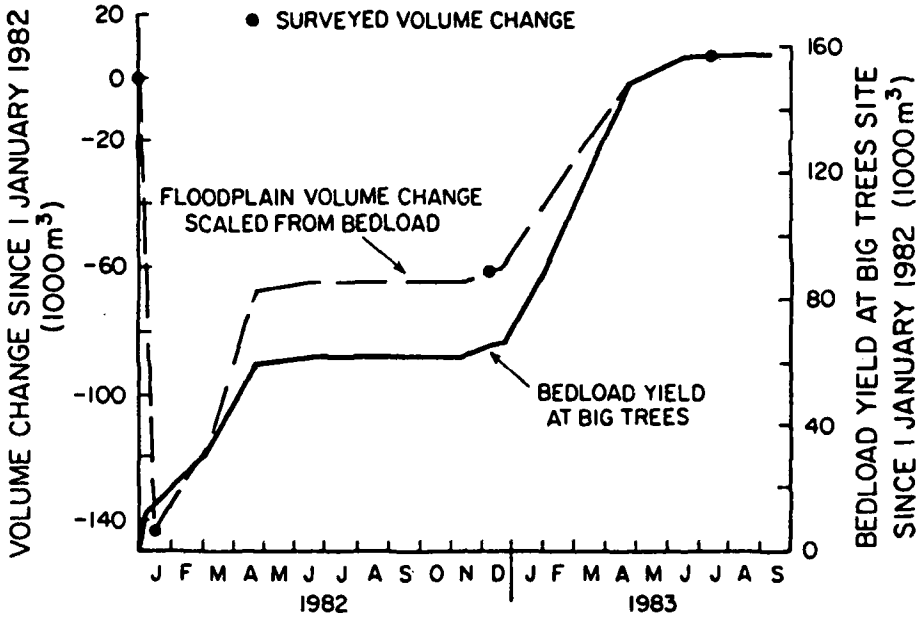
SURVEYED VOLUME CHANGE
FLOODPLAIN VOLUME CHANGE SCALED FROM BEDLOAD
BEDLOAD YIELD AT BIG TREES
VOLUME CHANGE SINCE 1 JANUARY 1982 (1000 m³)
BEDLOAD YIELD AT BIG TREES SITE SINCE 1 JANUARY 1982 (1000 m³)
20
0
-20
-60
-100
-140
160
120
80
40
0
J F M A M J J A S O N D J F M A M J J A S
1982
1983

Figure 12. Size distributions of bed-material from the San Lorenzo River floodplain channel and of bedload at the Big Trees gaging site.

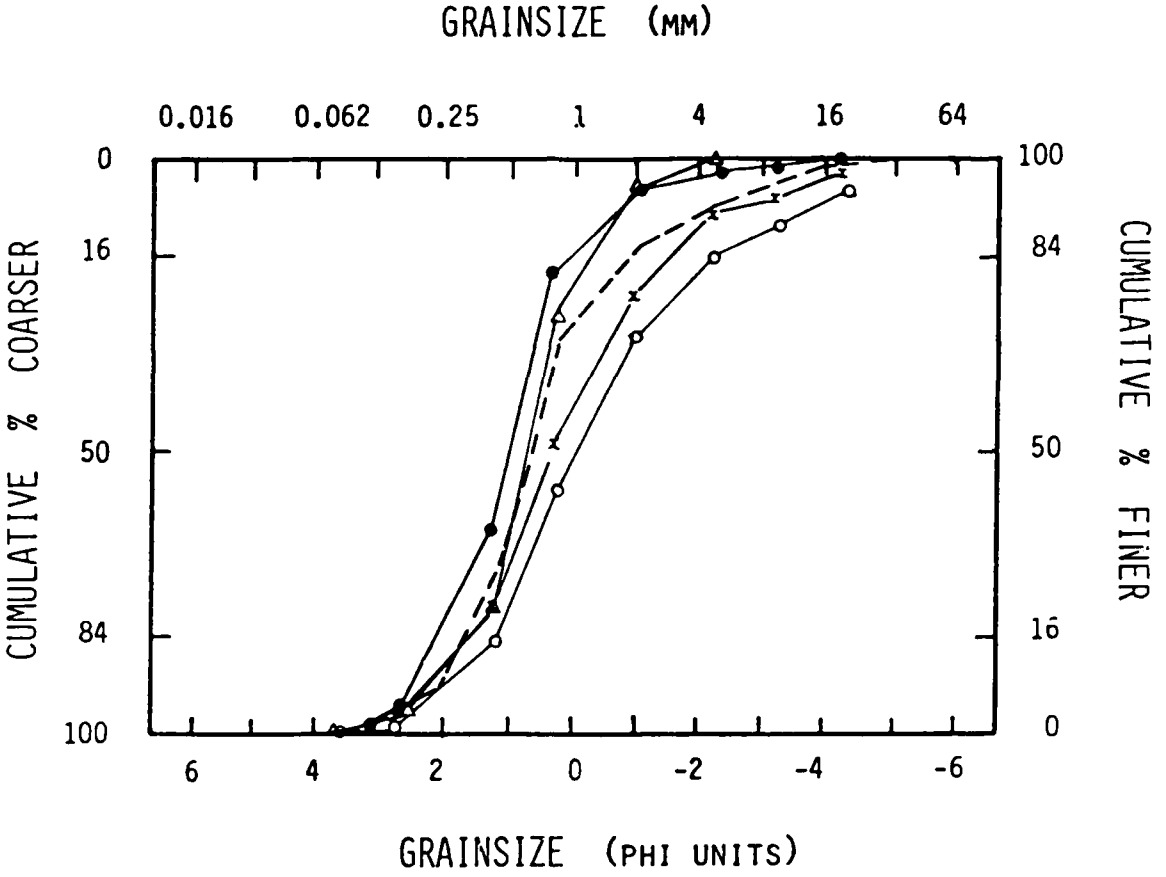

—●— San Lorenzo River bed-material, between Water St. * & Highway 1

—△— " " " , Pedestrian Bridge *

—x— " " " , Laurel St. Bridge *

—○— " " " , SPPR Bridge *

- - - - San Lorenzo River bedload, average of 12 samples + collected with Helley-Smith bedload sampler at Big Trees gaging site

* Reported by Jones-Tillson & Associates (1979)

\+ Reported by USGS, Water Resources Division, annual data reports

records, and is 1-2 times the various estimates of mean annual longshore transport potential past the Santa Cruz beaches. These figures highlight the intermittent nature of the littoral sand delivery and the ability of the major floods to overwhelm the longshore transport potential.

4.2 Longshore Transport

The cumulative longshore transport past the east end of Seabright Beach, predicted by equation (2) and by the records of sediment storage in the harbor entrance channel, is shown in Fig. 13. The harbor entrance is an imperfect trap to sand moving around the breakwater from Seabright Beach. Therefore, the harbor sedimentation and dredgings indicate only a lower limit to the easterly transport. The fact that the dredged volumes exceed the surveyed changes suggests that sand entered the harbor as dredging proceeded.

The variations in longshore transport rate along the length of the control cell, totalled monthly and between survey dates and based on the back-refraction analysis, are plotted in Fig. 14. Also shown on this figure, for comparison, are: the longshore transport just west of the harbor predicted by equation (2); the accretion in the harbor entrance; and the "background" transport near the river mouth obtained from refracting wave rays over an assumed "no-delta" nearshore bathymetry. Fig. 15 shows the longshore variation in transport divergence between survey dates. Negative transport divergence, at sites where the transport rate decreases in the transport direction, implies accretion. Positive divergence implies erosion. For comparison, the surveyed accretions and erosions are also plotted in Fig. 15.

The time-cumulative net longshore transport and transport divergence for the period January-November 1982 are plotted in Fig. 16. Again, the "background" longshore transport, surveyed accretion and erosion, longshore transport west of the harbor predicted by equation (2), and harbor accretion are plotted for comparison.

Figure 13. Record of sediment storage in the entrance channel to the Santa Cruz small craft harbor. The storage volumes are with respect to a datum plane at -9.14 m MLLW. Also shown are the sand volumes dredged from the harbor entrance each spring and the cumulative longshore transport past the harbor's western breakwater predicted by equation (2).

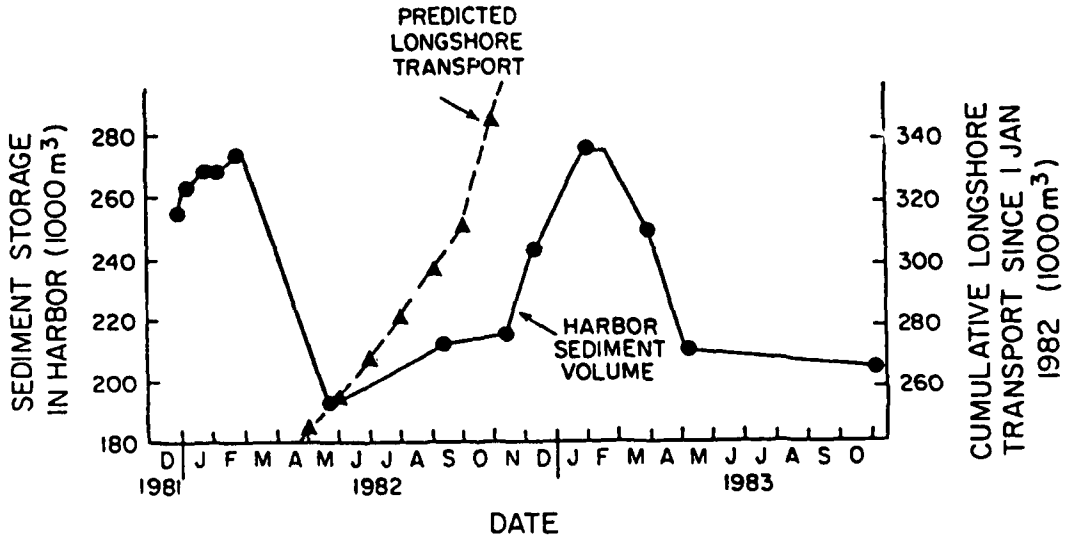

Spring 1982:

Vol dredged = 105,000 m^3
Surveyed loss = 81,000 m^3

Trapped during dredging = 24,000 m^3

Spring 1983:

Vol dredged = 118,000 m^3
Surveyed loss = 65,000 m^3

Trapped during dredging = 53,000 m^3

Figure 14. Longshore variation in longshore-transport potential predicted by the back-refraction analysis for the periods between surveys. The solid-line plots show the results when waves were refracted over the actual surveyed bathymetry. The dashed-line plots show the results when waves were refracted over a fictitious bathymetry wherein there was no delta at the river mouth. The longshore transport shoreward of the wave array predicted by the Seymour-Higgins method and the concurrent accretion in the harbor are shown also. Easterly transport is positive. Four littoral sub-cells are identified: each sub-cell is a closed system of longshore sediment movement.

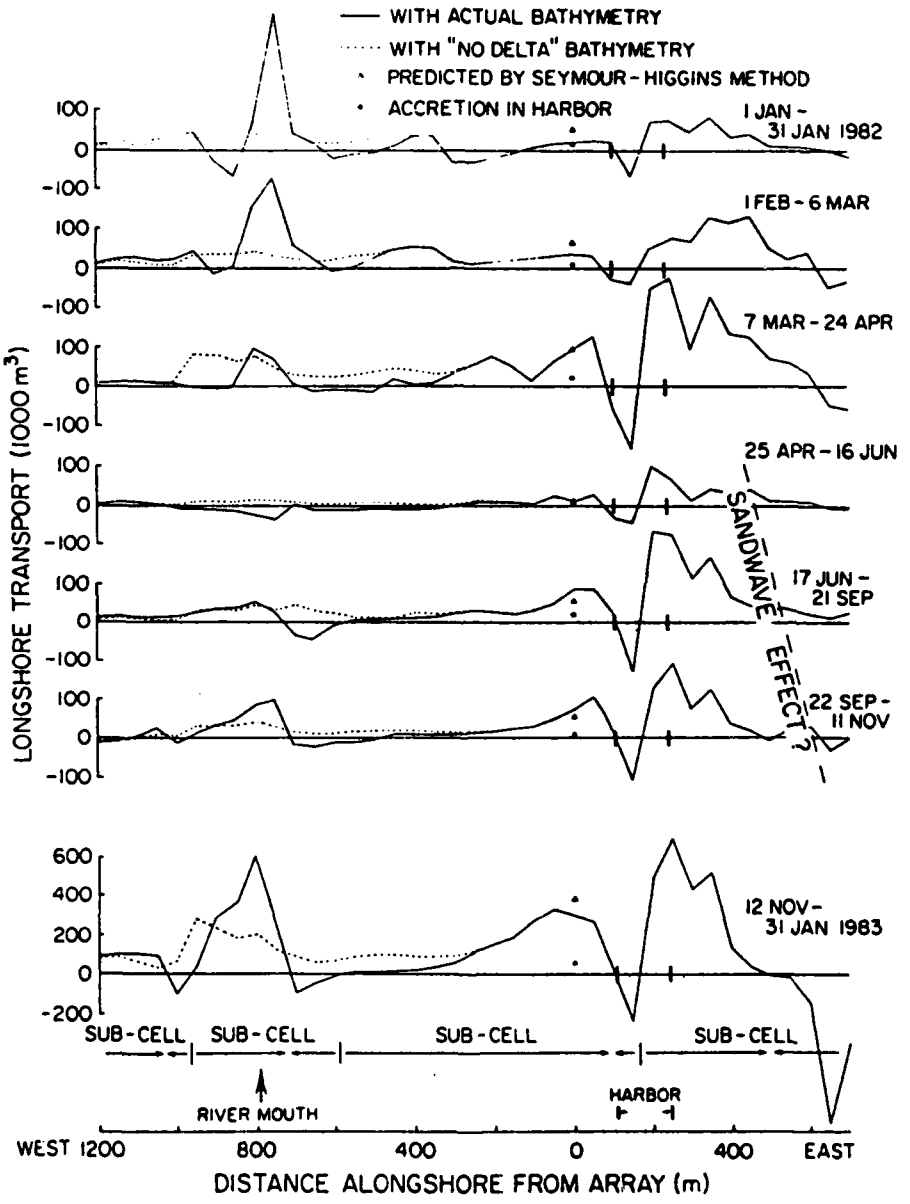
WITH ACTUAL BATHYMETRY
WITH "NO DELTA" BATHYMETRY
PREDICTED BY SEYMOUR-HIGGINS METHOD
ACCRETION IN HARBOR
1 JAN - 31 JAN 1982
1 FEB - 6 MAR
7 MAR - 24 APR
25 APR - 16 JUN
17 JUN - 21 SEP
22 SEP - 11 NOV
12 NOV - 31 JAN 1983
SANDWAVE EFFECT?
LONGSHORE TRANSPORT (1000 m³)
SUB-CELL
SUB-CELL
SUB-CELL
SUB-CELL
RIVER MOUTH
HARBOR
WEST 1200
800
400
0
400
EAST
DISTANCE ALONGSHORE FROM ARRAY (m)

Figure 15. Longshore variation in longshore-transport divergence predicted for the periods between surveys. Positive transport divergence induces erosion; negative divergence induces accretion. The computed divergence (solid-line plots) is compared with the surveyed accretion and erosion (dashed-line plots). To improve the comparison, external sand inputs have been subtracted from the surveyed volume changes; river sand and harbor dredge spoil inputs were assumed to be spread uniformly over 100 m of shoreline at the river mouth and on Twin Lakes Beach respectively.

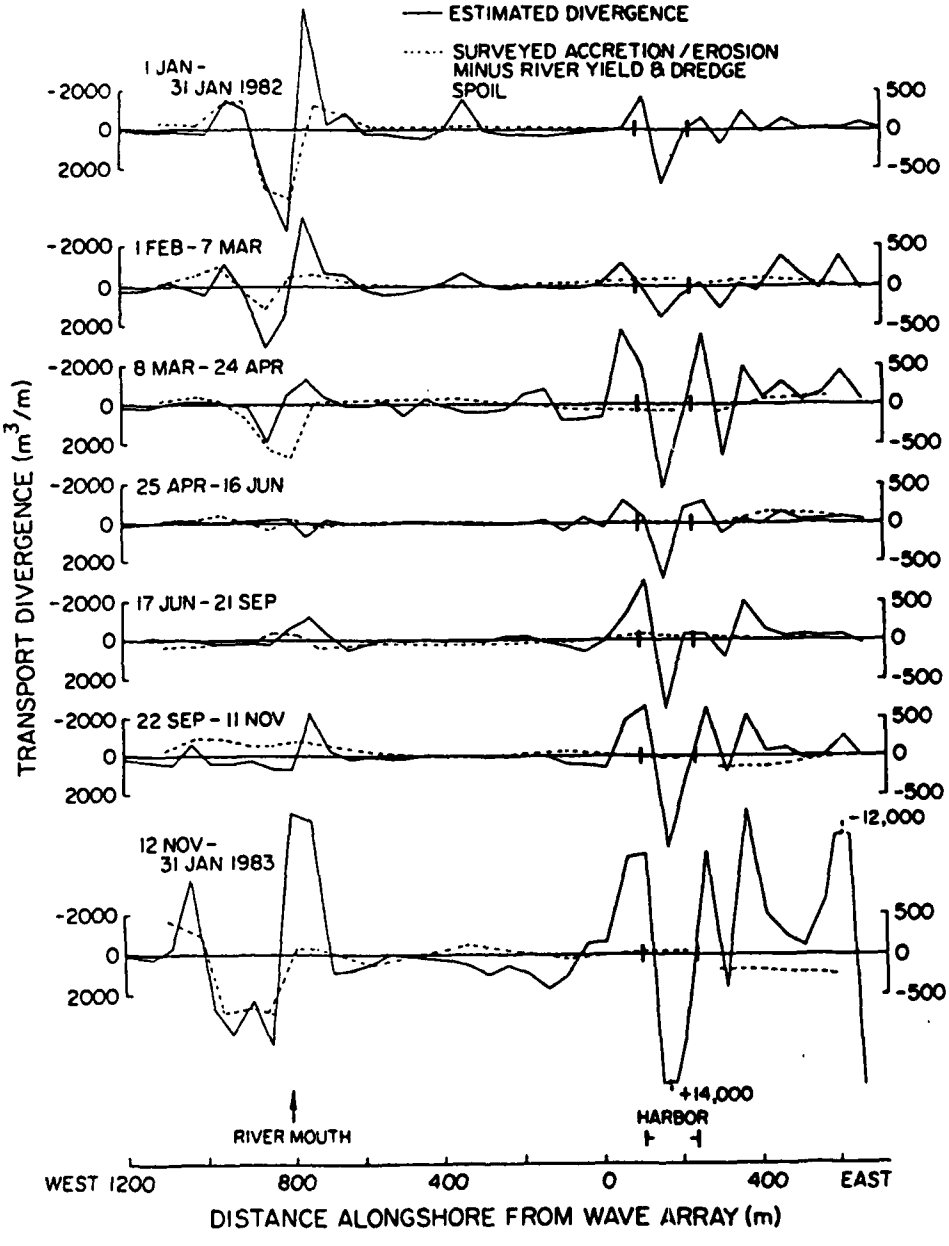
ESTIMATED DIVERGENCE
SURVEYED ACCRETION / EROSION MINUS RIVER YIELD & DREDGE SPOIL
1 JAN - 31 JAN 1982
1 FEB - 7 MAR
8 MAR - 24 APR
25 APR - 16 JUN
17 JUN - 21 SEP
22 SEP - 11 NOV
12 NOV - 31 JAN 1983
-2000
0
2000
500
0
-500
-12,000
+14,000
TRANSPORT DIVERGENCE (m³/m)
RIVER MOUTH
HARBOR
WEST 1200
800
400
0
400
EAST
DISTANCE ALONGSHORE FROM WAVE ARRAY (m)

Figure 16. Longshore variation in net longshore-transport and net transport-divergence for the period January-November 1982. As in Fig. 14, the transport predictions are compared for actual and "no delta" bathymetries. As in Fig. 15, the divergence predictions are compared with the observed accretion and erosion after making allowances for sand inputs from the river and from harbor dredging.

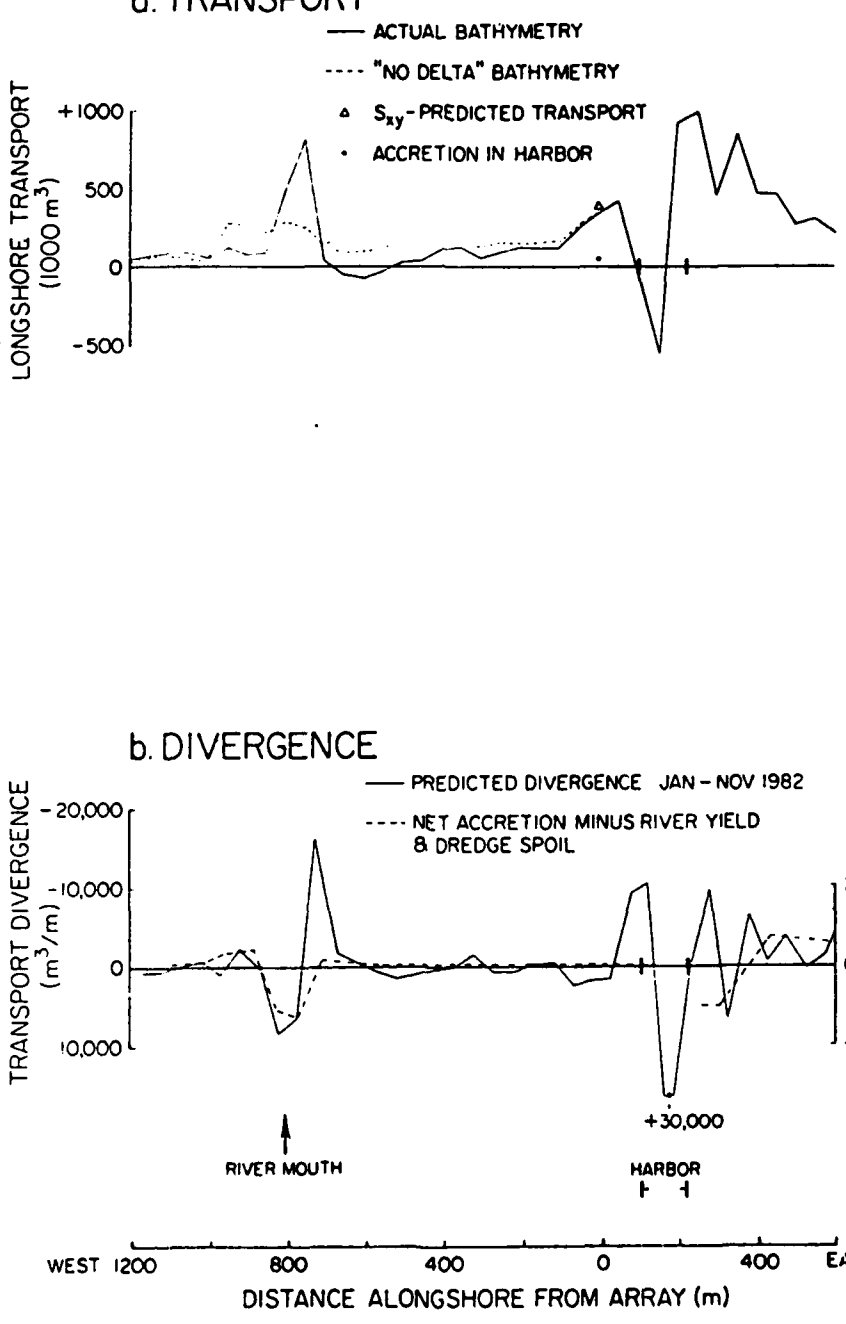
a. TRANSPORT
ACTUAL BATHYMETRY
"NO DELTA" BATHYMETRY
S_{xy} - PREDICTED TRANSPORT
ACCRETION IN HARBOR
LONGSHORE TRANSPORT (1000 m³)
+1000
500
0
-500
b. DIVERGENCE
PREDICTED DIVERGENCE JAN - NOV 1982
NET ACCRETION MINUS RIVER YIELD & DREDGE SPOIL
TRANSPORT DIVERGENCE (m³/m)
-20,000
-10,000
0
10,000
2500
0
-2500
SURVEYED ACCRETION (m³/m)
+30,000
RIVER MOUTH
HARBOR
WEST 1200
800
400
0
400
EAST
DISTANCE ALONGSHORE FROM ARRAY (m)

4.2.1 Longshore Transport Past the Harbor: Comparison of Estimates

The estimates of longshore transport potential opposite the slope-array computed from equation (2) and from the back-refraction procedure appear to be in reasonable agreement. While the monthly transport estimates sometimes differ by up to a factor of 2 between methods, the transport directions always agree and the net transport estimates for January-November 1982 agree to within 15%.

The estimate predicted by the Seymour-Higgins method is expected to be more accurate since it utilizes the wave-directional spectrum. In contrast, the back-refraction procedure uses an idealistic representative wave. However, as discussed previously, the Seymour-Higgins method is subject to a number of assumptions, a critical one requiring a planar bottom between the array and the breakpoint. The bathymetric surveys showed that this assumption was often violated. Another difference between the two methods is that they do not always predict the transport at the exact same point on the shoreline. The back-refraction procedure uses linear interpolation to compute the transport rate at a fixed station shoreward of the array. The transport at the fixed station is interpolated from the transports predicted at the arrival points of rays hitting the shore on either side of the fixed station. Conversely, the Seymour-Higgins method predicts the transport at a station fixed less precisely. The importance of this difference depends on the presence of strong longshore gradients in the wave field.

Both computation methods predict close to 400,000 m^3 of eastward transport for January-November 1982, and about as much again for the stormy period of December 1982 - January 1983. These figures are

somewhat higher than expected from the observed sand volume shifts in the control cell and from the earlier estimates of mean annual longshore transport potential. In comparison, the sediment volumes trapped in the harbor over these two periods were 83,000 m^3 and 42,000 m^3 respectively. Assuming the bulk of the sand trapped in the harbor came around the western jetty (after Walker et al, 1978; and Seymour et al, 1980), these latter figures indicate the minimum bound on the eastward transport from Seabright Beach.

There are several possible contributing explanations for the difference between these maximum and minimum estimates.

First, the estimates of transport potential may be reasonably accurate and a large proportion of the eastward-moving sand by-passed the harbor entrance. It is clear that sand was by-passing in January-March 1982 and December 1982 - January 1983 because a tip-shoal spanned the harbor entrance during these periods. Furthermore, although dredging removed the tip-shoal during the intervening months, it is likely that much of the sand transported east from Seabright Beach during this period never moved as far as the harbor entrance. Rather, it was deposited in a zone of negative transport divergence off the western jetty; most of it only moved on during the following period of winter storm waves. Evidence for this is found both in the bathymetric surveys and in the analysis of transport divergence, and will be discussed in the following sections.

Second, the value 0.77 used for the dimensionless coefficient K in the transport relations may be too high. As discussed in Appendix D, according to White and Inman's (1985) relation, K might be as low as 0.4

for high, spilling, storm waves arriving at Seabright Beach. Since the bulk of the longshore transport occurs in the high-wave events (as demonstrated by Seymour and Castel, 1985, and as apparent in equation (2) where transport is porportional to $H^{2.5}$), the time-averaged value of K might be closer to 0.4 than to the assumed 0.77.

Third, the longshore transport computations are influenced by uncertainties in the absolute orientation of the array (about +/- 2°) and in the relative orientation between the array and the beach normal or shoreline (at least +/- 2°). A sensitivity analysis showed that large differences in transport potential are induced through changing the wave incidence angle by only a few degrees. For example, a +/- 4° systematic uncertainty in the incidence angle resulted in a +/- 45% uncertainty in the net transport opposite the wave array over the record period. This analysis suggests that the computations of longshore transport shoreward of the array are accurate only to within a factor of 2.

4.2.2 Longshore Variation in Longshore-transport

Transport Direction

Predominantly eastward transport was predicted along the Santa Cruz beaches over the 13 month wave-record period. However, this general transport was interrupted by two promontories: the river delta and the harbor entrance. Because of refraction effects, short reaches on either side of these promontories generally experienced a net westward transport. When this occurred, the study shoreline was effectively divided into four isolated littoral sub-cells. These sub-cells are

apparent in Fig. 14. (A fifth sub-cell appeared briefly in January 1982 on Seabright Beach and is linked to a slight topographic bulge in the middle of the beach.) The surveyed sand volume changes, which will be discussed in detail in the next section, suggest sand leaked eastwards between neighboring sub-cells. However, this does not discredit the results of the refraction study given its uncertainties and the fact that longshore transport also occurs outside the surfzone, notably as a longshore component to the massive, seasonal, cross-shore sand migrations.

In contrast, the "background" longshore transport past the river mouth area, predicted by refracting the wave data over a hypothetical "no-delta" bathymetry, was everywhere eastward.

Divergence of Transport

Along the study shoreline, the predicted patterns of longshore-transport divergence generally compare qualitatively, but not always quantitatively, with the observed accretion and erosion when sediment inputs from the river and harbor dredgings are subtacted from the latter.

One explanation for the lack of quantitative agreement is the uncertainty in wave direction. A sensitivity analysis was done to test the effect of a +/- 2° systematic error in wave direction, such as might be induced by an error in the measured orientation of the array. The results showed that while in places alongshore the transport magnitude varied considerably as wave direction varied, the transport directions and divergence trends remained essentially the same.

AD-A154 352 SAND DISPERSION FROM AN EPHEMERAL RIVER DELTA ON THE WAVE-DOMINATED CENTRAL CALIFORNIA COAST(U) CALIFORNIA UNIV SANTA CRUZ D M HICKS MAR 85 N00014-80-C-0440 2/3

UNCLASSIFIED F/G 8/3 NL

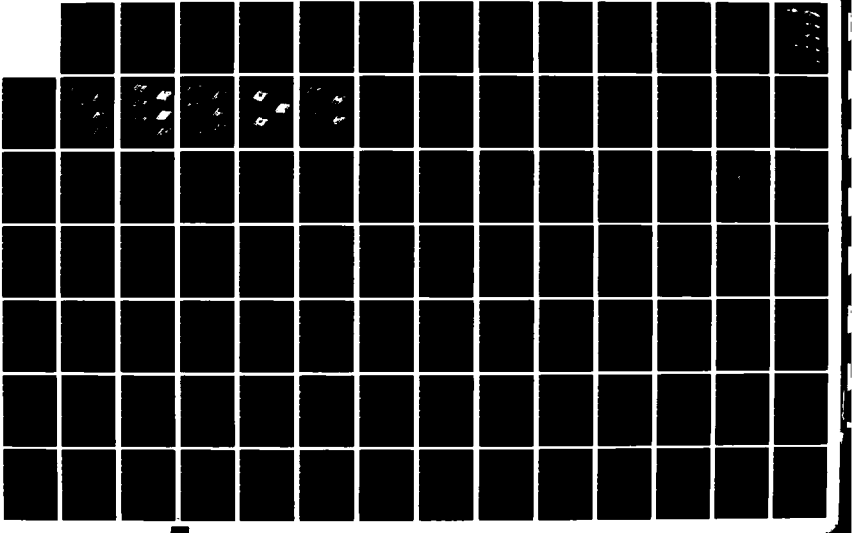

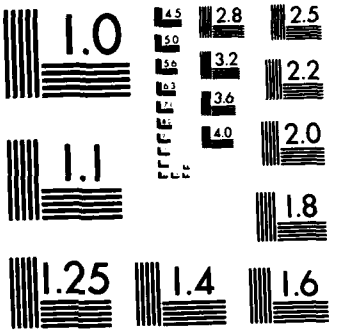

Another explanation concerns wave diffraction, wherein energy is transferred along the crest of a wave, from higher to lower points, as the wave travels. (Crest-wise variations in wave height can be induced by irregular bathymetry.) This process was ignored in the refraction model as there is no simple refraction model that incorporates diffraction as well. Yet, in reality, diffraction must dampen considerably the longshore energy gradients predicted by refraction procedures. If diffraction could be modelled, it would undoubtedly remove much of the "high frequency noise" seen on the divergence plots but not seen in the prototype.

Other uncertainties in the analysis are discussed below, in conjunction with the results predicted for individual segments of the control cell.

Around the river mouth, accretion was predicted on the delta's flanks and erosion was predicted at its apex. Qualitatively, this pattern agreed with the observed accretion and erosion when sediment inputs from the river were subtracted, as shown in Fig. 15. Quantitatively, the predicted volume changes at the river mouth averaged about four times those observed. There are several factors contributing to this discrepancy. These include: the transport formula and the assumed coefficient, K; the method of refracting an ideal representative wave and not a spectrum; the inaccuracy in refracting wave rays across the steep bottom slopes of the delta margins; uncertainties in the bathymetry and the assumption that it remained constant over 1-2 month periods; and uncertainties in the shoreline orientation. The "shoreline" orientation was assumed parallel to the -1 m MSL isobath

whose position was considered representative of the average breaker line. There must be great uncertainty with this assumption around the delta where the curvature of the isobaths increased shoreward and there was a strong gradient in wave height (and hence breaker depth and position) away from the apex. As shown in Fig. 14, the transport divergence predicted around the river mouth was reduced considerably when "no delta" bathymetry was substituted for the real bathymetry.

Along Seabright Beach, reasonable agreement was found between observed and predicted sand shifts except for those occurring between the September and November surveys in 1982 (Fig. 15). During this period, sand apparently "leaked" eastward from the eastern delta sub-cell, as discussed in the next section.

Around the harbor, the transport and divergence results cannot be considered too seriously for several reasons. First, wave diffraction, certainly an important effect near the jetties, was ignored in the refraction analysis. Second, even the refraction is not expected to be too accurate there. This is because the surface-fitting routine used to create the bathymetry grid for the refraction program creates inaccurate bathymetry off steeply sloping seawalls since it forces a smooth surface to pass across the shoreline. Third, the longshore transport model and formula, which relate to waves breaking on a beach, have dubious applicability there where all but the highest storm waves reflect off the jetties without breaking. Fourth, the open harbor entrance is not modelled. Fifth, during coastal storms, strong rip currents run past each jetty and are probably the locally-dominant littoral forcing

function. Nonetheless, the accretion predicted off the west jetty was often observed.

East of the harbor, along Twin Lakes Beach, the predicted and observed accretion/erosion patterns are qualitatively similar through to September 1982. From September on, erosion was observed despite predicted accretion (Fig. 15). This can be explained by the eastward transport potential exceeding the supply of sand. The divergence prediction model does not account for the sand trapped in the harbor entrance and the paucity of sand stored on this beach - it was quickly eroded bare during the 1983 winter storms.

In conclusion, while the absolute magnitudes of the potential longshore transport and divergence along the control cell shoreline are uncertain, the transport directions and divergence trends appear reasonably accurate. This is important because, at least through to January 1983, it removes the ambiguities in interpreting the direction of sand movement from the isopach plots of surveyed erosion and accretion. For example, while the March-April accretion/erosion patterns in Fig. 21c could support either net eastward or westward transport, the refraction analysis confirms eastward transport.

4.3 Sand Movements, Morphology and Volume Changes

Sand movements, morphologic features, and volume gains and losses within the control cell are interpreted from the results of the bathymetric surveys. These results are presented in several formats, each of which highlights certain features but also has inherent uncertainties and limitations.

The beach profiles shown in Figs 17a-f highlight cross-shore sand movements. The profiles selected are of Rangelines 1, 3, 5, and 8, as located in Fig. 8. The two-dimensional beach profiles most accurately portray the survey results since there is no longshore interpolation involved in bottom elevation fixes. However, their interpretation is made ambiguous by any longshore sand movements or external sand inputs.

The bathymetric (or topographic) maps and perspective block diagrams in Figs 18 and 19 show the three-dimensional detail of evolving morphologic features at the river mouth. Their uncertainty, and that of all subsequent plots mentioned below, lies in interpolating the bathymetry between survey lines. Topographic features in the whole study cell at each survey time and the elevation changes between surveys are shown on block diagrams in Fig. 20.

The isopach maps, Figs 21a-j, also show changes in bottom elevation between repeated surveys. They are the best format for observing bulk sand movements since they allow differentiation of longshore and cross-shore components. However, the interpreted directions of sand movement may be ambiguous without supporting information on the direction of the forcing functions. Plots showing the total change in sand volume across the nearshore zone (per unit shore length) are included in Figs 21a-j. Volume changes are shown for the period between surveys and the period since the "pre-January 1982 baseline survey". These plots show best the longshore component of sand migrations.

The x-t plots in Figs 22-24 summarise the history of sand volume changes (per unit beach length) above a baseline surface; they are the best means of portraying the bulk longshore dispersion of sand. Fig.

22a shows contours of volume change per meter shoreline since the pre-January 1982 baseline for the entire study period. The volume change at each point alongshore represents the net volume change within a meter-wide strip across the control cell. Fig. 23 highlights the volume changes since the November 1982 survey. Fig. 24a contours the volume change on the "visible beach" only, i.e., as far seaward as the mean lower low water line. Fig 22b, a replot of Fig. 10, shows the total volume gain (above the pre-January 1982 baseline surface) within the control cell and within individual longshore segments of the control cell. It can be obtained by integrating the area under Fig. 22a at given times and over given lengths of shoreline. For comparison, the cumulative littoral sediment yield from the river is also plotted on Fig. 22b. Fig. 24b is similar to Fig. 22b except that the volume changes are for the "visible beach" only. Note that the lower plots in Figs 21a-j are actually cross-sections of Fig. 22a at the survey times. The block diagram equivalents of the x-t plots are shown in Fig. 25.

The essential results contained in these plots will be described and discussed in time sequence. Fig. 26 illustrates the nomenclature employed to descibe morphologic features of the nearshore zone. Fig. 27, showing x-t plots for several idealized situations, aids interpretation of the prototype x-t plots.

4.3.1 Sequential Changes in the Control Cell

In terms of dominant coastal processes and the resultant morphologic responses and sand movements, the study period naturally subdivides into five phases. These are: the January 1982 flood delta

Figure 17. Beach profiles at selected rangelines.

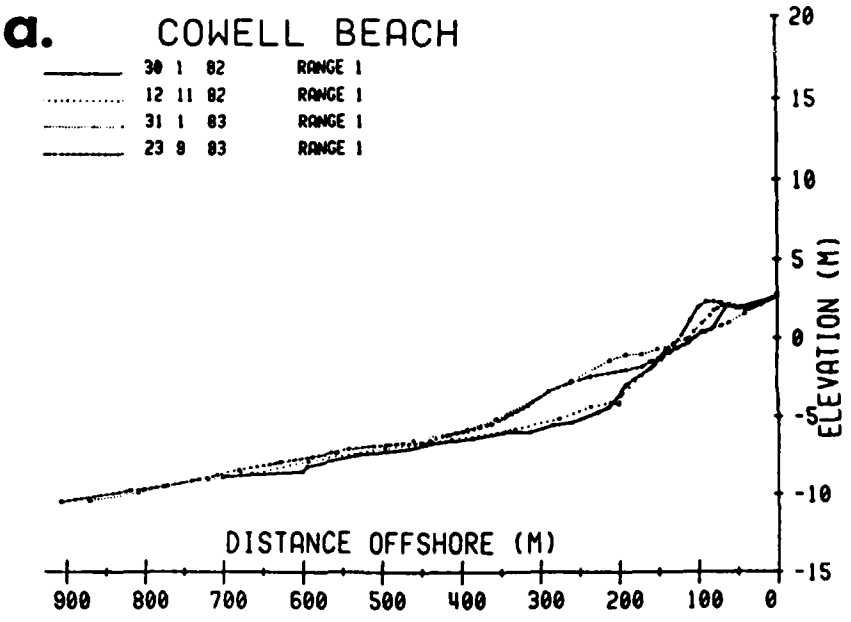
a.
COWELL BEACH
30 1 82 RANGE 1
12 11 82 RANGE 1
31 1 83 RANGE 1
23 9 83 RANGE 1
ELEVATION (M)
DISTANCE OFFSHORE (M)
20
15
10
5
0
-5
-10
-15
900
800
700
600
500
400
300
200
100
0

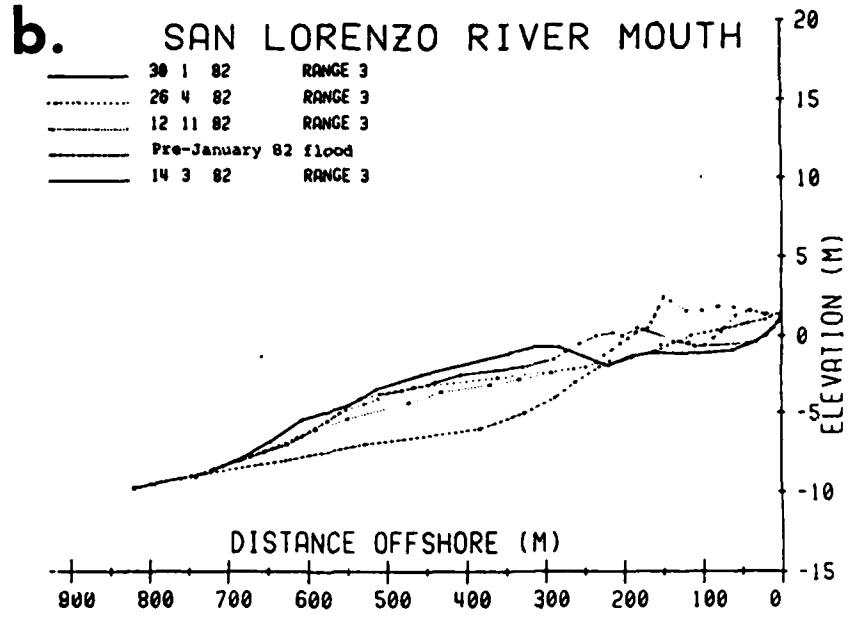
b.
SAN LORENZO RIVER MOUTH
30 1 82 RANGE 3
26 4 82 RANGE 3
12 11 82 RANGE 3
Pre-January 82 flood
14 3 82 RANGE 3
ELEVATION (M)
DISTANCE OFFSHORE (M)
20
15
10
5
0
-5
-10
-15
900
800
700
600
500
400
300
200
100
0

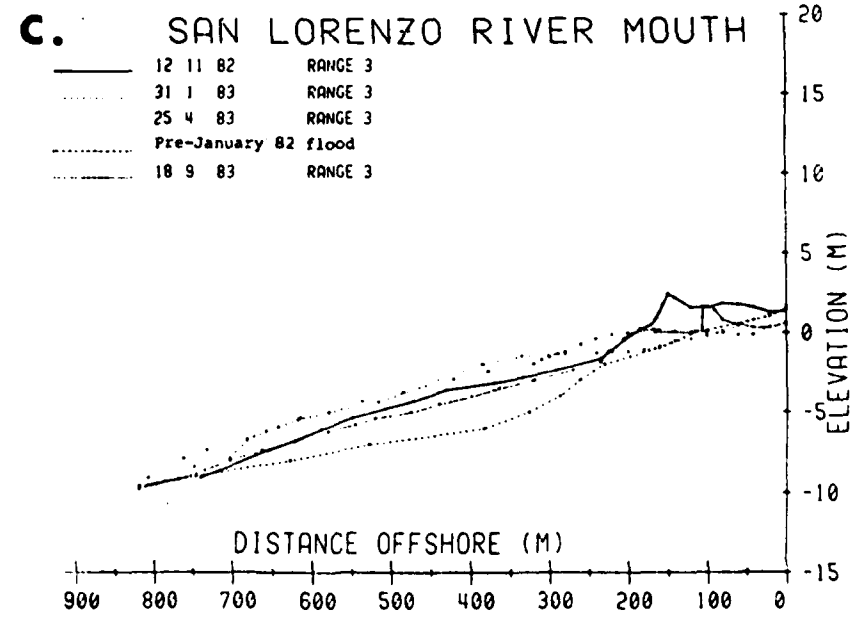
c.
SAN LORENZO RIVER MOUTH
12 11 82 RANGE 3
31 1 83 RANGE 3
25 4 83 RANGE 3
Pre-January 82 flood
18 9 83 RANGE 3
ELEVATION (M)
DISTANCE OFFSHORE (M)
20
15
10
5
0
-5
-10
-15
900
800
700
600
500
400
300
200
100
0

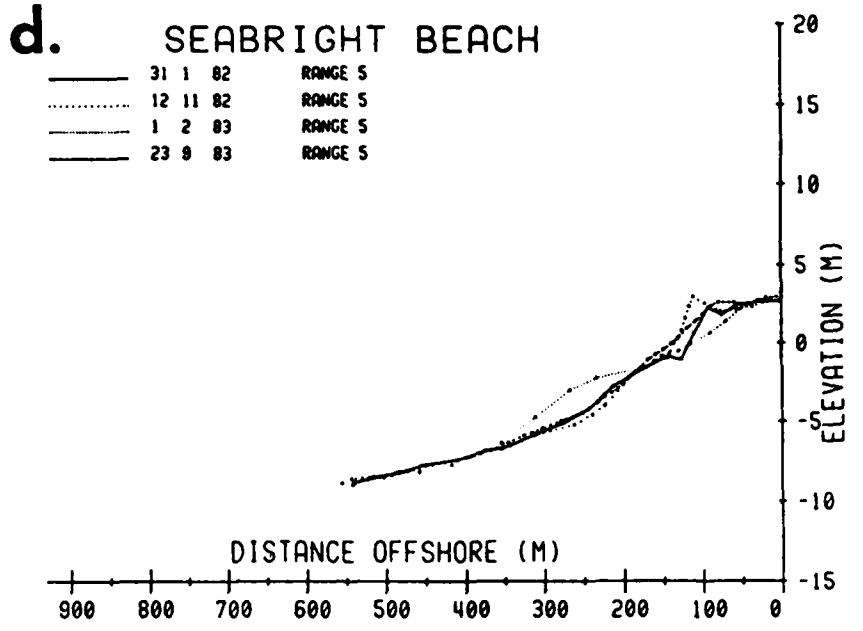
d.
SEABRIGHT BEACH
31 1 82 RANGE 5
12 11 82 RANGE 5
1 2 83 RANGE 5
23 9 83 RANGE 5
ELEVATION (M)
DISTANCE OFFSHORE (M)
20
15
10
5
0
-5
-10
-15
900
800
700
600
500
400
300
200
100
0

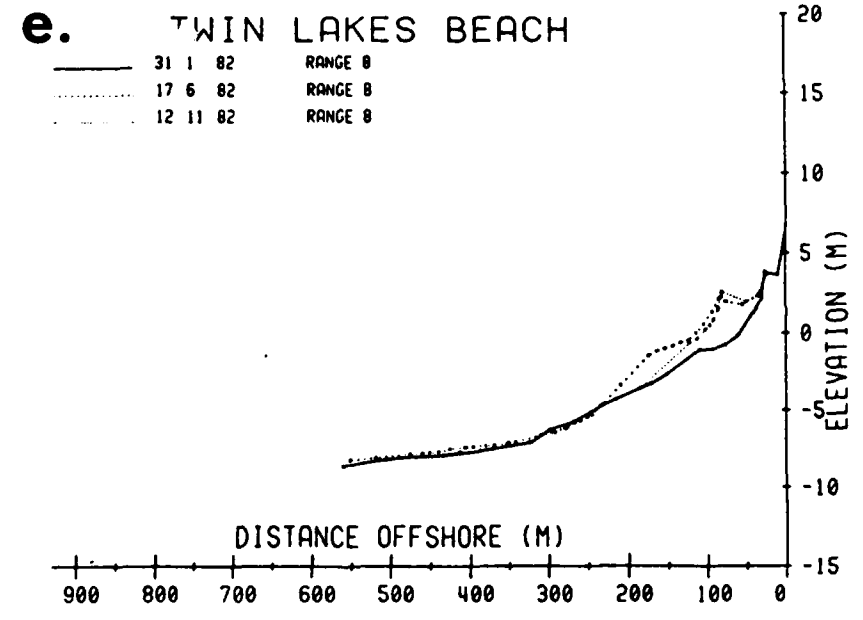
e.
TWIN LAKES BEACH
31 1 82 RANGE 8
17 6 82 RANGE 8
12 11 82 RANGE 8
ELEVATION (M)
DISTANCE OFFSHORE (M)
20
15
10
5
0
-5
-10
-15
900
800
700
600
500
400
300
200
100
0

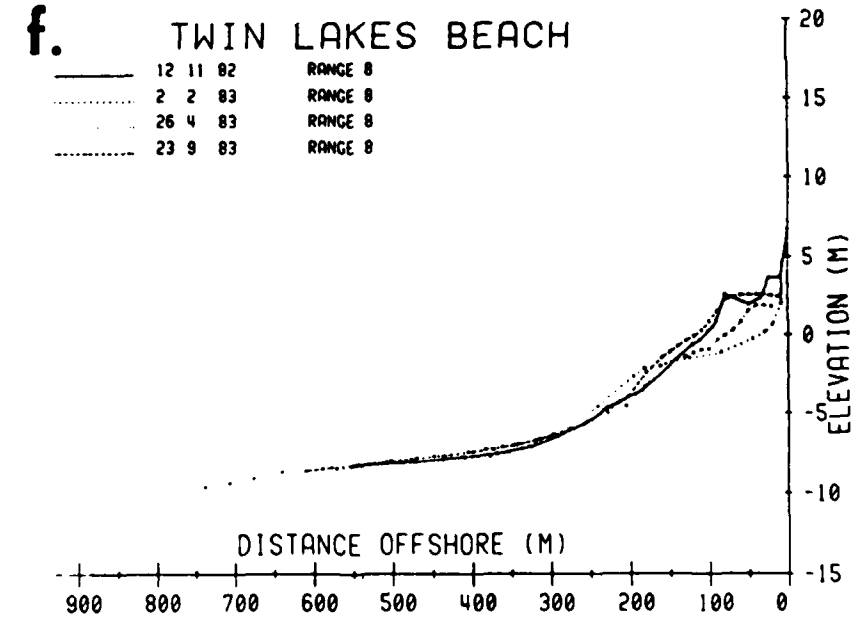
f.
TWIN LAKES BEACH
12 11 82 RANGE 8
2 2 83 RANGE 8
26 4 83 RANGE 8
23 9 83 RANGE 8
ELEVATION (M)
DISTANCE OFFSHORE (M)
20
15
10
5
0
-5
-10
-15
900
800
700
600
500
400
300
200
100
0

Figure 18. Charts depicting the changing morphology at the mouth of the San Lorenzo River.

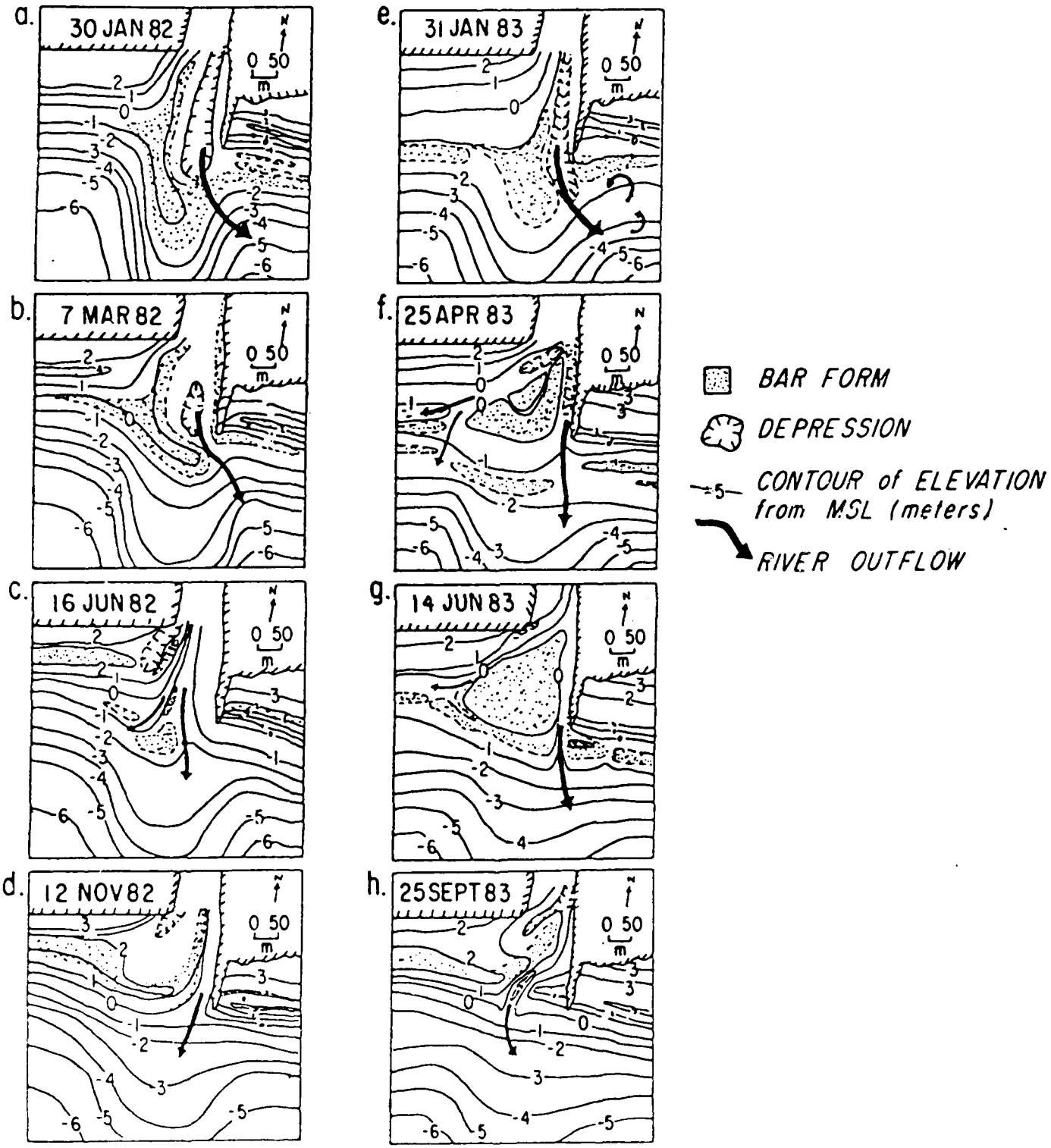
a.
30 JAN 82
b.
7 MAR 82
c.
16 JUN 82
d.
12 NOV 82
e.
31 JAN 83
f.
25 APR 83
g.
14 JUN 83
h.
25 SEPT 83
N
0 50
m
BAR FORM
DEPRESSION
-5- CONTOUR of ELEVATION from MSL (meters)
RIVER OUTFLOW

Figure 19. Computer-graphics block diagrams depicting the changing morphology of the San Lorenzo delta.

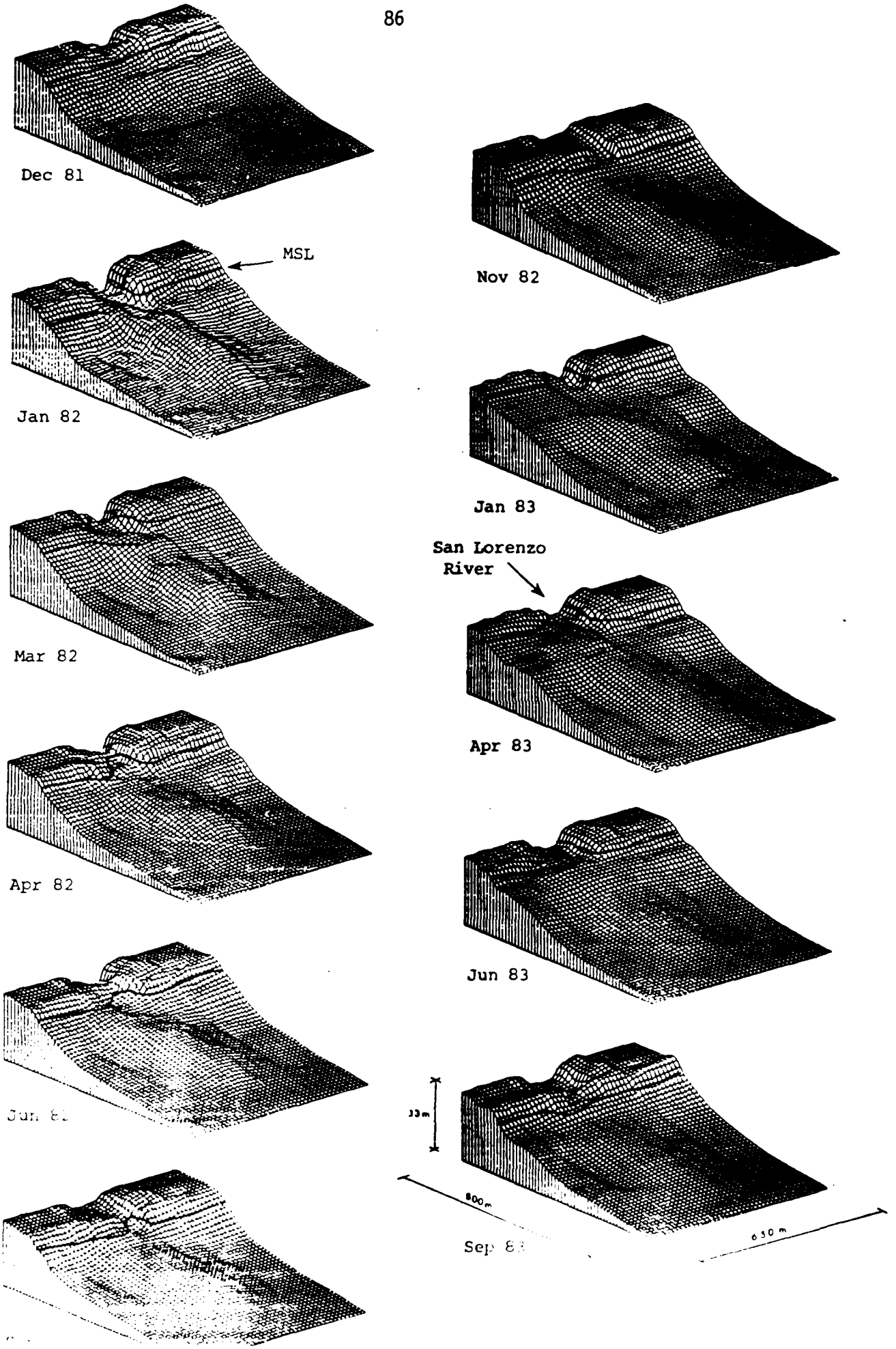
Dec 81
MSL
Jan 82
Mar 82
Apr 82
Jun 82
Sep 82
Nov 82
Jan 83
San Lorenzo River
Apr 83
Jun 83
Sep 83
33m
800m
650m

Figure 20. Block diagrams showing the morphology within the control cell at survey times and the changes in elevation occurring between surveys. On the elevation change plots, hills and ridges indicate accretion while valleys and depressions indicate erosion.

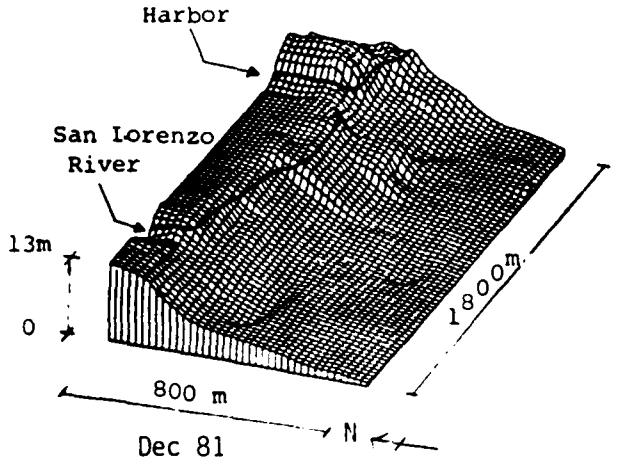

Dec 81

a. December 1981 - April 1982

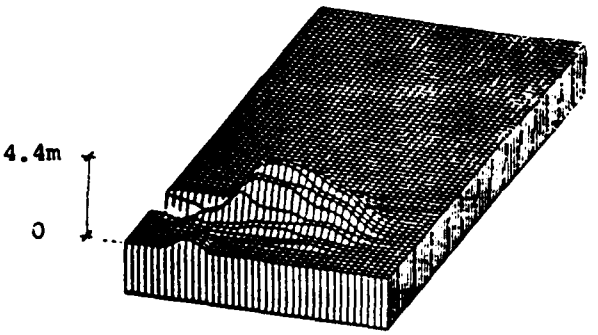

Dec 81 - Jan 82

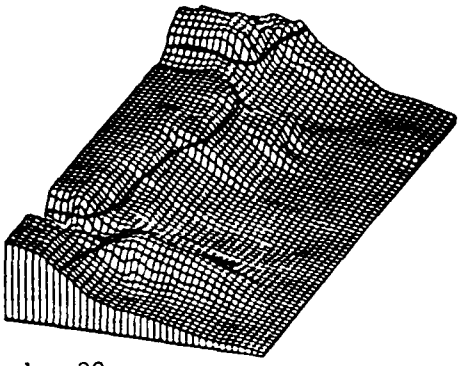

Jan 82

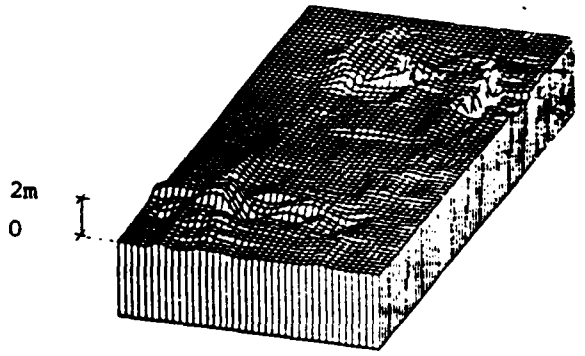

Jan-Mar 82

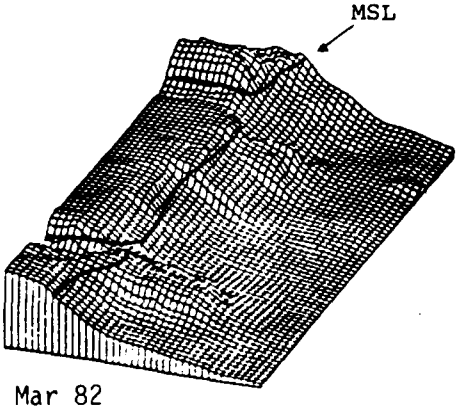

Mar 82

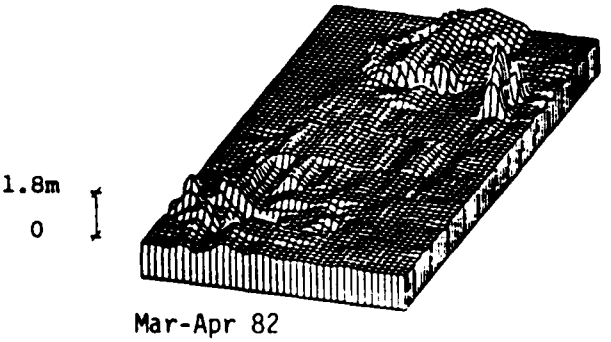

Mar-Apr 82

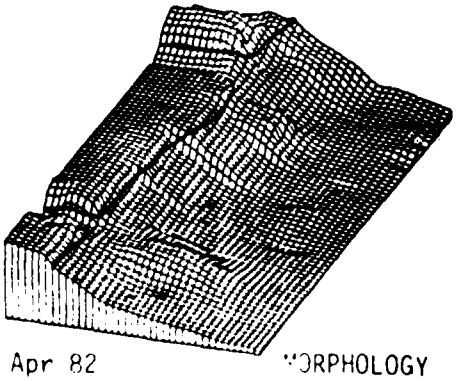

Apr 82

MORPHOLOGY

ELEVATION CHANGE

b. April 1982 - November 1982

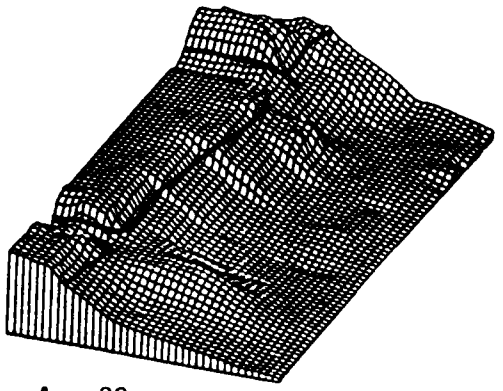

Apr 82

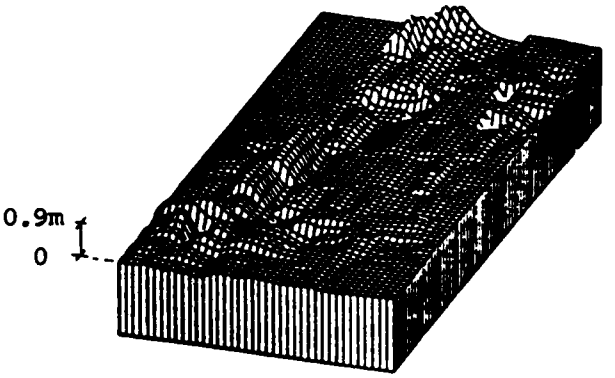

Apr-Jun 82

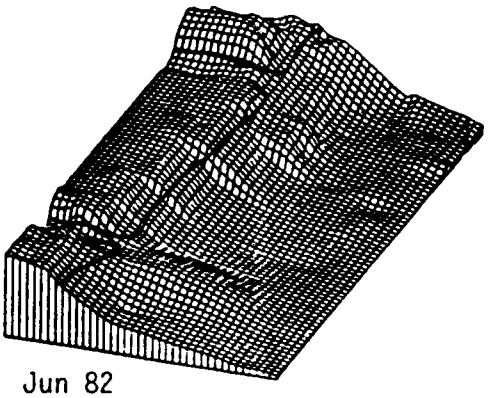

Jun 82

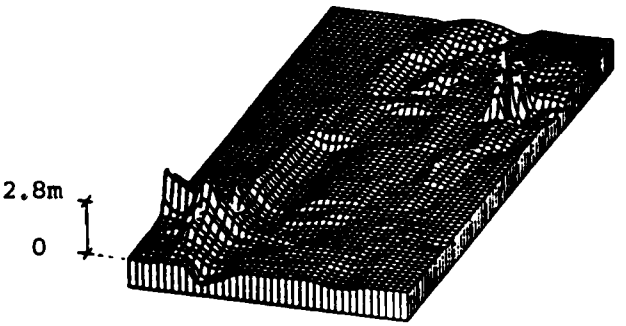

Jun-Sep 82

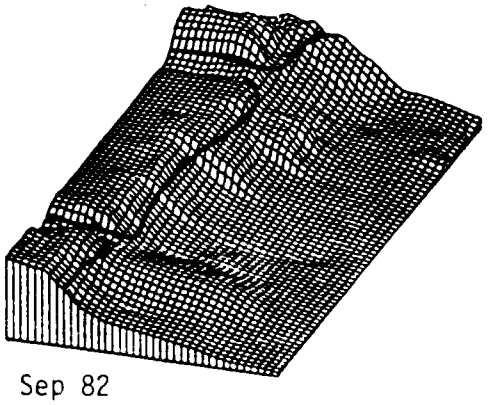

Sep 82

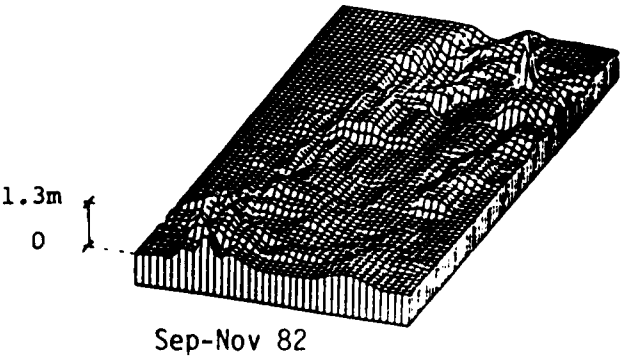

Sep-Nov 82

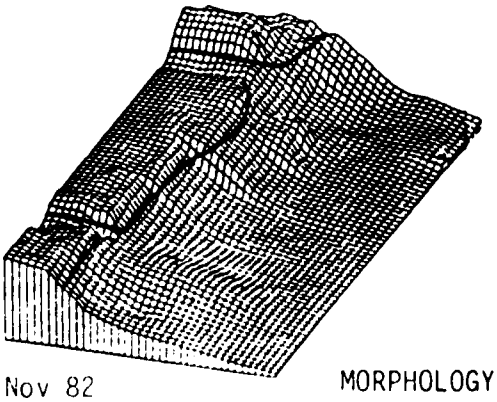

Nov 82

MORPHOLOGY

ELEVATION CHANGE

c. November 1982 - June 1983

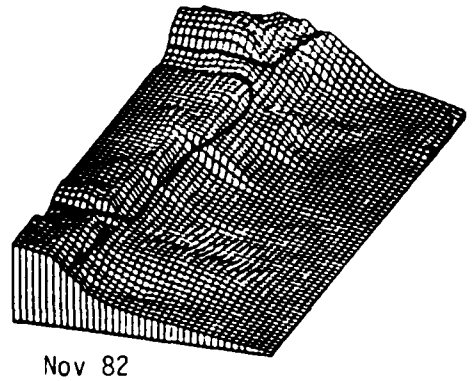

Nov 82

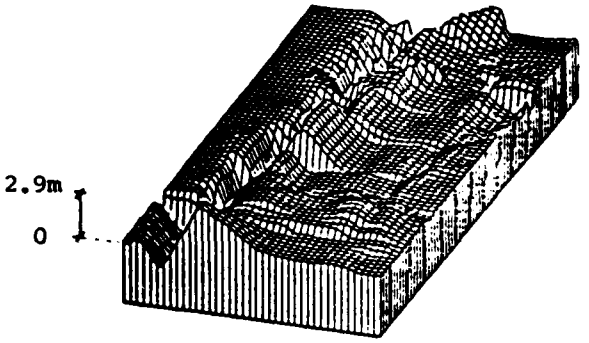

Nov 82 - Jan 83

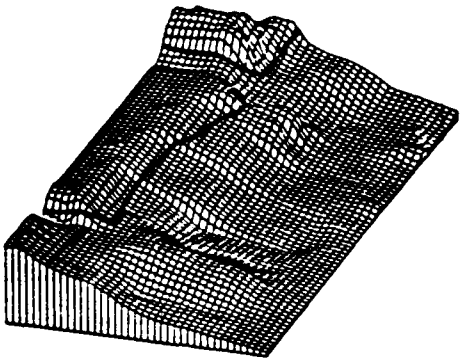

Jan 83

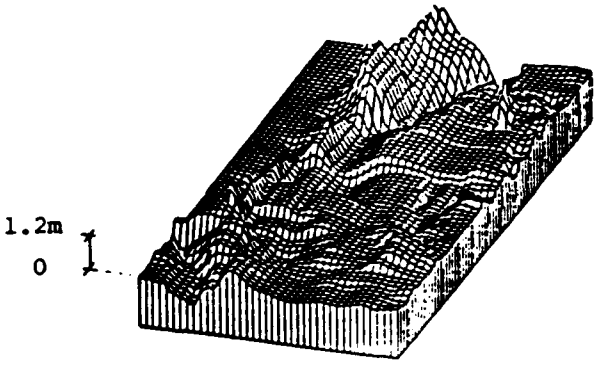

Jan-Apr 83

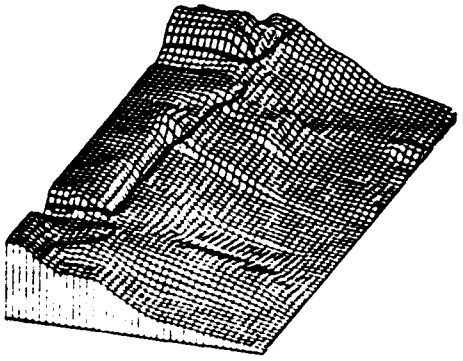

Apr 83

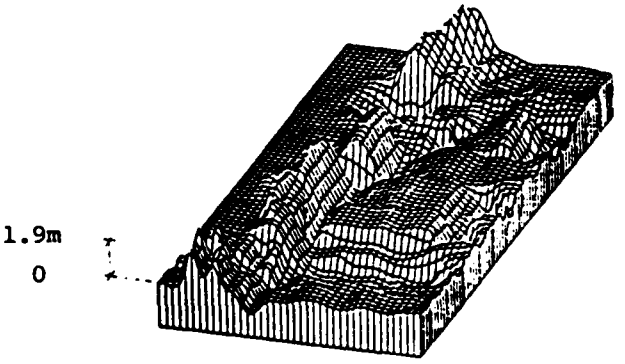

Apr-Jun 83

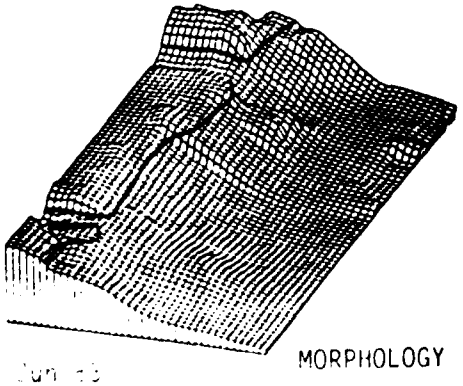

MORPHOLOGY

ELEVATION CHANGE

d. June - September 1983

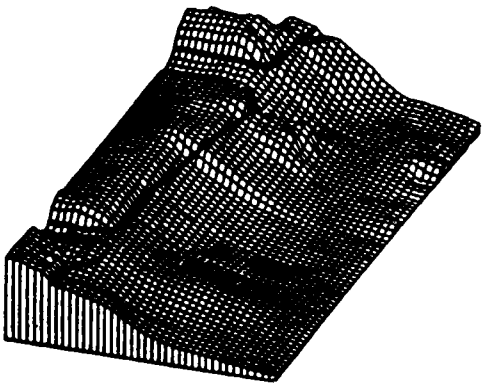

Jun 83

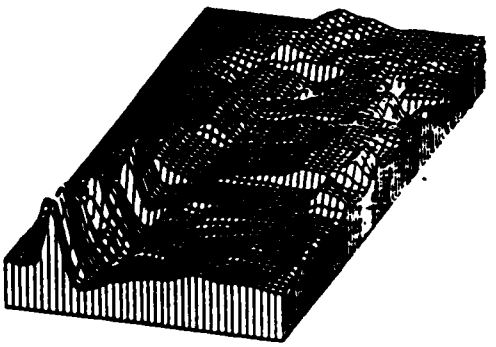

Jun-Sep 83

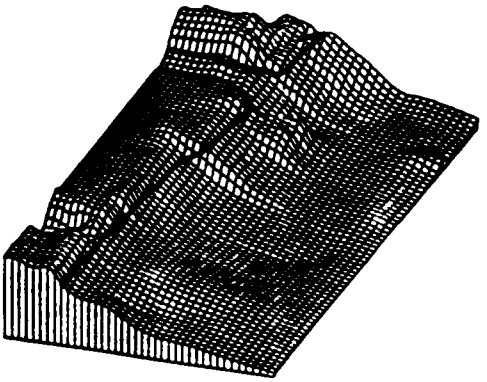

Sep 83

MORPHOLOGY

ELEVATION CHANGE

e. December 1981 - September 1983

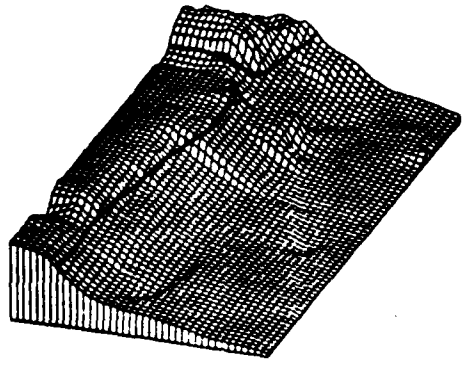

Dec 81

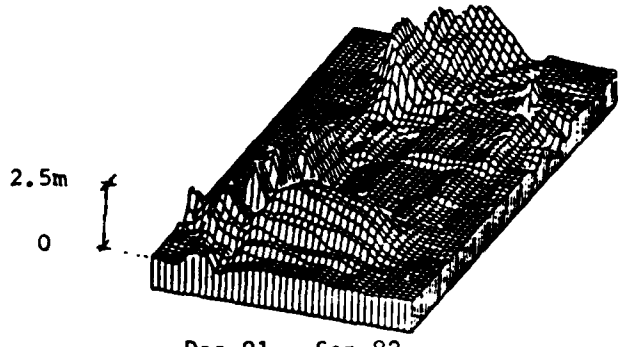

Dec 81 - Sep 82

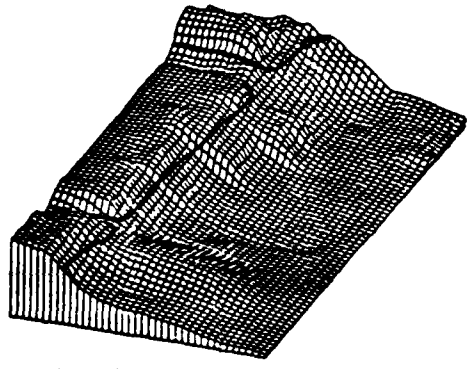

Sep 82

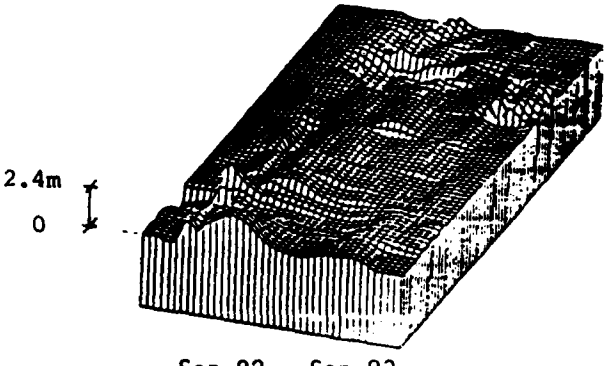

Sep 82 - Sep 83

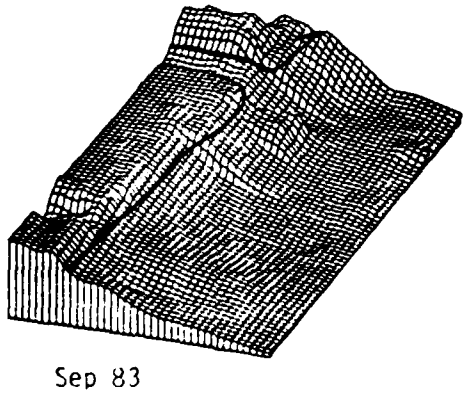

Sep 83

MORPHOLOGY

ELEVATION CHANGE

Figure 21. Isopach maps showing contours of equal change in elevation between surveys. The plots beneath each isopach map show the net volume change per meter length of shore. This is obtained from the isopach maps by integrating volume change across meter-wide strips of the control cell. The area under these plots gives the total volume change within the control cell for the given time interval. The net volume change at the harbor is plotted in terms of the volume change outside the harbor (dashed line) and the sum of volume changes inside and outside the harbor (solid line). The river yield, spread over 100 m of shoreline at the river mouth, is also shown.

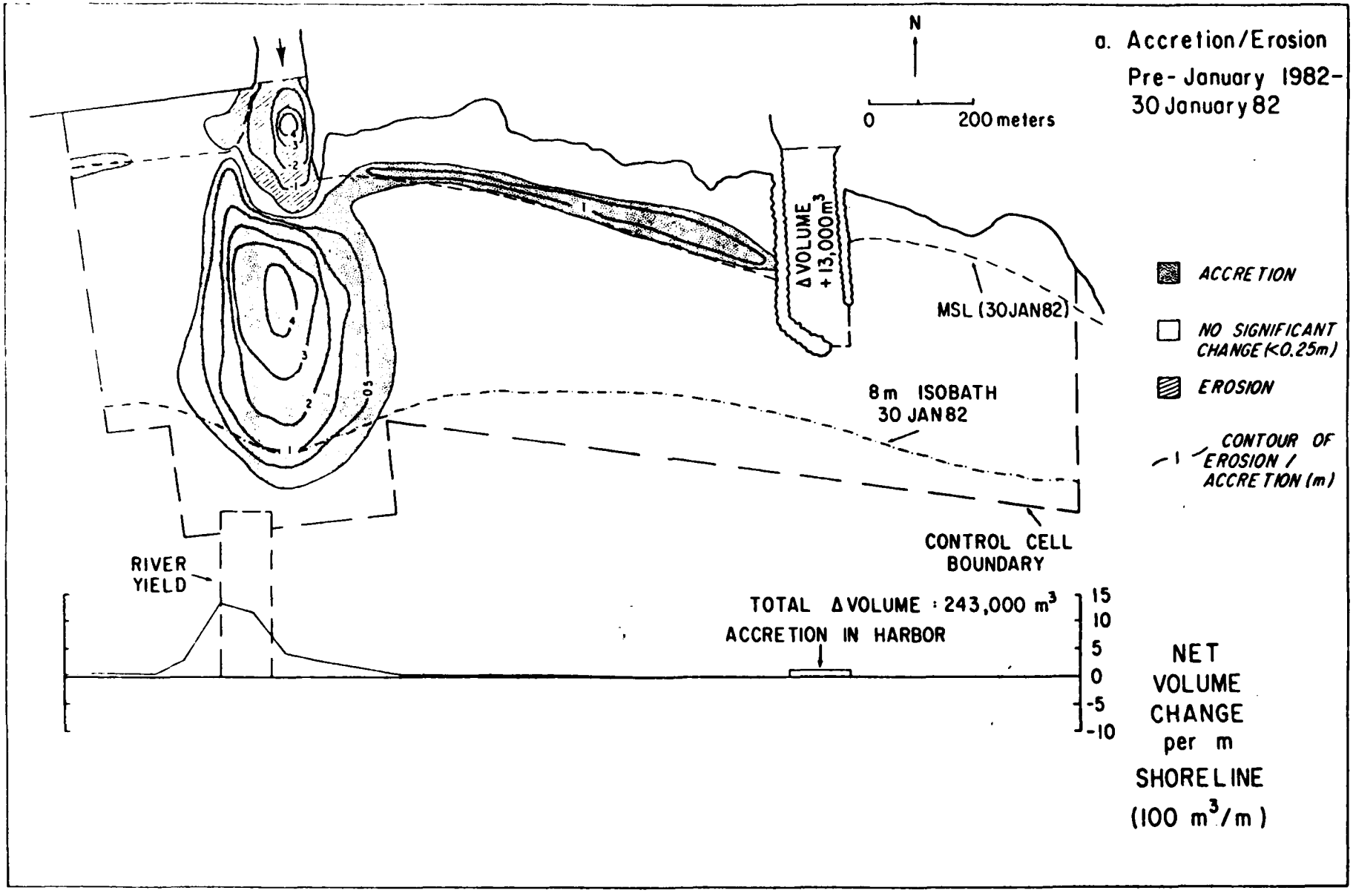
a. Accretion/Erosion
Pre-January 1982-
30 January 82
N
0
200 meters
ΔVOLUME
+13,000m³
MSL (30JAN82)
8m ISOBATH
30 JAN82
ACCRETION
NO SIGNIFICANT
CHANGE (<0.25m)
EROSION
CONTOUR OF
EROSION /
ACCRETION (m)
CONTROL CELL
BOUNDARY
RIVER
YIELD
TOTAL ΔVOLUME : 243,000 m³
ACCRETION IN HARBOR
15
10
5
0
-5
-10
NET
VOLUME
CHANGE
per m
SHORELINE
(100 m³/m)

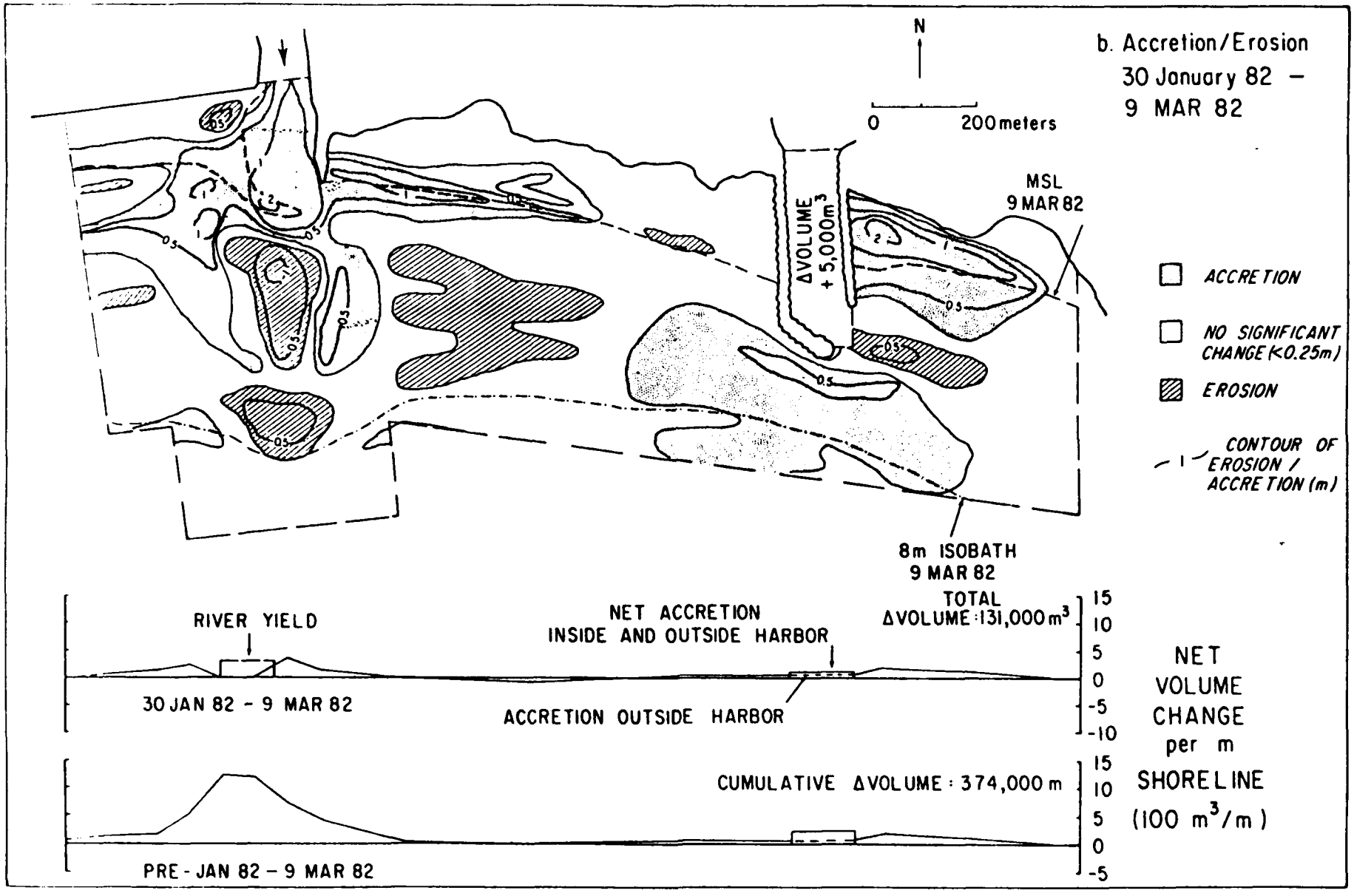
b. Accretion/Erosion
30 January 82 –
9 MAR 82
N
0
200 meters
ΔVOLUME
+5,000m³
MSL
9 MAR 82
ACCRETION
NO SIGNIFICANT
CHANGE (<0.25m)
EROSION
CONTOUR OF
EROSION / ACCRETION (m)
8m ISOBATH
9 MAR 82
RIVER YIELD
NET ACCRETION
INSIDE AND OUTSIDE HARBOR
TOTAL
ΔVOLUME: 131,000 m³
30 JAN 82 - 9 MAR 82
ACCRETION OUTSIDE HARBOR
CUMULATIVE ΔVOLUME: 374,000 m
PRE - JAN 82 – 9 MAR 82
NET
VOLUME
CHANGE
per m
SHORELINE
(100 m³/m)

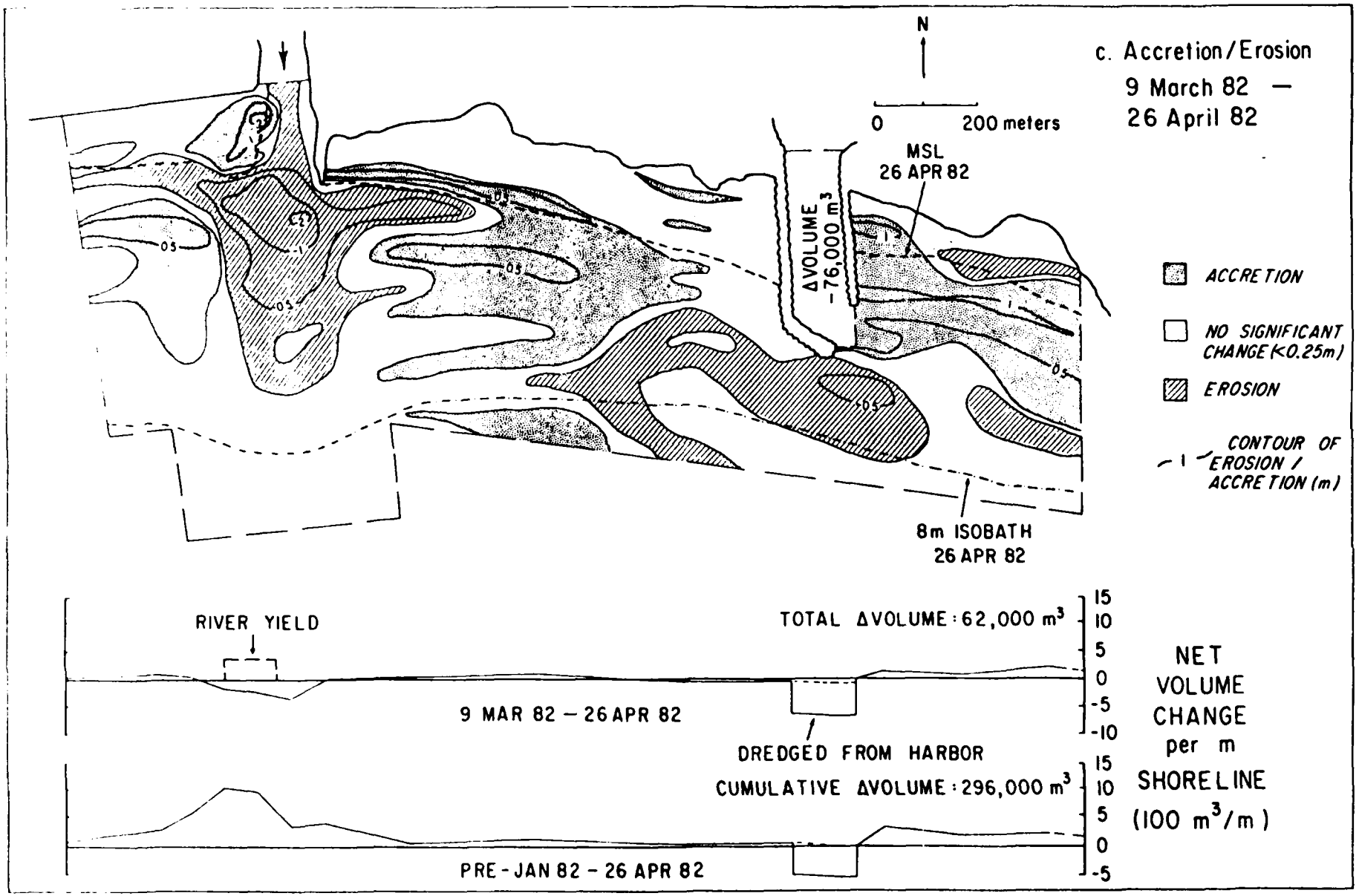
N
0
200 meters
c. Accretion/Erosion
9 March 82 —
26 April 82
MSL
26 APR 82
ΔVOLUME
-76,000 m³
ACCRETION
NO SIGNIFICANT
CHANGE (<0.25m)
EROSION
CONTOUR OF
EROSION /
ACCRETION (m)
8m ISOBATH
26 APR 82
RIVER YIELD
TOTAL ΔVOLUME: 62,000 m³
9 MAR 82 – 26 APR 82
DREDGED FROM HARBOR
CUMULATIVE ΔVOLUME: 296,000 m³
PRE-JAN 82 – 26 APR 82
15
10
5
0
-5
-10
NET
VOLUME
CHANGE
per m
SHORELINE
(100 m³/m)

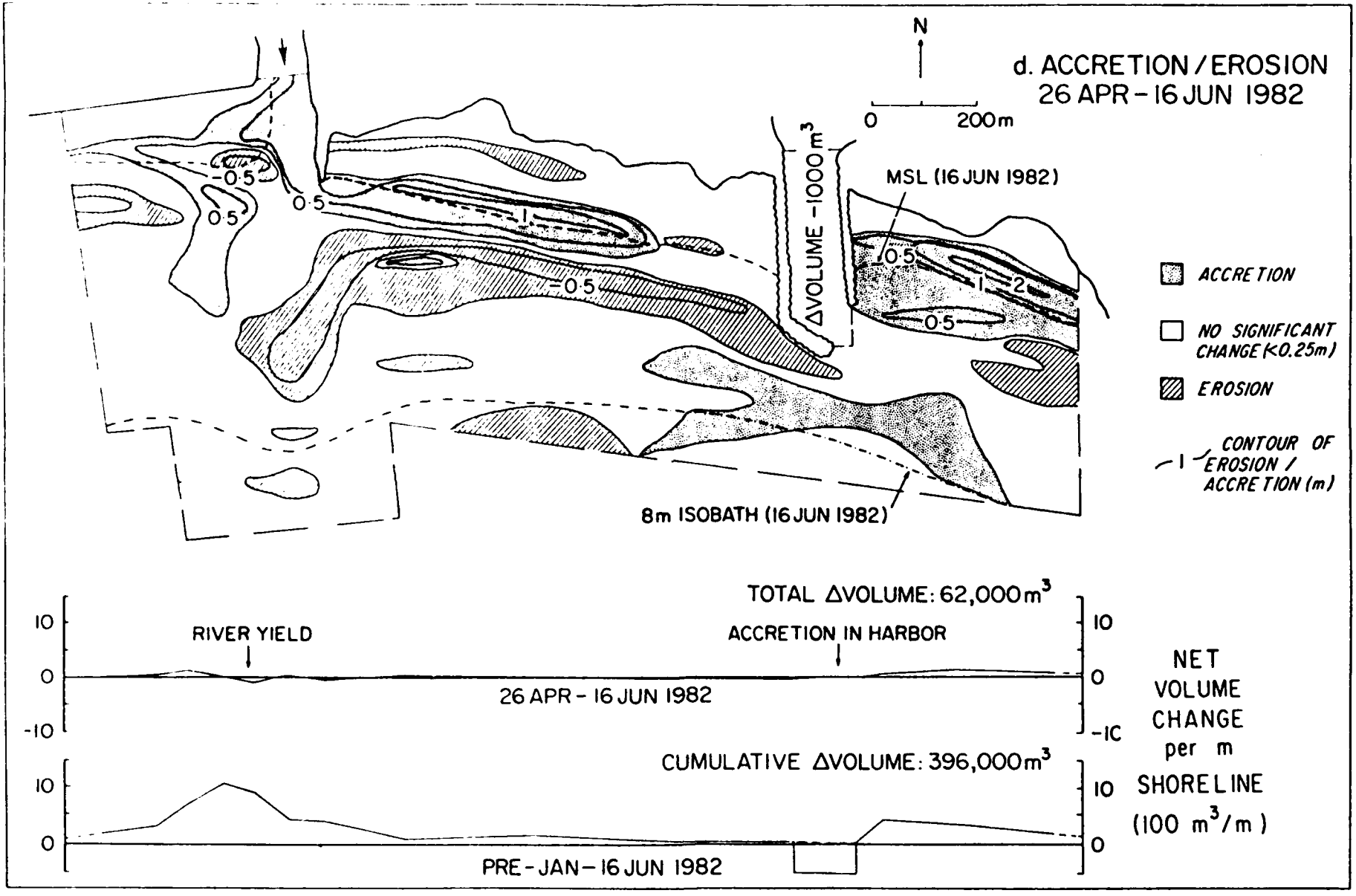
d. ACCRETION / EROSION
26 APR - 16 JUN 1982
N
0
200m
ΔVOLUME -1000 m³
MSL (16 JUN 1982)
-0.5
0.5
0.5
1
-0.5
0.5
1
2
0.5
8m ISOBATH (16 JUN 1982)
ACCRETION
NO SIGNIFICANT CHANGE (<0.25m)
EROSION
1 CONTOUR OF EROSION / ACCRETION (m)
TOTAL ΔVOLUME: 62,000 m³
RIVER YIELD
ACCRETION IN HARBOR
10
0
-10
26 APR - 16 JUN 1982
CUMULATIVE ΔVOLUME: 396,000 m³
PRE-JAN - 16 JUN 1982
NET VOLUME CHANGE per m SHORELINE (100 m³/m)

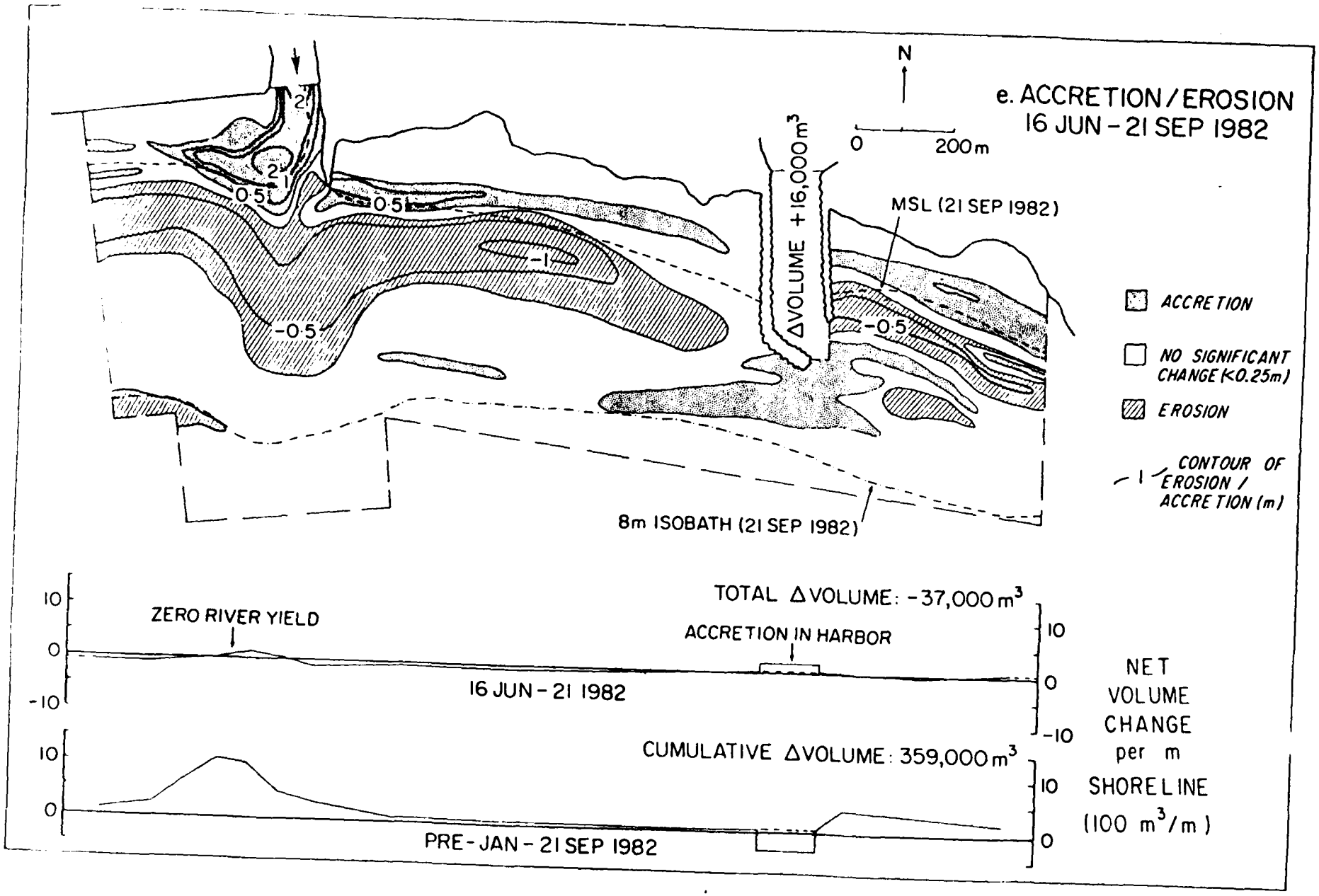
e. ACCRETION / EROSION
16 JUN - 21 SEP 1982
N
0
200m
ΔVOLUME +16,000 m³
MSL (21 SEP 1982)
2
1
0.5
-0.5
-1
8m ISOBATH (21 SEP 1982)
ACCRETION
NO SIGNIFICANT CHANGE (<0.25m)
EROSION
CONTOUR OF EROSION / ACCRETION (m)
TOTAL ΔVOLUME: -37,000 m³
ZERO RIVER YIELD
ACCRETION IN HARBOR
16 JUN - 21 1982
CUMULATIVE ΔVOLUME: 359,000 m³
PRE-JAN - 21 SEP 1982
10
0
-10
NET VOLUME CHANGE per m SHORELINE (100 m³/m)

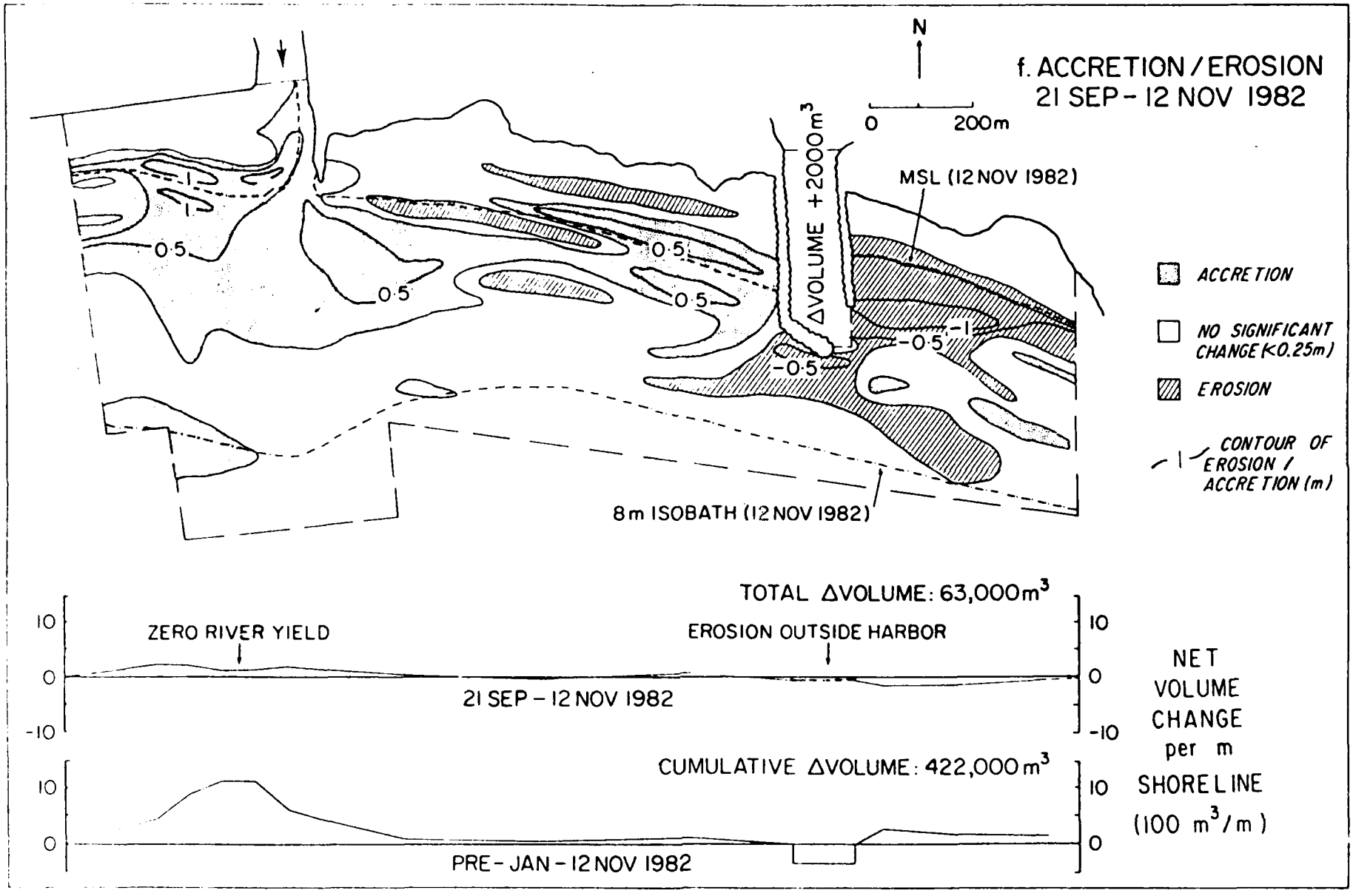
f. ACCRETION / EROSION
21 SEP - 12 NOV 1982
N
0
200m
ΔVOLUME +2000m³
MSL (12 NOV 1982)
-1
-0.5
0.5
0.5
0.5
0.5
-0.5
-0.5
-1
8m ISOBATH (12 NOV 1982)
ACCRETION
NO SIGNIFICANT CHANGE (<0.25m)
EROSION
CONTOUR OF EROSION / ACCRETION (m)
TOTAL ΔVOLUME: 63,000m³
ZERO RIVER YIELD
EROSION OUTSIDE HARBOR
10
0
-10
21 SEP - 12 NOV 1982
CUMULATIVE ΔVOLUME: 422,000m³
PRE - JAN - 12 NOV 1982
NET VOLUME CHANGE per m SHORELINE (100 m³/m)

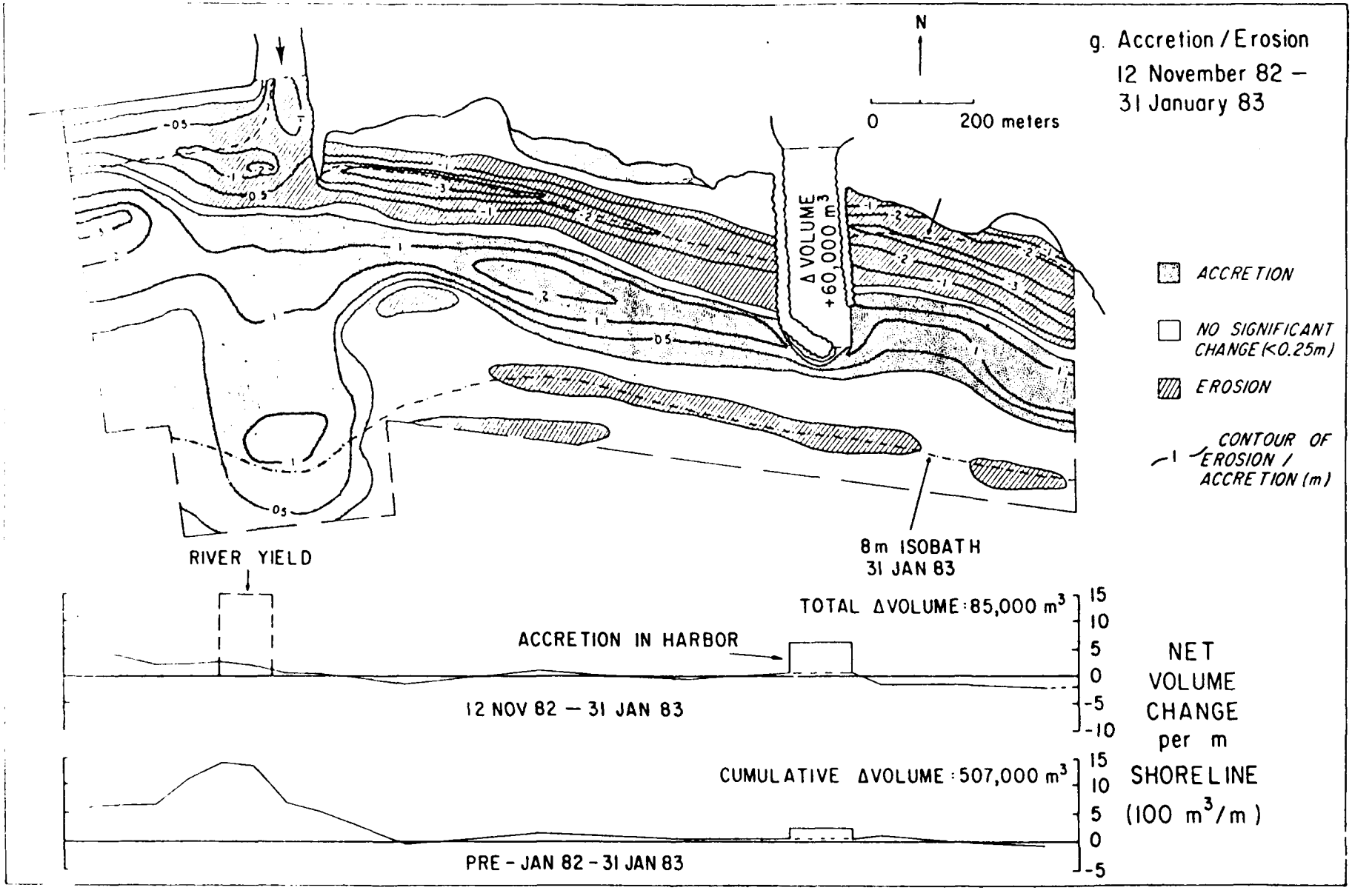
N
0
200 meters
g. Accretion / Erosion
12 November 82 –
31 January 83
ΔVOLUME
+60,000 m³
ACCRETION
NO SIGNIFICANT
CHANGE (<0.25m)
EROSION
CONTOUR OF
EROSION /
ACCRETION (m)
RIVER YIELD
8m ISOBATH
31 JAN 83
TOTAL ΔVOLUME: 85,000 m³
ACCRETION IN HARBOR
12 NOV 82 – 31 JAN 83
CUMULATIVE ΔVOLUME: 507,000 m³
PRE - JAN 82 - 31 JAN 83
NET
VOLUME
CHANGE
per m
SHORELINE
(100 m³/m)

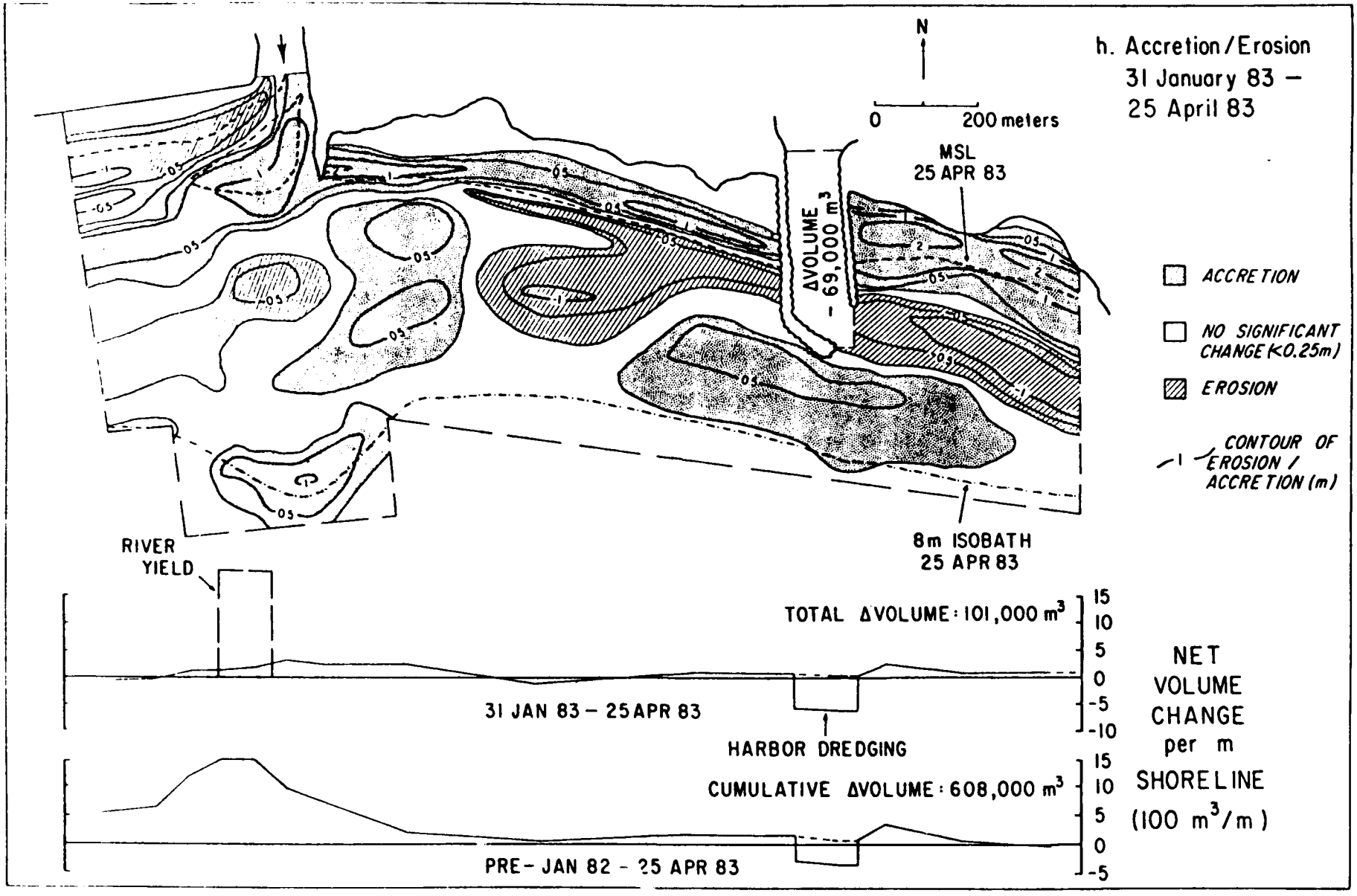
h. Accretion / Erosion
31 January 83 –
25 April 83
N
0
200 meters
MSL
25 APR 83
ΔVOLUME
- 69,000 m³
ACCRETION
NO SIGNIFICANT
CHANGE (<0.25m)
EROSION
CONTOUR OF
EROSION /
ACCRETION (m)
RIVER
YIELD
8m ISOBATH
25 APR 83
TOTAL ΔVOLUME: 101,000 m³
31 JAN 83 – 25 APR 83
HARBOR DREDGING
CUMULATIVE ΔVOLUME: 608,000 m³
PRE-JAN 82 - 25 APR 83
NET
VOLUME
CHANGE
per m
SHORELINE
(100 m³/m)

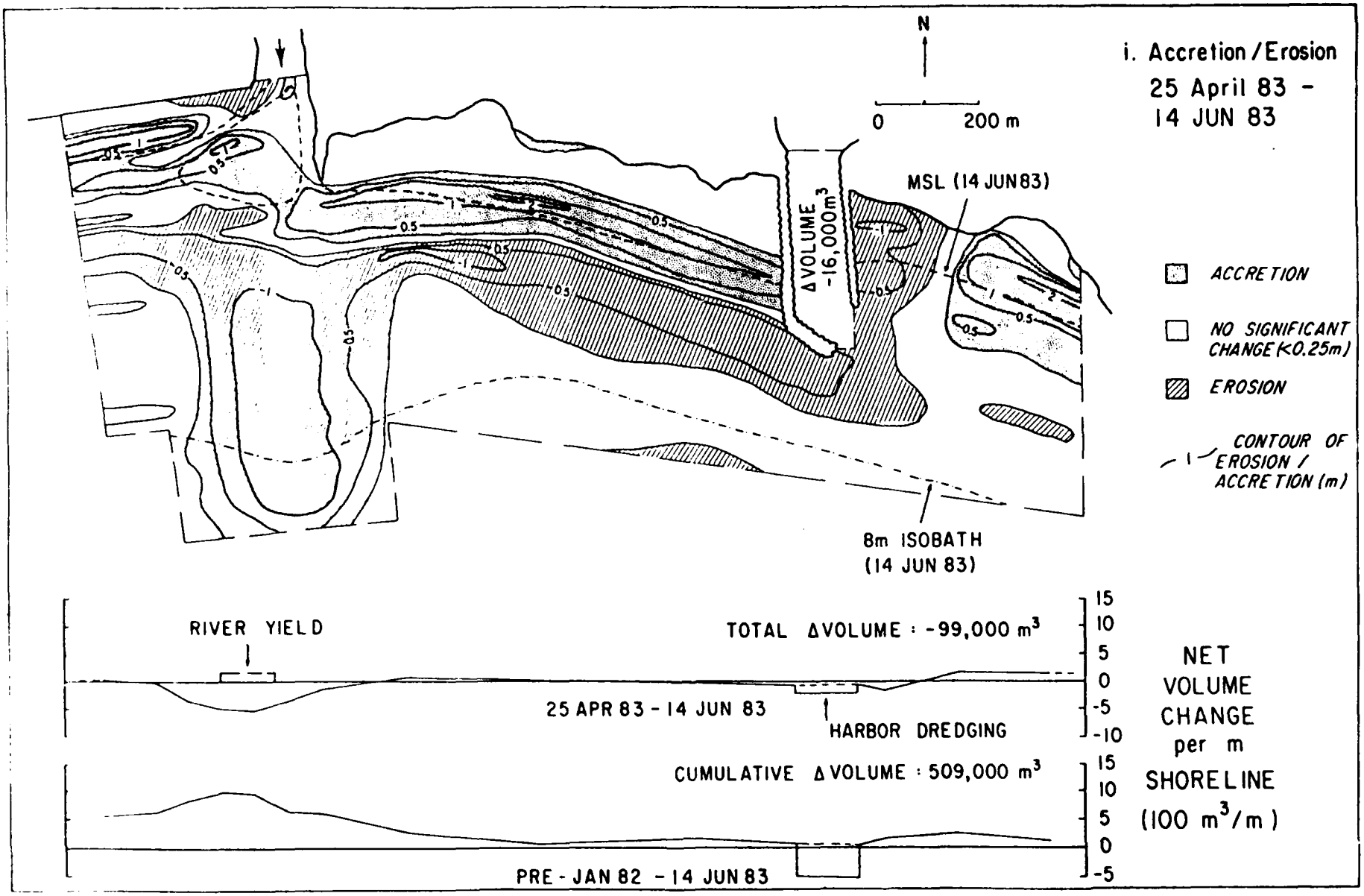
i. Accretion / Erosion
25 April 83 -
14 JUN 83
N
0
200 m
MSL (14 JUN83)
ΔVOLUME
-16,000m³
ACCRETION
NO SIGNIFICANT
CHANGE (<0.25m)
EROSION
CONTOUR OF
EROSION /
ACCRETION (m)
8m ISOBATH
(14 JUN 83)
RIVER YIELD
TOTAL ΔVOLUME : -99,000 m³
25 APR 83 - 14 JUN 83
HARBOR DREDGING
CUMULATIVE ΔVOLUME : 509,000 m³
PRE - JAN 82 - 14 JUN 83
NET
VOLUME
CHANGE
per m
SHORELINE
(100 m³/m)

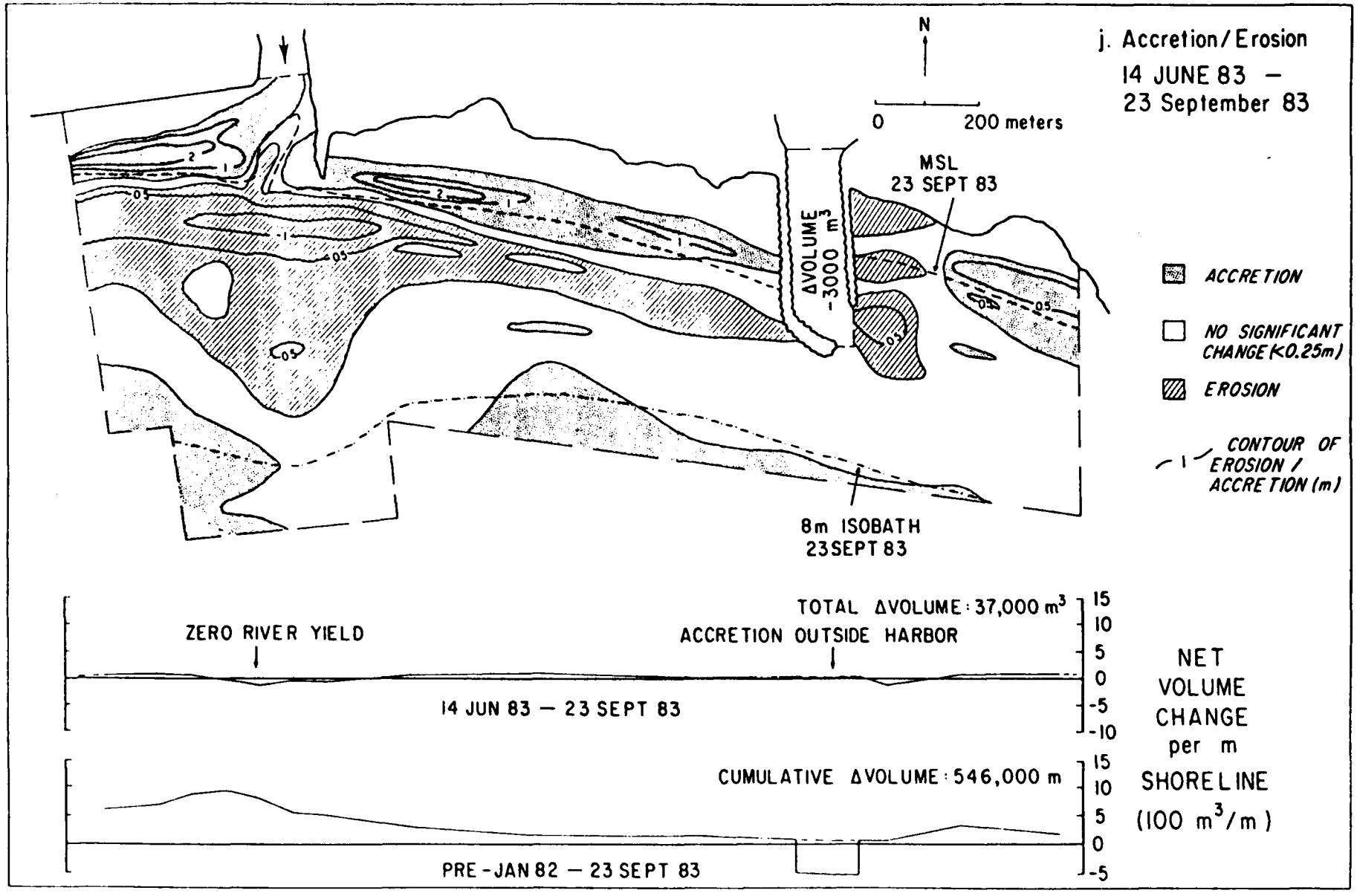
j. Accretion/Erosion
14 JUNE 83 –
23 September 83
N
0
200 meters
MSL
23 SEPT 83
ΔVOLUME
-3000 m³
ACCRETION
NO SIGNIFICANT
CHANGE (<0.25m)
EROSION
CONTOUR OF
EROSION / ACCRETION (m)
8m ISOBATH
23SEPT 83
TOTAL ΔVOLUME: 37,000 m³
ZERO RIVER YIELD
ACCRETION OUTSIDE HARBOR
14 JUN 83 – 23 SEPT 83
CUMULATIVE ΔVOLUME: 546,000 m
PRE-JAN 82 – 23 SEPT 83
NET
VOLUME
CHANGE
per m
SHORELINE
(100 m³/m)

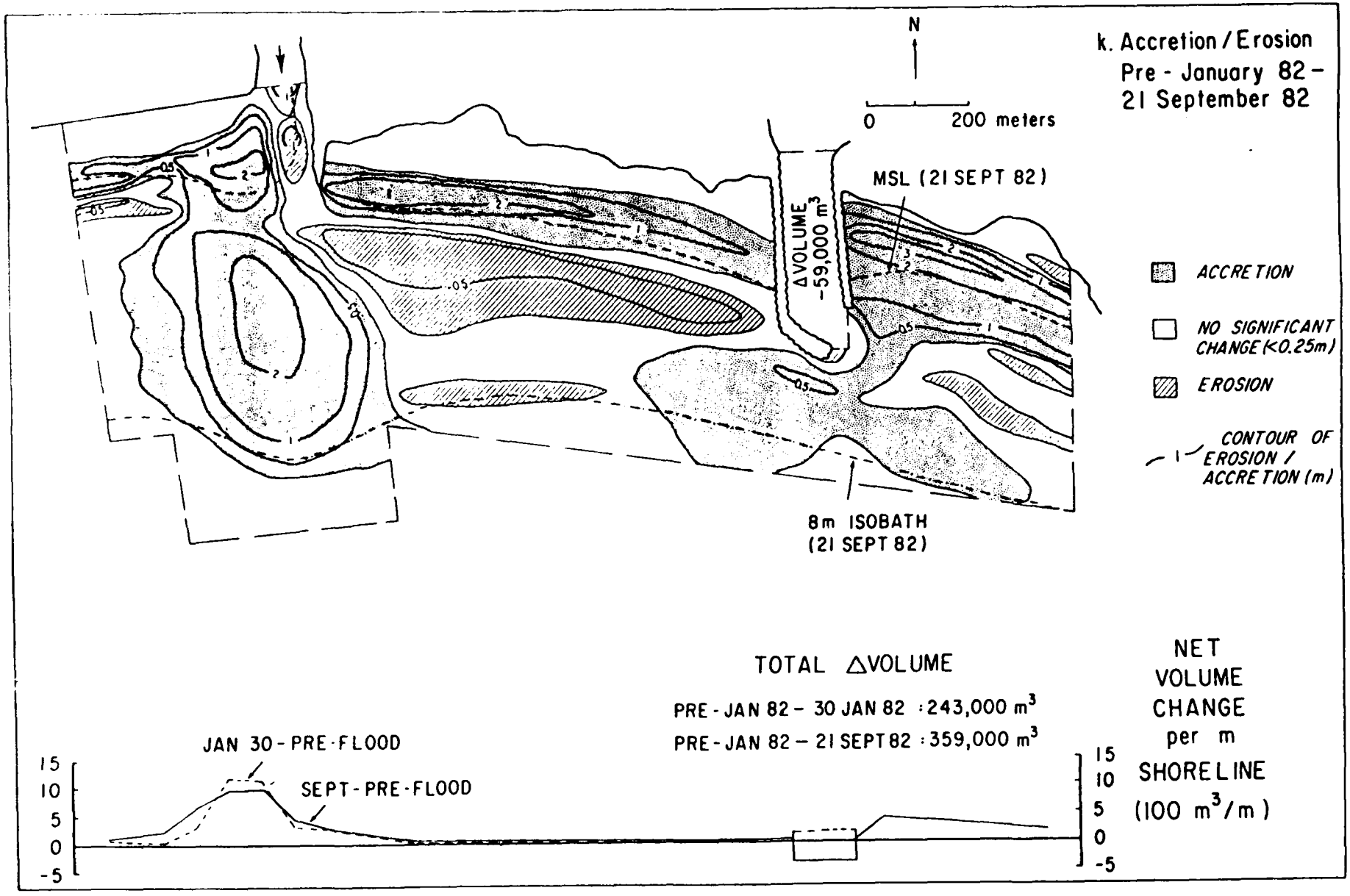
k. Accretion / Erosion
Pre - January 82 -
21 September 82
N
0
200 meters
MSL (21 SEPT 82)
ΔVOLUME
-59,000 m³
ACCRETION
NO SIGNIFICANT
CHANGE (<0.25m)
EROSION
CONTOUR OF
EROSION /
ACCRETION (m)
8m ISOBATH
(21 SEPT 82)
TOTAL ΔVOLUME
PRE - JAN 82 - 30 JAN 82 : 243,000 m³
PRE - JAN 82 - 21 SEPT 82 : 359,000 m³
JAN 30 - PRE - FLOOD
SEPT - PRE - FLOOD
15
10
5
0
-5
NET
VOLUME
CHANGE
per m
SHORELINE
(100 m³/m)

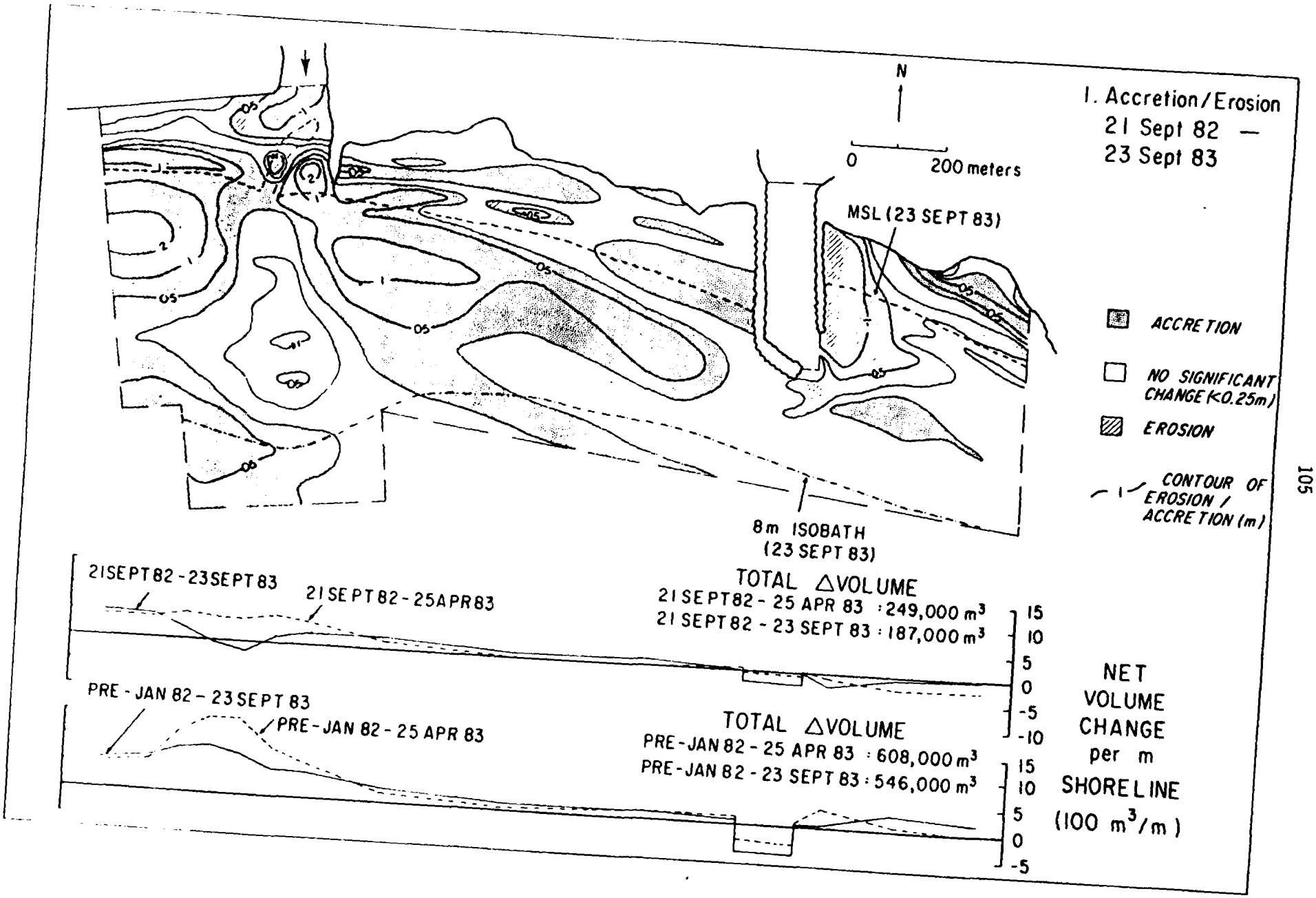
1. Accretion/Erosion
21 Sept 82 — 23 Sept 83
N
0
200 meters
MSL (23 SEPT 83)
ACCRETION
NO SIGNIFICANT CHANGE (<0.25m)
EROSION
CONTOUR OF EROSION / ACCRETION (m)
8m ISOBATH (23 SEPT 83)
21SEPT82 - 23SEPT83
21SEPT82 - 25APR83
TOTAL ΔVOLUME
21SEPT82 - 25 APR 83 : 249,000 m³
21SEPT82 - 23 SEPT 83 : 187,000 m³
PRE - JAN 82 - 23 SEPT 83
PRE - JAN 82 - 25 APR 83
TOTAL ΔVOLUME
PRE-JAN 82 - 25 APR 83 : 608,000 m³
PRE-JAN 82 - 23 SEPT 83 : 546,000 m³
15
10
5
0
-5
-10
NET VOLUME CHANGE per m SHORELINE (100 m³/m)

Figure 22. (a) X-t diagram showing time-cumulative accretion/erosion within the control cell for the entire study period. The values contoured at given times (t-coordinates) and points alongshore (x-coordinates) indicate the net accretion/erosion since 1 January 1982 across meter-wide strips of the control cell. (b) Time-cumulative sediment gains within longshore segments of the control cell - a replot of Fig. 10. The plotted values are obtained by integrating from the x-t diagram the accretion/erosion along segments of the control cell shoreline at given times.

b. Net accretion in control cell segments

Figure 23. X-t diagrams showing time-cumulative accretion/erosion within the control cell after the 13 November 1982 survey only.

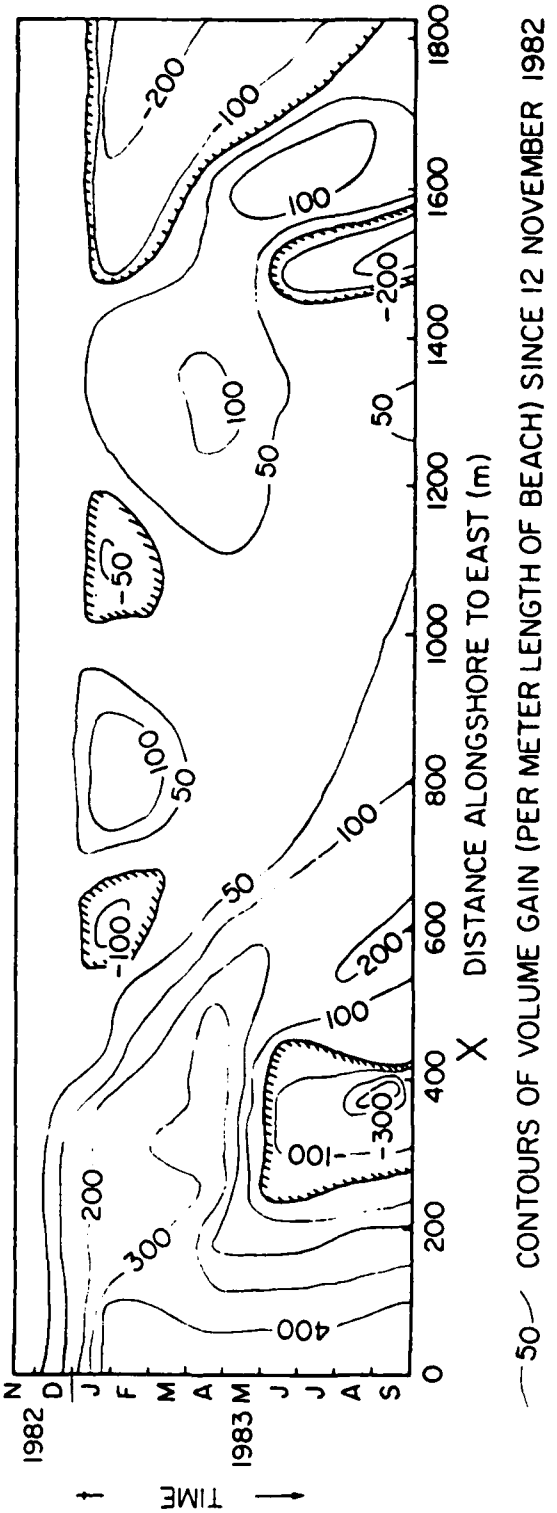
TIME
1982
N
D
1983
J
F
M
A
M
J
J
A
S
0
200
400
600
800
1000
1200
1400
1600
1800
X DISTANCE ALONGSHORE TO EAST (m)
50 CONTOURS OF VOLUME GAIN (PER METER LENGTH OF BEACH) SINCE 12 NOVEMBER 1982

Figure 24. (a) X-t diagram showing time-cumulative accretion/erosion within the portion of the control cell shoreward of the MLLW line. (b) Time-cumulative volume gains shoreward of the MLLW line within longshore segments of the control cell.

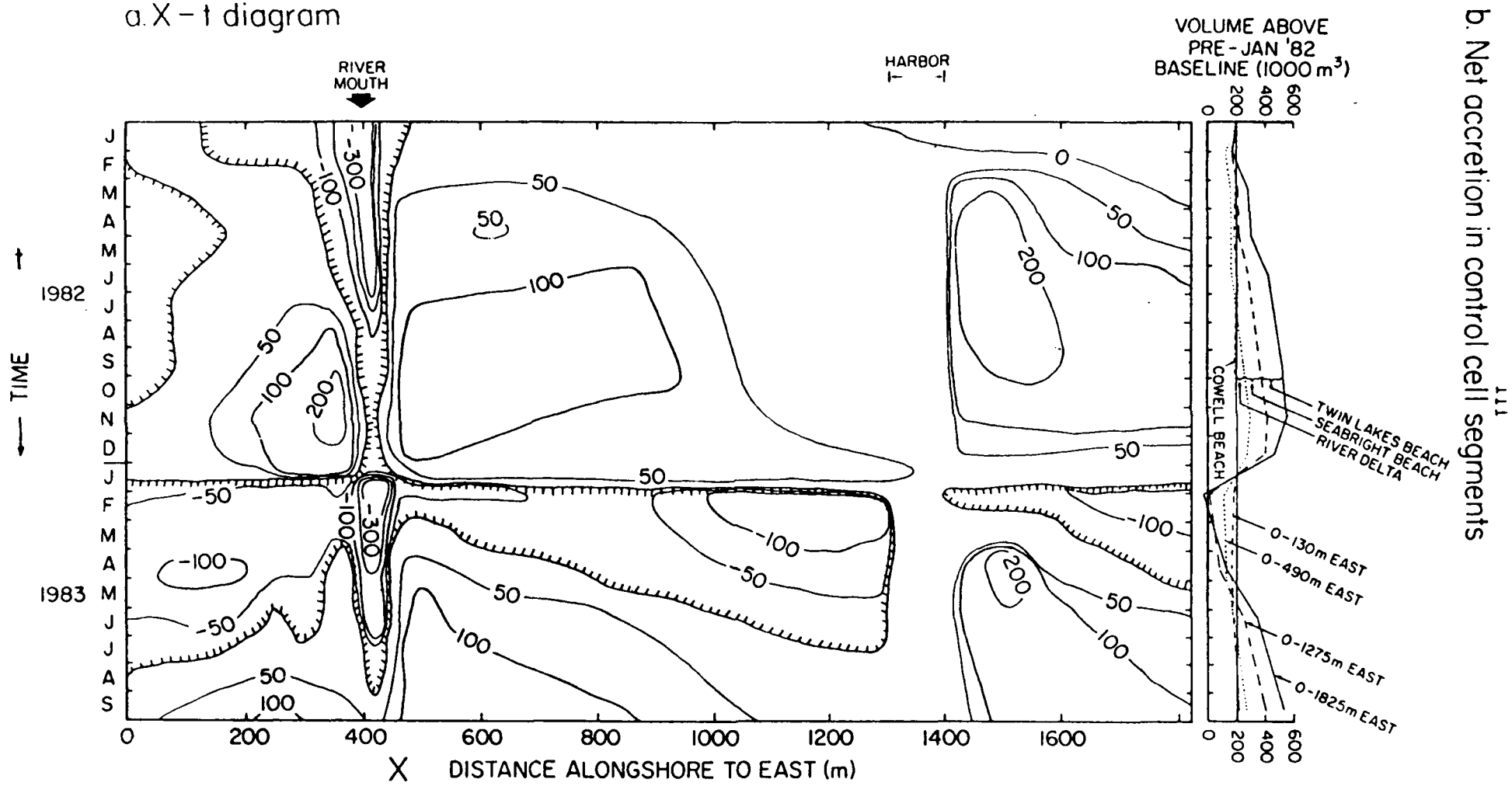
a. X – t diagram
RIVER MOUTH
HARBOR
VOLUME ABOVE PRE-JAN '82 BASELINE (1000 m³)
b. Net accretion in control cell segments
t
TIME
1982
1983
J F M A M J J A S O N D J F M A M J J A S
X DISTANCE ALONGSHORE TO EAST (m)
0 200 400 600 800 1000 1200 1400 1600
COWELL BEACH
TWIN LAKES BEACH
SEABRIGHT BEACH
RIVER DELTA
0-130m EAST
0-490m EAST
0-1275m EAST
0-1825m EAST
100 CONTOURS OF VOLUME GAIN (PER METER LENGTH OF BEACH) ABOVE MLLW (VISIBLE BEACH)

Figure 25. Block diagram representations of the x-t diagrams in Figs 22-24. The relief in these diagrams shows the accretion/erosion per meter length of shoreline as time progresses.

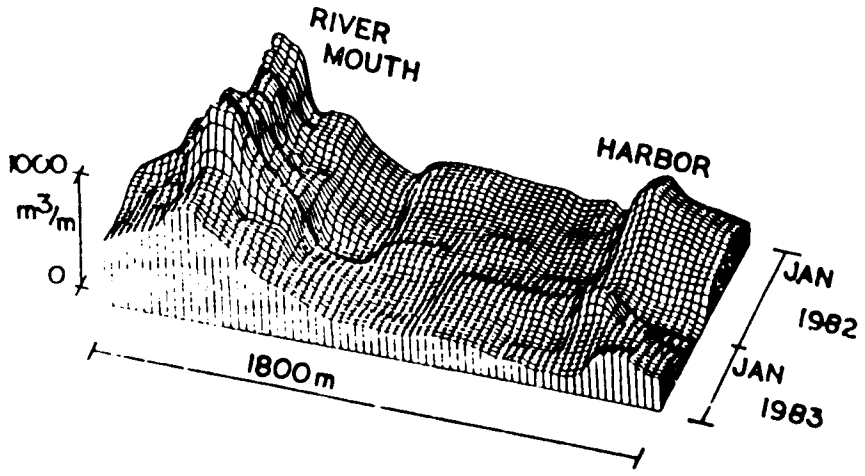

a. Entire control cell, 1982-83
(c.f. Fig. 22a)

b. Control cell shoreward of MLLW line, 1982-83
(c.f. Fig. 24a)

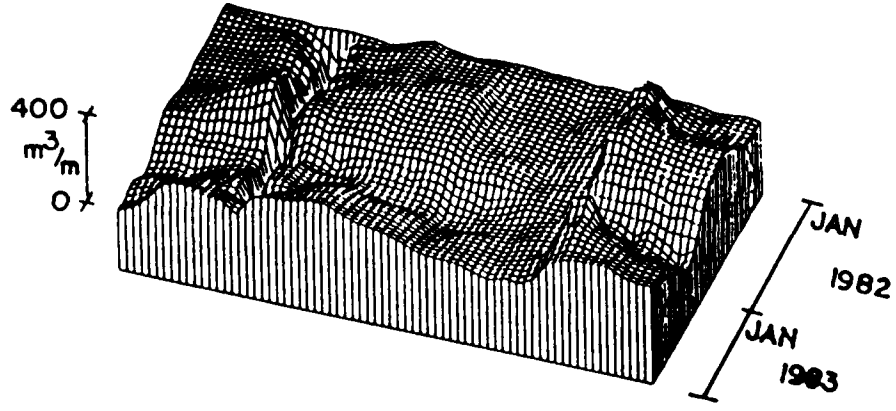

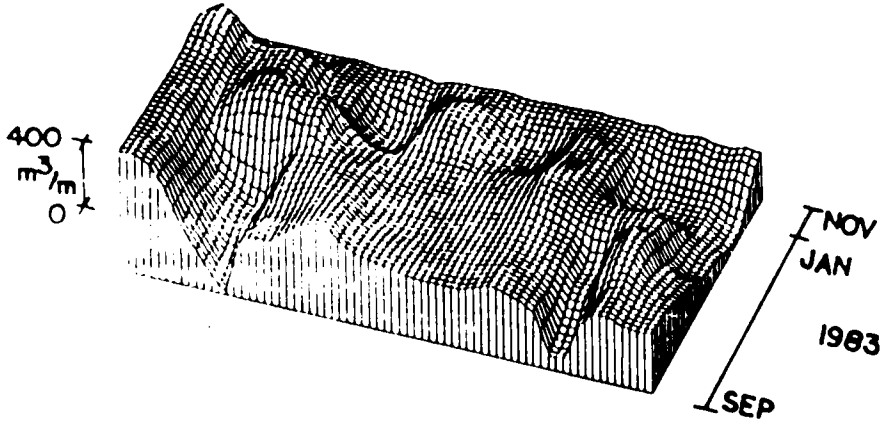

c. Entire control cell, Nov. 1982 - Sep. 1983
(c.f. Fig. 23)

Figure 26. Nomenclature and schematic diagram for the summer profile of the shore zone of coasts with sea cliffs. Storm waves modify the beach profile as shown by the storm bar and scarp (after Inman, 1971).

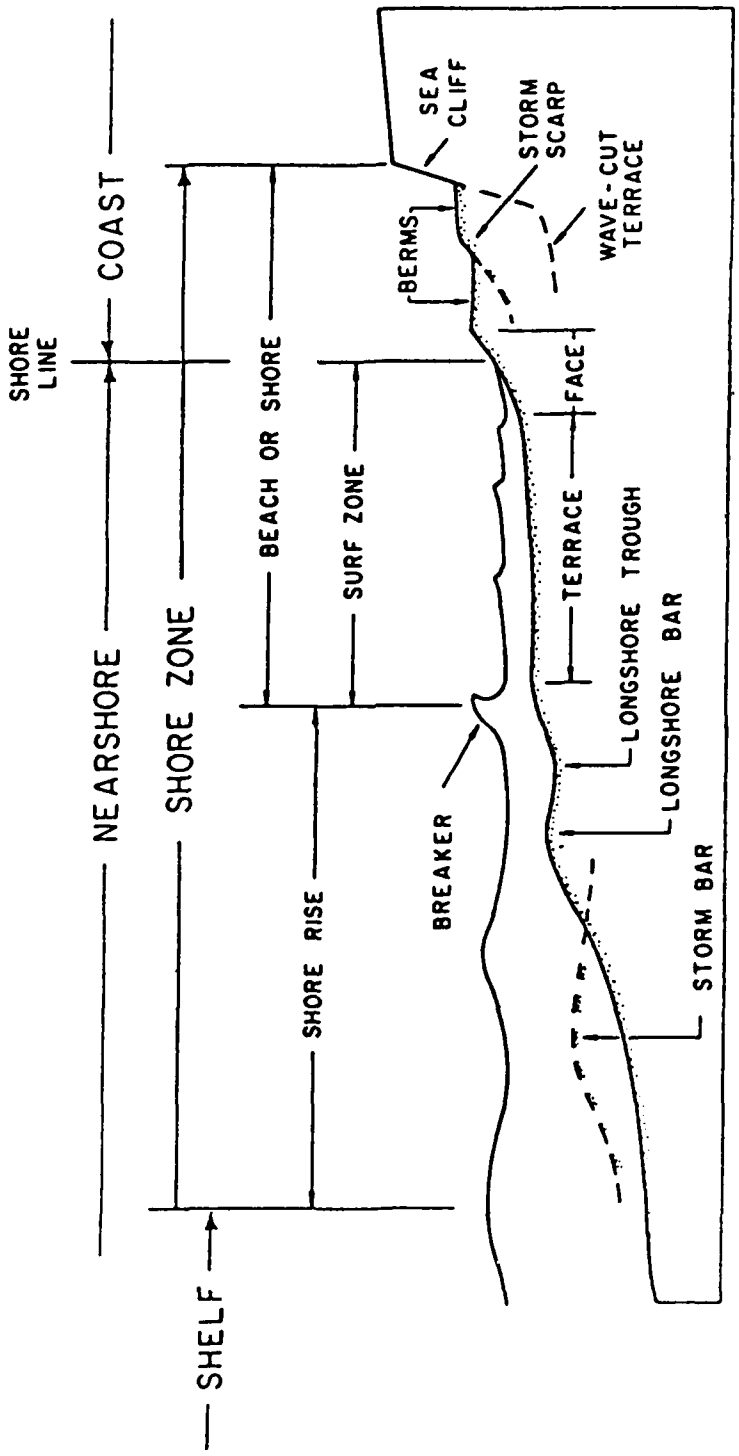
SEA CLIFF
STORM SCARP
WAVE-CUT TERRACE
BERMS
COAST
SHORE LINE
BEACH OR SHORE
FACE
SURF ZONE
TERRACE
LONGSHORE TROUGH
LONGSHORE BAR
NEARSHORE
SHORE ZONE
BREAKER
SHORE RISE
STORM BAR
SHELF

Figure 27. Idealized x-t diagrams depicting simple cases of sediment dispersion from a river mouth. In each case, the contours show relative accretion per unit length of shoreline as time progresses.

a. Uniform bi-directional dispersion with net loss from control cell

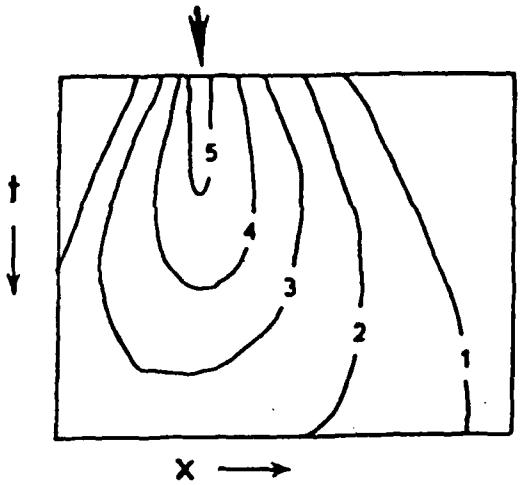

b. Unidirectional dispersion with net loss

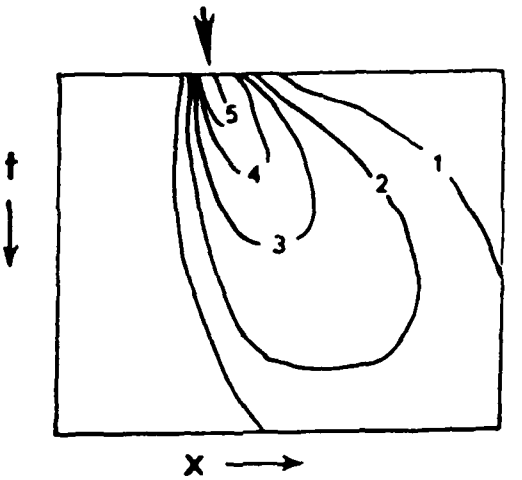

c. Unidirectional dispersion with net gain

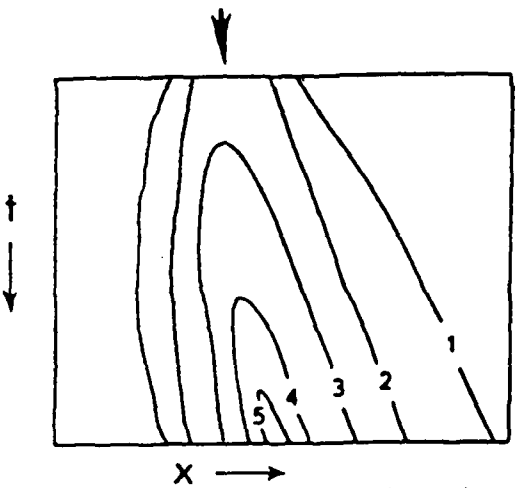

d. Sandwave propagation; no dispersion; no net gain or loss

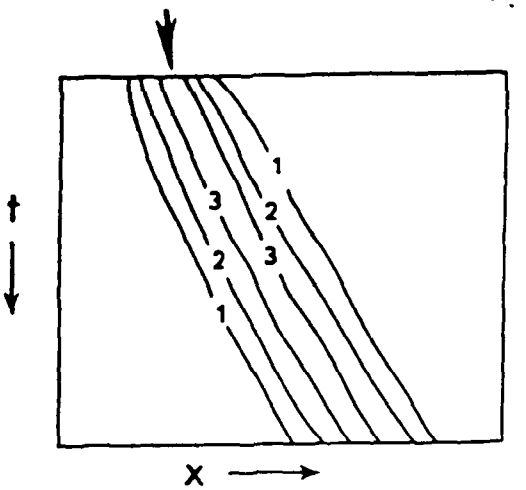

e. Bi-directional dispersion with net gain

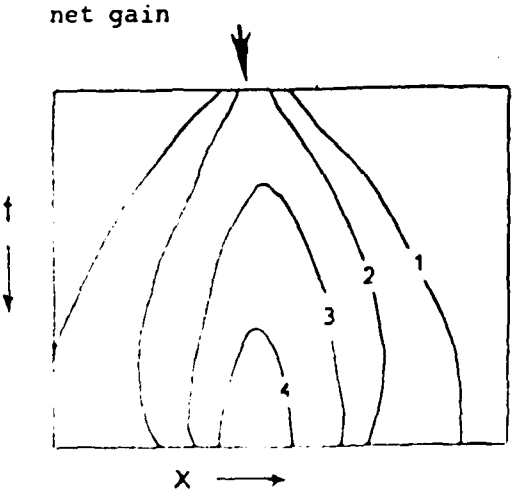

River mouth position

t time

X distance alongshore

4 Contour of cumulative volume change since t = 0

deposition; the spring-summer 1982 reworking of the delta by swell waves; the fall 1982 episode of longshore movement; the 1982-83 winter period of coastal storms and high riverflow that resulted in beach erosion and delta rebuilding; and the spring-summer 1983 period that saw recovery of the beaches, reworking of the delta, and longshore migration of the river sand.

January 1982

The dominant event in January 1982 was the flood which built the delta off the river mouth. While high storm waves occurred concurrently with the flood on 3-4 January, they apparently induced little dispersion of the delta sediment and little change in the beaches away from the river mouth. Some eastward transport is indicated by the sand trapped in the harbor entrance but the refraction analyses suggest much of the littoral drift was confined within individual sub-cells.

The river apparently behaved something like a plane-jet during the flood (c.f. Figs 3a and 19a). It dominated the concurrent wave conditions, scouring a deep hole at its mouth and depositing an offshore bar elongated in the offshore direction. The profile off the river mouth on 30 January, plotted in Fig. 17b, shows the offshore bar and must approximate the centerline cross-section under the flood outflow. Fig. 18a shows the river mouth morphology on 30 January. The eastward deflection of the outflow and the connection of the bar to the west beach suggest that waves approaching obliquely from the west had already begun to reshape the flood deposit.

Away from the river mouth, morphologic changes through January can only be "hindcast" from the 30 January and later beach surveys, since

there was no pre-January survey. Fig. 17a suggests little change occurred on the western beach. Fig. 17d suggests the eastern beaches were slightly eroded during the early January storm but they recovered quickly, as evidenced by a low offshore storm bar and a possibly new berm on the 30 January profile.

As shown in Fig. 22, the control cell as a whole gained a considerable sand volume through January and this was concentrated offshore of the river mouth. In contrast, Fig. 24 shows how the "visible" beach lost sand due to flood scour at the river mouth.

Spring-Summer 1982

The spring-summer period of 1982, from February until September, saw mainly onshore reworking of the delta deposit by swell waves, plus some superimposed, mainly eastward, longshore dispersion. No major coastal storms struck during this period. The river continued to supply sediment in significant quantities until May. Sand was continually trapped in the harbor entrance, but in comparatively small quantities. Close to 100,000 m^3 was dredged from the harbor entrance channel between February and June and was released subaerially at the west end of Twin Lakes Beach. The total sand volume in the control cell remained essentially constant after February. There was a net loss off the river mouth, balanced by a net gain on the beaches to either side. This gain was weighted to the eastern beaches. In contrast, the "visible" sand volume grew steadily due to shoreward sand migration around the river mouth and to the placement of the harbor dredge spoil on Twin Lakes Beach.

At the river mouth, as shown on Figs 17b and 18, the offshore bar grew in elevation, migrated shoreward, and apparently "bent" around into the channel throat. The January flood scour-hole was filled partly with this material and partly with sand dropped by the waning river flows. By June, the center of the river mouth was sufficiently plugged with sediment that a secondary high-tide outflow-channel was forced open to the west of the main bar. Through the entire spring-summer period, there was also a continual shoreward migration of small longshore bars, spaced several meters apart and composed of coarse sand and fine gravel, all around the river mouth area. This sediment apparently came from two sources: fresh deposits at the mouths of the low-flow and tidal channels, and the main flood delta deposit to seaward. The end result of these bar migrations was a high berm and prograded shoreline around the river mouth.

Longshore sand dispersion from the river mouth is demonstrated in Figs 21b-e. The bulk of the sand appears to have dispersed eastward. Westward dispersing river sand converged with sand arriving from upcoast on the western delta flank. The resultant accretion was spread across the whole nearshore zone. For some periods, e.g. February-early March, the eastward dispersing river sand appears to have been confined within the eastern delta convergence zone. In other periods, e.g. March-April, the river sand undoubtedly "leaked" eastward, across the width of the nearshore zone, into the Seabright Beach sub-cell.

Through the entire period, there was a superimposed onshore migration that saw much of the "leaked" river sand accreted to the Seabright Beach berm. This is demonstrated best on Fig. 21b-e. Through

most of this period, there was a general tendency for erosion at the eastern end of Seabright Beach and accretion off the harbor jetty, as predicted by the refraction analysis. However, some eastward "leakage" past the breakwater is evidenced by the continued trapping of sand in the harbor entrance.

The changes to Twin Lakes beach in March-June were dominated by the input of the harbor dredge spoil. While this sand was released subaerially onto the beach face, it quickly dispersed offshore and alongshore. From June onward, some of the sand that had dispersed offshore was returned to the beach face. As seen on Fig. 17e, the sand volume under Rangeline 8, 150 m east of the outflow pipe, peaked in June, soon after the dredging was completed, and gradually decreased thereafter. Fig. 22a shows the locus of maximum accretion migrating eastwards with time, indicating that the dredge spoil moved along Twin Lakes Beach as a sandwave. The similarity between Figs 22a and 24a for this location demonstrate that the bulk of the sandwave moved along the beach face.

Fall 1982

During the 1982 fall, from September through November, the river flow and sediment yield were essentially nil and the coast received generally mild swell. Onshore migration continued about the river mouth, but the dominant sand movements appear to have been longshore, to the east. The control cell gained sand around and west of the river mouth, but lost sand east of the harbor. The total sand volume in the control cell increased slightly.

At the river mouth, the shoreward migration of small bars continued. These welded to the beach face, building a high berm (Fig. 17b) and sealing-off all channels but the main low-flow river channel (Fig. 18d). Accretion was greatest on the western delta flank, the result of the delta ponding sand transported from the west, both inside and outside of the surfzone, as shown on Fig. 21f. Lesser accretion occured on the eastern delta flank in the zone of transport convergence predicted by the refraction analysis.

On Seabright Beach, an overall sand gain indicates that sand must have "leaked" eastward from the delta sub-cells. The accretion-erosion patterns observed there can be reconciled with the predicted patterns (Fig. 15), provided the predicted accretions are smeared alongshore somewhat.

A general sand loss occurred off Twin Lakes Beach: the result of eastward transport and insufficient replenishment from the west. The harbor continued to trap small amounts of sand. The sand volume changes on the "visible" beach were similar to those across the whole control cell width.

Winter 1982-1983

The 1982-83 winter period, extending from December through to April, saw high river flows and sediment yields, and concurrent destructive coastal storms. The high sediment yield from the river rebuilt the subaqueous delta, and was spread over a wider area compared to the previous winter. The highest storm waves in December-January flattened and eroded the visible beach and built offshore bars. Some beach recovery occurred in February-April. A strong easterly longshore

transport was superimposed through the whole period: it caused significant net accretion west of the river mouth, eastward migration of delta material onto Seabright Beach, and net erosion east of the harbor. The harbor entrance trapped sand until, by late January 1983, it was almost completely shoaled. It was subsequently dredged and the spoil assisted the recovery of Twin Lakes Beach. The control cell volume increased, but not as fast as sediment was apparently supplied by the river. This indicates a net loss of sand to eastward transport and perhaps to offshore.

Conditions and processes around the river mouth during the height of the severe coastal and hydrological storm of 27 January 1983, a day when waves exerted a major control on sedimentation, are sketched in Fig. 28 and described below. The 2-3 m high storm waves approached obliquely from the southwest. The river outflow, stained by suspended mud, was deflected diagonally eastward off Seabright Beach at both high and low tides. Strong eddies circulated at the western corner of Seabright Beach, exacerbating erosion. A strong eastward longshore current swept the surfzone of the eastern two-thirds of Seabright Beach and ran seaward as a rip past the western harbor jetty. This rip intersected the river effluent stream some distance off the breakwater and dispersed it further seaward. Logs, brought by the river, were strewn along Seabright Beach while only a few were observed west of the river mouth - further evidence of the dominantly eastward currents. When observed at low tide, the river flowed between broad flat levees before deflecting eastward inside of a broad submerged bar. The waves broke across this bar which extended obliquely shoreward to the western beach, almost parallel to the approaching wave crests.

Figure 28. Field observations at the San Lorenzo river mouth during the storm of 27 January 1983. (a) At high tide at 0830 hours. (b) At low tide at 1500 hours.

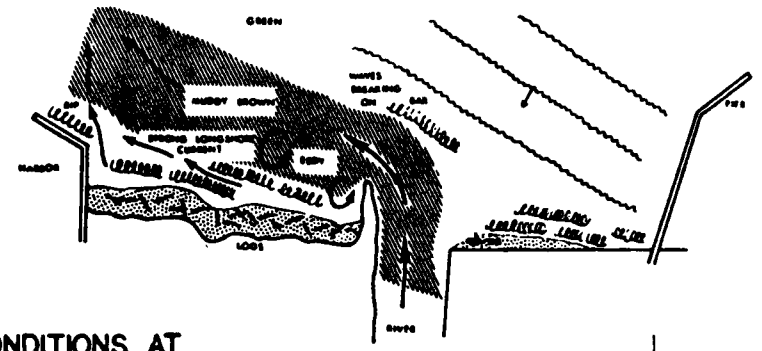

CONDITIONS AT
HIGH TIDE

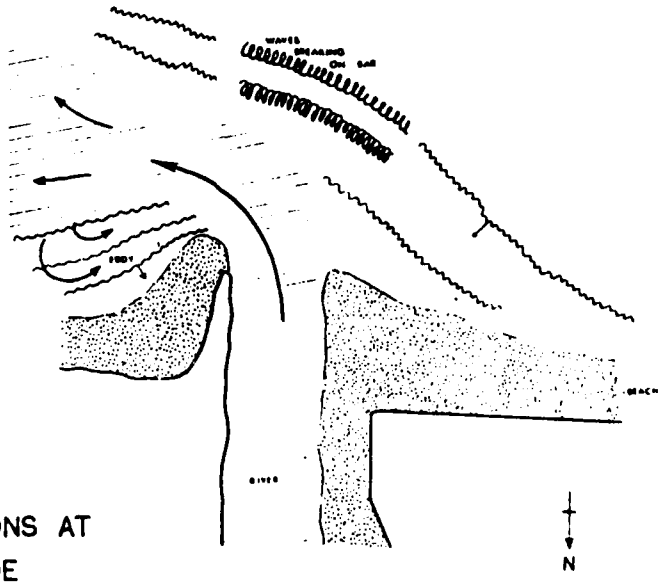

CONDITIONS AT
LOW TIDE

This description, and the results of the refraction analysis, help explain the winter period accretion/erosion patterns shown in Fig. 21g. The most obvious features on this plot are: the ubiquitous cross-shore transfer of sand from the beach face to an offshore bar, the result of storm waves and high tides; and the broad zone of offshore accretion opposite and west of the river mouth.

The net accretion observed off Cowell Beach and the western delta flank must have resulted from longshore transport convergence. Fig. 17a shows how the bar volume there greatly exceeded the volume eroded from the beach face: this imbalance can only be supported by lateral influxes of sand. Presumably, littoral drift from the west initially stalled in the surfzone; then it was moved to the offshore bar. This situation is the reverse of that observed during the previous summer, when stalled drift moved shoreward to accrete on the beach face.

The widespread deposition off the river mouth can be explained by initial deposition of part of the river's sand load on the river mouth bar, and its subsequent removal further offshore by the storm waves. The combined effect of exceptionally low tides and very high waves saw the river sand spread further offshore than during the previous winter - out of the control cell, in fact. The locus of maximum deposition on the delta must have varied in response to the oscillating dominance of river and wave forces, the size and position of the river mouth bar, the state of the tide, and the dynamic feedback between all of these controls.

As noted in section 4.1, the river yield estimated for the 1982-83 winter period differed significantly from the net deposition. Three

explanations are offered to account for the apparent surplus of river sand. The first is that the river yield might be overestimated, as discussed previously. The second explanation is that river sand dispersed rapidly eastward, at least some ending up on the large bar off Seabright Beach. The third alternative is that the delta suffered net erosion, losing sediment alongshore, before the larger river flows and sand inputs occurred in mid January. This is predicted by the refraction analysis (Fig. 15). Probably, all explanations apply.

Twin Lakes Beach was eroded severely during the storms of January-February 1983, as shown in Fig. 17f. There, insufficient sand was available above the wave-cut bedrock terrace and fronting the seacliffs to form an adequate wave-energy-dissipating storm bar. This factor, plus the high tides, saw the waves reach and reflect off the low cliffs and riprap seawalls. As a result, the shoreline was essentially stripped of sand. Much of the eroded sand was lost to eastward transport.

Spring-Summer 1983

February-April 1983 saw the beaches begin to recover with the onshore exchange of sand between storm bar and berm. The river's sand yield continued to be high; much of it was apparently dispersed and deposited east of the delta, although the delta's seaward margin also accreted. The central delta lost sand, apparently to shoreward and eastward. The center of the river mouth rapidly became choked with coarse sand and fine gravel so that a secondary high-tide and high riverflow channel opened to the west. This caused some erosion of the face of Cowell Beach. Net accretion occurred at the east end of

Seabright Beach, probably a result of longshore transport convergence, and on Twin Lakes Beach, due to the input of spoil from harbor dredging.

From May through September, the riverflow was insignificant, and the dominant wave condition was mild swell. This period saw the continued recovery of the beach faces as sand migrated shoreward between bar and berm. It also saw some major eastward sand migrations that resulted in widespread erosion across the delta and a net sand loss from the control cell. Although there were no directional wave data available for this period, the direction of net transport is apparent from the accretion-erosion patterns (Figs 21 i and j). The visible beach gained sand almost everywhere; the greatest accretions occurring around the river mouth as delta sand was moved shoreward. By September, a high broad berm, cut only by a small outflow channel, fronted the river mouth.

The sand losses from the delta were significant, particularly between the April and June surveys when the average erosion across the outer 500 m was about 1 m and over 100,000 m^3 was lost. Both eastern beaches experienced a net gain in sand as a result of this migration. It was apparent from the distribution of pebbles and coarse angular sand in swashzones of Seabright and Twin Lakes Beaches that the delta sediment had moved all the way through the control cell; it had not simply replaced the sediment transported from the beach beside the delta. This longshore dispersion of delta sand contrasts with the situation of the previous year when the vast bulk of the river yield remained opposite the river mouth. Probably the greater spread of the delta in 1983 induced less refraction and less transport divergence.

At Twin Lakes Beach, the harbor dredge spoil again migrated along the beach face as a sandwave, as indicated in Figs 17f, and 22-24.

Interestingly, Fig. 21j shows accretion seaward of the 8 m isobath along much of the control cell. This may indicate the shoreward return of sand that was originally moved far offshore from the control cell by the winter storm waves. More likely, it shows an influx of "fresh" sand that was moved by storm waves around Point Santa Cruz, in relatively deep water, and dispersed into the Santa Cruz Bight.

4.3.2 Summary of Sand Movements and Volume Changes

The x-t plots, Figs 22-25, the block diagrams on Fig. 20e, and the isopach maps on Figs 21 a, k, and l, summarise the sand movement trends and volume changes within the control cell through the study period.

Through most of 1982, delta sediment of the January 1982 flood dispersed only a short distance alongshore; the bulk of it remained opposite the river mouth (Fig. 22). The beaches to either side of the delta gained only a small volume of sand. In contrast, the spring harbor-dredging spoil migrated eastward along Twin Lakes Beach as an attenuating sandwave. A comparison of Figs 21 a and k shows that the dominant sand movements around the river mouth during this period were onshore: the end result was a prograded shoreline and a plugged river mouth. Even so, the sand that migrated shoreward represented only a slice from the delta top; much of the delta material remained offshore, invisible to a casual observer. From late 1982, Cowell Beach and the western delta gained sand as littoral drift from the west was trapped against the delta (Figs 22 and 23).

The whole delta grew through the stormy months of January-April 1983, gaining sediment from the river and from longshore transport. Concurrently, river sediment dispersed eastward and everywhere the beach face eroded. The eastward dispersion continued through the spring-summer of 1983 when the river ceased contributing sediment. The result was a significant sand loss from the delta but sand gains on the beaches to the east. (The direction of the dispersion is evident from the trends of the iso-volume contours on Fig. 23.) At Twin Lakes Beach, the spring harbor-dredging spoil again migrated eastward as a sandwave, filling-in the scour-hole that was eroded by the 1983 winter storm waves as it progressed.

Between September 1982 and September 1983, the control cell gained sand (Fig. 21 1). The large gains west of the delta occurred at two nodes: a nearshore node, consisting of trapped littoral drift; and an offshore node, consisting of dispersed river sand or perhaps sand migrating shoreward following a headland by-passing event. The delta lost sand, but this was balanced by accretion all across Seabright Beach. Twin Lakes Beach lost sand, possibly as a result of the continuity imbalance created by the ponding of littoral drift west of the delta.

4.4 Extended Discussion

Several phenomena stand out from the study results and will be expanded upon. These include the effects of the river flood-delta on the local nearshore regime, the importance of cross-shore sand movements

in the longshore migration of the river sand, the bulk sand dispersion patterns, and the morphologic cycle followed at the river mouth.

4.4.1 Effects of the Delta on the Local Nearshore Regime

The presence of a subaqueous flood-delta off the San Lorenzo River mouth had several effects on the local beaches and on the longshore transport past them. These include the division of the shoreline into several littoral sub-cells, the ponding of littoral drift west of the delta, some erosion east of the delta, and an overall gain in sand.

The change that the delta induced in the local longshore transport patterns is best appreciated by comparing the transport predictions for "delta" and "no delta" bathymetries, shown in Figs 14 and 16. Without the delta, the net transport should have been eastward everywhere around the river mouth. With the delta, the net transport directions reversed locally. The resultant transport convergence caused beach accretion on both sides of the delta, particularly on the west side, where, for a time, apparently all littoral drift entering the control cell from the west was stalled. The sand losses observed at times on the beaches east of the harbor can be partly blamed on the resultant continuity imbalance.

The amount of littoral drift ponded against the western side of the delta was estimated with the aid of two approximations. These concerned the boundaries of the accretion zone and the accretion patterns along the unsurveyed part of Cowel Beach west of the control cell.

The criteria for defining the eastern boundary of the accretion zone changed with time, depending on whether reversed, westerly, transport occurred along the west flank of the delta. If so, the boundary must occur at the point of transport reversal where the easterly transport along Cowell Beach met westerly transport from the delta. If not, the boundary must lie at the point of minimum easterly transport on the delta's west flank. Inspection of Figs 14 and 15 suggests that the average position of this eastern boundary was about 1000 m west of the wave array.

Two approaches were used to estimate the accretion patterns west of the control cell, along Cowell Beach. The first, conservative, approach involved linear extrapolation of the surveyed accretion trend at the western end of the control cell. The second, less conservative, approach assumed that the accretion zone was 750 m long and the accretion decreased linearly west of the control cell.

The results suggest 40,000-90,000 m^3 accretion for January-November 1982, and 170,000-230,000 m^3 accretion for December 1982 - September 1983. Even with a factor of 2 uncertainty assigned to these figures, they show that the delta trapped a significant portion of the expected littoral drift arriving from the northwest around Point Santa Cruz.

The sand gains within the control cell through the study period, recorded in Figs 10 and 22b, therefore reflect inputs from the river and from longshore transport. Apparently, most of the sand supplied by the river was retained in the control cell. As time went on, the largest sand gains passed from the delta area to the eastern beaches. The only significant net loss occurred to eastward longshore transport in the

spring of 1983. Even after this, every segment of the control cell contained more sand at the end of the 21 month study period than at the beginning.

In contrast, the "visible" portion of the control cell, the area above the mean lower low water level, gained and lost sand seasonally, as shown in Fig. 24b. While the summer gains far outweighed the winter losses, the overwhelming abundance of sand in the control cell was not obvious. This surplus sand, to a large degree, protected much of the shore from erosion during the 1983 winter storms as it sat offshore on large wave-energy-dissipating storm bars. Only the beaches east of the harbor suffered a net sand loss during this period. This loss was undoubtedly exacerbated by the continuity effect of sand accretion against the delta and by the slow migration of river sand eastward from the delta through 1982. The arrival of significant volumes of river sand at the harbor appeared to lag the river floods by about a year.

4.4.2 Longshore and Cross-shore Sand Movements

The longshore movement of sand away from the river mouth was apparently not restricted to transport within the surfzone. Net longshore translations often accompanied cross-shore migrations to and from deeper water. Even if the transport was more rapid within the "littoral river of sand", it was apparent that the supply of sand to the surfzone was regulated by the cross-shore migrations. For example, the greatest longshore movement by far occurred in the spring-summer of 1983, in conjunction with the shoreward return of sand dispersed offshore by the past winter's storms (Fig. 21i). The erosion-accretion

patterns across the control cell clearly demonstrate that this shoreward migration had a longshore component, while the composition of swashzone sediments indicated that some river-derived sediment was also quickly sluiced alongshore within the surfzone.

In terms of total sand fluxes, the cross-shore sand movements were of the same order of importance as the longshore movements. On-offshore transports associated with the seasonal sand exchanges between berm and bar are shown in Fig. 29. The magnitudes of these sand fluxes varied alongshore, ranging from 500 m^3 per m beach length at the delta to 100-200 m^3/m elsewhere. The average seasonal flux, about 250 m^3/m, when taken over 1 km of shoreline and twice per year, represents a gross annual cross-shore flux of 500,000 m^3.

Even modest longshore components to these cross-shore migrations would result in significant sand shifts alongshore. For example, seasonal cross-shore sand fluxes of 500 m^3 per m shore length, migrating at a 20° angle to the shore normal over a bar-berm separation distance of 300 m, incorporate a longshore flux of 109,000 m^3 per year. We can visualize these cross-shore events remobilizing sand "stalled" in the nearshore zone at sites of longshore transport convergence - thus providing a mechanism for "leaking" sand between littoral sub-cells.

4.4.3 Bulk Sand Dispersion Patterns

The integral role played by cross-shore transport must account for some of the complexity in the overall pattern of sand dispersion from the river mouth, shown in Figs 22a and 23. Nonetheless, after making allowances for seasonal changes, fresh inputs of river sand, and

Figure 29. Longshore variation in on-offshore sand fluxes as approximated by the seasonal gains and losses of sand on the onshore and offshore segments of the surveyed beach profiles. (a) Onshore sand migration over the summer season between January and November 1982. (b) Offshore sand migration over the winter season between November 1982 and January 1983. (c) Onshore sand migration over the summer season between January and September 1983.

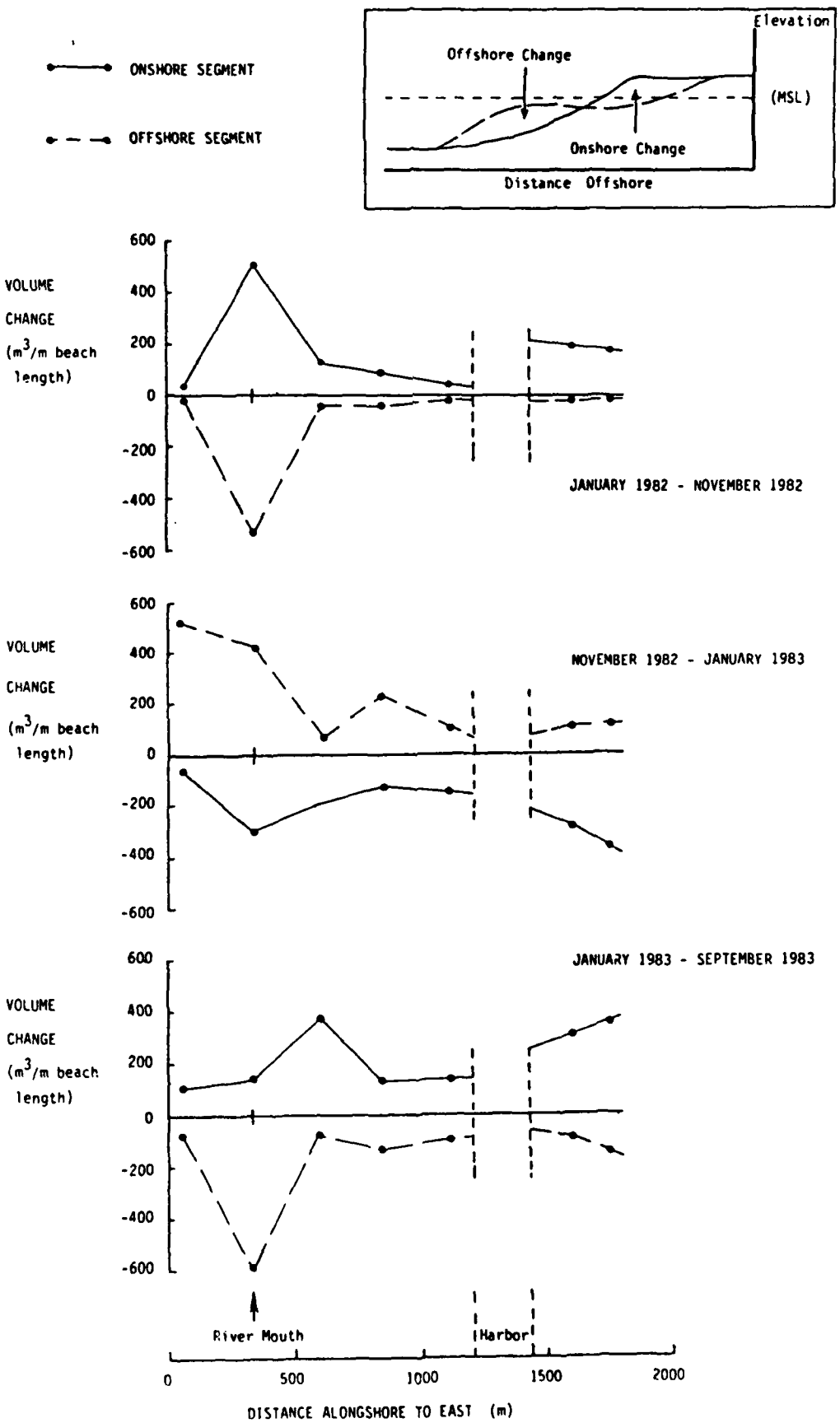
ONSHORE SEGMENT
OFFSHORE SEGMENT
Elevation
Offshore Change
(MSL)
Onshore Change
Distance Offshore
VOLUME CHANGE (m^3/m beach length)
600
400
200
0
-200
-400
-600
JANUARY 1982 - NOVEMBER 1982
NOVEMBER 1982 - JANUARY 1983
JANUARY 1983 - SEPTEMBER 1983
River Mouth
Harbor
0
500
1000
1500
2000
DISTANCE ALONGSHORE TO EAST (m)

drift-ponding west of the delta, the overall pattern off the river mouth is similar to the sandwave pattern left each year on Twin Lakes Beach by the eastward-dispersing harbor-dredge spoil and to the idealized sandwave patterns in Fig. 27. The Twin Lakes Beach sandwave was clearly defined and was moved along the beach face by surfzone longshore transport. However, it was small enough to be destroyed in the winter by large cross-shore movements. In contrast, the much larger sandwave off the river mouth, extending across the whole nearshore zone, relied, to some extent, on cross-shore sand movements as its means of propagation and dispersion. Consequently, its signature was more diffuse over the time and length scales of the study.

A year after completing the surveys, in the summer of 1984, observations by the author and by local residents showed considerable recent sand gains along the shore for several km east of the control cell. There, continuous sandy beaches were present for the first time in many years. These observations support the picture of a progressive, albeit dispersing, sandwave originating from the 1982-83 San Lorenzo River floods. The celerity of this mega sandwave was of the order of 1,000 m/year. The x-t plots show the short-lived dredge-spoil sandwaves moving along Twin Lakes Beach at similar rates, about 50-100 m/month (600-1200 m/yr).

In order for any sandwave to propagate alongshore, there must be some mechanism operating that causes the longshore transport rate to vary alongshore in phase with the sandwave form. In the case of the dredge-spoil sandwave, there is a suggestion in the 1982 predictions of longshore transport potential in Fig. 13 that the necessary transport

divergence was induced, in part, by refraction across the sandwave bathymetry. Sand supply effects also must have contributed to the transport divergence pattern there since the harbor trapped part of the sand supplied from upcoast. In the case of the wave of river sand, the propagation mechanism may lie partly in the longshore-varying magnitude of the cross-shore transport fluxes, shown in Fig. 29, and their longshore components. Intuitively, the cross-shore fluxes should be larger where the bathymetry deviates most from the concave-up equilibrium profile, and where refraction focusses wave energy, as at the river delta.

4.4.4 River Mouth Morphology

The river mouth morphology followed a cyclic seasonal pattern which repeated twice over the study period. Stages of its morphological evolution are shown in Figs 18 and 19.

Each winter, the high river flows scoured the channel throat and deposited the scour-debris with additional coarse sediment brought from upstream onto a subaqueous bar off the mouth. From the bar, sand was further dispersed by storm waves and so the delta was built. As the river flow waned, swell waves caused the main bar cresting the delta to migrate shoreward towards the river mouth, building it higher in the process. Concurrently, longshore transport converged at the western end of this bar: the resultant deposition attached the bar to the western beach.

By late spring in both years, the main bar feature occupied the center of the river mouth, filling the flood scour-hole along with

sediment dropped from the lower river flows. This central plug forced the temporary opening of a secondary outflow channnel to the west. By late summer, however, the secondary channel was closed off. Sand, in the form of small bars, continued to migrate shoreward from off the delta through both summers. These bars eventually welded onto the beach face, building a berm and locally prograding the shoreline.

It is interesting how the major shoreward sand migration occurred under the one large bar that originated during the flood deposition process. It is also interesting how, in planform, the bar apparently rotated 180° as it migrated from its initial construction site offshore to its eventual terminus in the river mouth, as suggested in Figs 18a-c and e-f.

By the end of each summer, the river mouth - delta shoreline had attained a low-amplitude cuspate planform. Theoretically, such a planform is expected only where the ratio of river sand supply to longshore transport potential is low (Grijm 1960, 1964; Bakker and Edelman, 1964). At Santa Cruz, where this ratio was close to unity when averaged over the study period, the planform actually reflects the low rate-of-return of river flood sand - sand that had initially overshot the shorezone with the flood outflow - from offshore, under the regulation of the cross-shore transport potential.

Each year, the net accretion on the "visible" beach at the river mouth was only about one quarter of the preceding winter's supply of river sand. Given no further high yields of river sediment in the next few years, and an approximate balance between the cross-shore and longshore transport potentials, we might expect this modest local

progradation of the summer shoreline to persist for a number of years until most of the delta deposit has been brought ashore. Over this period, the shoreline perturbation might be expected to migrate unobtrusively alongshore - due to net easterly longshore surfzone transport and an easterly creep associated with cross-shore sand movements.

4.5 Conceptual Model for River Sand Dispersion

From the preceding description and discussion a conceptual model for dispersion of the San Lorenzo delta sediment is synthesized.

Following the initial wintertime deposition of the sediment from the flood flows, two processes act to disperse it: longshore motions within the surfzone immediately transport sand alongshore, and cross-shore motions induced by storm waves generally disperse sand offshore. The opportunity for longshore transport of river sand by surfzone processes is limited as the combined effects of riverflow inertia and storm waves see the bulk of the sediment yield deposited seaward of the surfzone. Furthermore, the rapidly-growing submerged offshore delta causes wave refraction which increases longshore transport convergence on either side of the river mouth. The result is that much of the initial littoral drift from the delta is trapped within the newly-created littoral sub-cells. Also trapped is littoral drift from the beach upcoast. This upsets the pre-flood continuity of longshore transport past the river mouth and sometimes results in sand losses from beaches downcoast.

In the subsequent summer season, swell waves return a portion of the delta sand shoreward. Any longshore component to this migration induces a net longshore-shift of the flood deposit as a whole. The sand is liable to be moved rapidly alongshore as it recrosses the surfzone. Some of the sand passing the surfzone is trapped in the flood-scour hole left in the river channel throat - and remains there until removed by the next flood. Concurrently, sand accumulations on the delta flanks, deposited by convergence of longshore transport, alter the delta

bathymetry and so also the wave refraction. The transport convergence is reduced and more sand may be able to by-pass or escape eastward from the delta. Winter storm waves focus on and attack the prograded shoreline around the river mouth, returning sand offshore again.

The cycle should repeat over several seasons until the flood delta material is dispersed alongshore and the bathymetry off the river mouth is in general equilibrium with the wave climate - or until another flood occurs. The overall pattern of bulk longshore dispersion of the delta is that of a progressive attenuating sandwave. Its propagation is driven by two mechanisms: the regular surfzone longshore transport, and a net creep associated with longshore components of the seasonal cross-shore migrations.

The complexity of process involved and the currently limited state of integrated longshore and cross-shore transport theory render impractical the quantitative testing of this model.

5. GENERAL APPLICATION OF RESULTS: COMPARISON WITH OTHER CALIFORNIA COASTAL DELTAS

In many respects, the events studied at Santa Cruz are typical of the general problem pertaining to river sand delivery to the California Coast: a large flood, of long return period, introduced a large volume of sediment to a coastline normally dominated by a regularly-operating longshore transport regime. The study was exceptional in that there were two consecutive years of high river sediment yield and also a period of extreme coastal storms. However, if anything, the second season of river floods and the coastal storms provided a clearer, "accelerated", picture of the dominant processes that incorporate the river sand into the longshore pathway.

The 1982 San Lorenzo flood and delta are compared with some previously studied Southern California examples in Table III. Perhaps the least representative aspect of the present study was the size of the river sediment outputs - the San Lorenzo River events were small compared to those at the other rivers. For example, the 10 million m^3 volume delta built by the 1969 Santa Clara River floods was 30 times larger than the 1982 San Lorenzo River delta.

The San Lorenzo delta was also exceptional in terms of its relative cross-shore and longshore dimensions. While it was elongated across-shore, the Southern California deltas were elongated alongshore. This difference must reflect the relative dominance of river flow inertia at the San Lorenzo mouth, a product of the high ratio of flood

Table III. California coast flood-delta comparisons

River	Mean Flow (m^3/sec)	Flood Period	Peak Flood Flow (m^3/sec)	Flood Return Period (yr)	Delta Volume ($10^6 m^3$)	Delta Length Along-shore (m)	Delta Width Off-shore (m)	Delta Limit of Deposition (m below MLLW)
San Lorenzo+	3.8	Jan 1982	840	30	0.3	400	700	11
Santa Clara*	4.1	Jan-Feb 1969	4670	100	10.1	1500	600	~15
Santa Ana*	1.3	Jan-Feb 1969	540	~50	2.2	1200	600	11
San Juan Ck*	0.7	Jan-Feb 1969	630	75	1.1	1000	400	6

\+ Data from this study

* Data from USACE, LAD (1970)

flow to sand yield, steep floodplain gradient, and narrow outlet channel (c.f. Figs 3 and 18).

Because of these differences in scale and geometry, the southern deltas also show some morphologic and behavioural differences. However, it appears that the same basic processes and mechanisms operate to move sand from the river mouth alongshore. In this, as at Santa Cruz, cross-shore sand transport and divergence patterns in the longshore transport potential play a major role.

The morphologic evolution, transport processes, and bulk sand migration mechanisms typical of several Southern California deltas are suggested schematically in Fig. 30. This figure was synthesized from maps, aerial photographs, and descriptions of the mouths of the Santa Clara, Santa Ana, and Ventura Rivers and of San Juan Creek presented by USACE LAD (1970) and USACE LAD (1980).

The behaviour of these river mouths is dominated by the morphologic evolution of the offshore bar. This bar is formed initially by the interaction of the river outflow and waves (Fig. 30b). After the river flood wanes, its evolution is dominated by wave action (Fig. 30c). Initially subaqueous, the bar gains height and becomes subaerial - a barrier island - as swell waves return river sand shoreward. Some sand is over-washed into the newly formed lagoon, while more sand is transported along the new shoreline. As a result, the bar migrates shoreward and a spit grows off its downcoast end.

The evolving nearshore topography and shoreline orientation induce changing patterns of longshore transport divergence. Transport

Figure 30. Morphological evolution of a typical Southern California river mouth following a flood.

a. Pre-flood

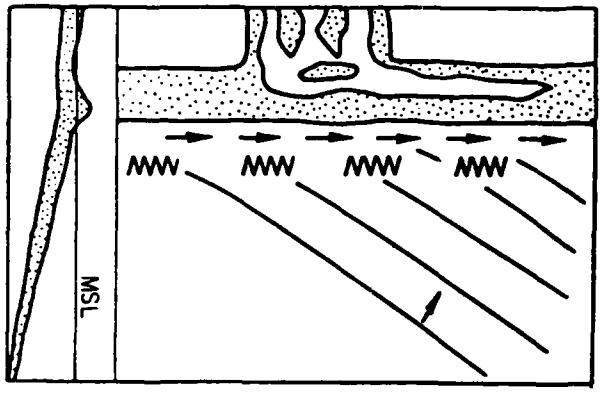

b. Flood

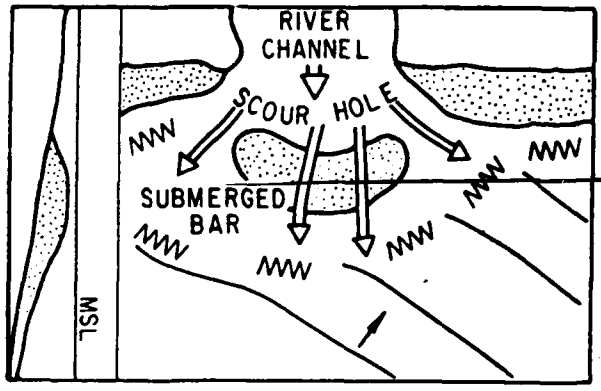

c. Several months post-flood

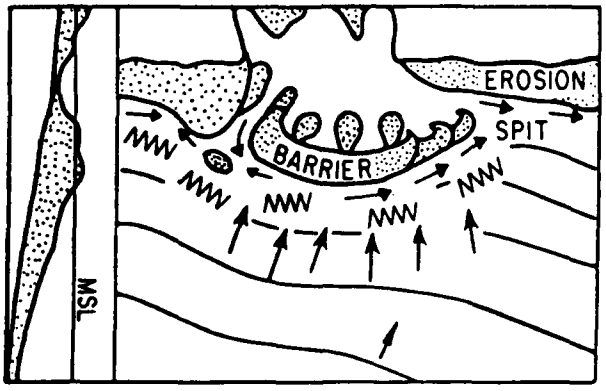

d. Several years post-flood

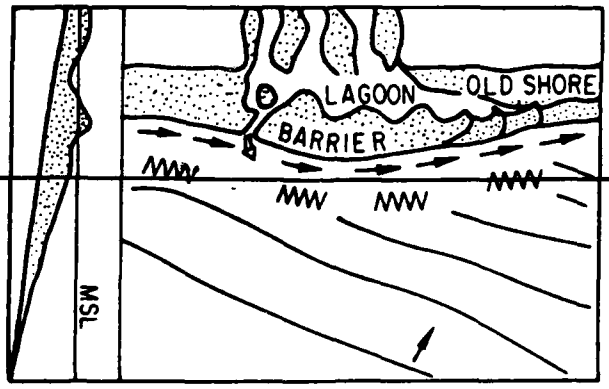

RIVER OUTFLOW

SAND TRANSPORT

WAVE CRESTLINE and DIRECTION

BREAKERLINE

convergence causes significant accretion on the upcoast beach and is also the mechanism for spit growth. Transport divergence occurs along the bar face as the wave incidence angle steepens in the downcoast direction. The shoreward-migration rates of the bar and spit reflect the excess of divergence-induced erosion over swell-induced accretion. Longshore transport divergence also causes a temporary phase of erosion on the downcoast shoreline. This ends when the spit welds to the old shoreline (Fig. 30d). Thereafter, the downcoast beaches experience a major phase of accretion. In essence, the spit becomes a ramp for sluicing sand onto the downcoast beaches from the sand supply zone - the area of maximum onshore transport at the bar apex. At this stage, with an essentially continuous shoreline again, the morphology and processes are similar to those observed at Santa Cruz.

As at Santa Cruz, the repeat surveys of the Southern California deltas show that only a portion of the total delta deposit is translated shoreward under the main bar form in the summer following the flood. The remaining sand returns shoreward, in mainly seasonal pulses, over several years (as Orme and Brown, 1982, suggested). As long as an approximate balance is maintained between onshore fluxes back to the river mouth area and longshore fluxes away from it, the visible signature of the submerged flood deposit might be obscure. Quite likely, a downcoast-moving shoreline erosion wave, initiated by the delta's ponding of the "background" littoral drift, might precede the passage of a subtle, dispersive, accretionary wave of river sand.

At the Southern California river mouths, the lagoons occupying the flood scour-holes behind the main bar become temporary traps for both

river and littoral sand. Low-flow deltas build from upstream, washover deltas build from the bar, and, until the outlet channel closes, sand can be transported into the lagoon by tide and wave action. The lagoon and lower river channel gradually accumulate sediment until they are flushed by the next capable flood.

6. CONCLUSIONS

The more important conclusions from this study are:

1. The 1982 and 1983 winter flood flows in the San Lorenzo River were exceptional in terms of return period and sediment yield. In both years, the river's supply of littoral-sediment-sized material was 10 times the mean annual supply and was probably equivalent to several times the mean annual longshore transport potential past the river mouth. As a result, the study conditions are representative of the general problem: the mechanism of incorporating the infrequently-delivered river sand supplies to the California coast into the more continuously-operating nearshore transport regime.

2. Only sediment coarser than about 0.18 mm is trapped in the nearshore zone at Santa Cruz. Through the study period, reasonable agreement was found between the yield of river sediment coarser than this "cut-off" size and accretion in the nearshore control cell about the river mouth. The estimated "littoral sediment load" of the river was equivalent to 28% of its total suspended load.

3. The river's sediment load was deposited initially opposite the river mouth on a subaqueous delta, the bulk of it seaward of the surfzone. This depositional pattern demonstrated the roles played by floodflow inertia and approximately concurrent storm waves in spreading much of the river sediment beyond the "littoral river of sand".

4. Bulk sand movements could be traced from incremental changes in bathymetry and from net longshore volume changes. These changes showed

how cross-shore movements, involving the entire nearshore zone, played an integral role in the longshore dispersion of the river sand - directly, through actual longshore components to the cross-shore movements, and indirectly, through the return of sand from offshore to the surfzone transport. In fact, the cross-shore transport potential served to regulate the shoreward return rate of the river sand.

5. The overall longshore-dispersion pattern shown by the river sediment through the study period - and observed afterwards - was that of a low-amplitude sandwave which migrated and dispersed gradually alongshore in the direction of the dominant longshore transport. The pattern of longshore-transport divergence necessary for the sandwave to migrate appeared to combine longshore variations in both the cross-shore sediment fluxes and the surfzone longshore transport.

6. Predictions of the longshore transport potential with and without the presence of a delta showed how, through wave refraction effects, the delta interrupted the continuous eastward motion of sand past the river mouth. For a time, the delta apparently divided the shoreline into several littoral sub-cells, each bounded by short segments experiencing net reverse transport. The surveyed sand volume changes generally supported this prediction but also indicated that sediment did "leak" alongshore from sub-cell to sub-cell. Transport convergence induced considerable accretion on the western delta flank.

7. By the second year of the study, the delta had broadened through the combined effects of transport convergence, further river sediment supplies, and sediment dispersion caused by storm waves. This

topographical smoothing apparently refracted the incident waves less, allowing accelerated longshore dispersion of delta sand.

8. The large inputs of river sand and the ponding of littoral drift from the west resulted in an abundance of sand within the control cell. This surplus sand was spread over the nearshore zone. While it's only visible effects were the wide "healthy" summer beaches, it also protected most of the beaches from severe erosion during the 1983 winter storms by providing the building material for large wave-energy-dissipating offshore bars. The exceptional erosion suffered by the beaches east of the harbor during these storms was undoubtedly exacerbated by the delta-induced break in longshore-transport continuity through the control cell.

9. Similar bulk sand transport mechanisms appear to operate at river mouths further south on the California coast. The flood deltas described there have been larger than the San Lorenzo delta. The morphologic response of this greater sand volume is a landward-migrating subaerially-exposed offshore bar and spit. Delta sand is moved shoreward to the bar face by swell waves. From there, it is transported along the spit to the downcoast beaches.

REFERENCES

Anderson, R.G., 1971, "Sand budget for Capitola Beach, California", M.S. Thesis, U.S. Naval Postgraduate School, Monterey, California.

Arnal, R.E., J.D. Dittmer, and R.C. Shumaker, 1973, "Sand transport studies in Monterey Bay", Moss Landing Marine Laboratory Technical Publication, p. 73-5.

Bailard, J.A., and S.A. Jenkins, 1982, "City of Carpenteria beach erosion and pier study", Final Report to the City of Carpenteria, April, 1982.

Bakker, W.T., and T. Edelman, 1964, "The coastline of river deltas", Coastal Engineering - 1964, A.S.C.E., Lisbon, p. 199-218.

Bakker, W.T., 1968, "A mathematical theory about sand waves and its application on the Dutch Wadden Isle of Vlieland", Shore and Beach, October 1968, p. 5-14.

Bates, C.C., 1953, "Rational theory of delta formation", Am. Assoc. Pet. Geols. Bull., vol. 37, p. 2119-2162.

Bowen, A.J., and D.L. Inman, 1966, "Budget of littoral sands in the vicinity of Point Arguello, California", Coastal Engineering Research Center, Tech. Memo. No. 19.

Brownlie, W.R., and B.D. Taylor, 1981, "Sediment management for Southern California mountains, coastal plains and shoreline. Part C: Coastal sediment delivery by major rivers in Southern California", Environmental Quality Laboratory Report No. 17-c, Cal. Inst. Tech., Pasadena.

Bruun, P., 1966, "Stability of coastal inlets", in "Tidal Inlets and Littoral Drift", vol. 2, Ed. H.S. Offsettrykkeri, Trondheim, Norway.

Chapman, D.M., 1978, "Management of sand budget - Kirra Beach, Gold Coast", 4th Australian Conference on Coastal and Ocean Engineering, Adelaide, November, 1978, p. 19-24.

Chapman, D.M., and A.W. Smith, 1981, "A ten year review of variability on an ocean beach", 5th Australian Conference on Coastal and Ocean Engineering, Perth, p. 162-170.

Clark, R.A., and R.H. Osborne, 1982, "Contribution of Salinas River sand to the beaches of Monterey Bay, California, during the 1978 flood period: fourier grain-shape analysis", J. Sed. Petrology, vol. 52 (3), p. 807-822.

Coastal Data Information Program - Monthly Reports, Joint publication of U.S. Army Corps of Engineers and California Department of Boating and Waterways.

Coleman, J.M., and L.D. Wright, 1975, "Modern river deltas: variability of processes and sand bodies", in "Deltas", Ed. M.L. Broussard, Houston Geological Society.

Coleman, J.M., 1981, "Deltas: processes of deposition and models for exploration", 2nd Edition, Burgess Publishing Co., Minneapolis, 124p.

Dean, R.G., 1978, "Review of sediment transport relationships and the data base", Proceedings, Workshop on Coastal Sediment Transport, University of Delaware Sea Grant Program, p. 25-39.

Dean, R.G., E.P. Bock, C.G. Gable, and R.J. Seymour, 1982, "Longshore transport determined by an efficient trap", Coastal Engineering - 1982, A.S.C.E., Cape Town, p. 954-968.

Dobson, R.S., 1967, "Some applications of a digital computer to hydraulic engineering problems", Tech. Rep. 80, Dept. of Civil Eng., Stanford University, Stanford, California.

Everts, C.H., A.E. Dewall, and M.T. Czerniak, 1974, "Behaviour of beach fill at Atlantic City, New Jersey", Coastal Engineering - 1974, A.S.C.E., Copenhagen, p. 1370-1387.

Everts, C.H., A.E. Dewall, and M.T. Czerniak, 1980, "Beach and inlet changes at Ludlam Beach, New Jersey", Coastal Engineering Research Center, Misc. Report No. 80-3, 146p.

Fairchild, J.C., 1972, "Longshore transport of suspended sediment", Coastal Engineering - 1972, A.S.C.E., Vancouver, p. 1062-1088.

Griggs, G.B., and R.E. Johnson, 1976, "Effects of the Santa Cruz Harbor on coastal processes of Northern Monterey Bay", Environmental Geology, vol. 1, p. 299-312.

Griggs, G.B., 1983, "Impact of the January 3-4, 1982 floods in Santa Cruz County, California", Draft Report, University of California, Santa Cruz.

Grijm, W., 1960, "Theoretical forms of shoreline", Coastal Engineering - 1960, A.S.C.E., The Hague, p. 197-202.

Grijm, W., 1964, "Theoretical forms of shorelines", Coastal Engineering -1964, A.S.C.E., Lisbon, p. 219-235.

Griswold, G.M., 1964, "Surf forecasting", Navy Weather Research Facility, Norwalk, Virginia, Report no. 36-1264-099.

Hunter, R.C., 1946, "Report on cooperative beach erosion study, Santa Barbara, California", Los Angeles District, U.S. Army Corps of Engineers.

Inman, D.L., 1953, "Areal and seasonal variations in beach and nearshore sediments at La Jolla, California", U.S. Army Corps of Engineers, Beach Erosion Board, Tech. Memo. no. 39, 134p.

Inman, D.L. and G.A. Rusnak, 1956, "Changes in sand level on the beach and shelf at La Jolla, California", U.S. Army Corps of Engineers, Beach Erosion Board, Tech. Memo. no. 82, p. 519-586.

Inman, D.L., and R.A. Bagnold, 1963, "Littoral processes", in "The Sea", vol IV, p. 529-553.

Inman, D.L., and J.D. Frautschy, 1966, "Littoral processes and the development of shorelines", Coastal Engineering, A.S.C.E., Santa Barbara Speciality Conference, 1965, p. 511-536.

Inman, D.L., 1971, "Nearshore processes", McGraw-Hill Encyclopedia of Science and Technology, vol. 9, p. 26-33.

Inman, D.L., and B.M. Brush, 1973, "The coastal challenge", Science, vol 181, p. 20-32.

Inman, D.L., 1976, "Summary report on man's impact on the California Coastal Zone", Report for the California Dept of Navigation and Ocean Development.

Inman, D.L., 1978, "Status of surfzone sediment transport relations", in Proceedings, Workshop on Coastal Sediment Transport with emphasis on the National Sediment Transport Study, Univ. of Delaware, Sea Grant Report DEL-SG-16-78, 106p.

Inman, D.L., and S.A. Jenkins, 1983, "Oceanographic report for Oceanside beach facilities", Report prepared for the City of Oceanside, August, 1983, 206p.

Inman, D.L., 1984, "The Nile littoral cell and man's impact on the coastal zone of the Southern Mediterranean", Coastal Engineering - 1984, A.S.C.E., Houston, in press.

Jones-Tillson and Associates, 1979, "San Lorenzo River reconnaissance study", Prepared for San Francisco District, U.S. Army Corps of Engineers, December 1979.

Komar, P.D., 1969, "The longshore transport of sand on beaches", Ph.D. thesis, University of California, San Diego, 143p.

Komar, P.D., and D.L. Inman, 1970, "Longshore sand transport on beaches", J. Geophysical Research, vol. 75 (30), p. 5914-5927.

Komar, P.D., 1973, "Computer models of delta growth due to sediment input from rivers and lonshore transport", Geol. Soc. Am. Bull., vol. 84, p. 2217-2226.

Langbein, W.B., and S.A. Schumm, 1958, "Yield of sediment in relation to mean annual precipitation", Am. Geophys. Union Trans., vol. 39, p. 1076-1084.

Longuet-Higgins, M.S., D.E. Cartwright, and N.D. Smith, 1963, "Observations of the directional spectrum of sea waves using the motions of a floating buoy", Proceedings, Conference on Ocean Waves Spectra, Prentice-Hall, Inc., New Jersey.

Longuet-Higgins, M.S., 1970, "Longshore currents generated by obliquely incident sea waves", J. Geophysical Research, vol. 75(33), p. 6778-6789.

Marine Advisers, 1961, "A statistical survey of ocean wave characteristics in Southern California waters", Prepared for the Los Angeles District, U.S. Army Corps of Engineers.

Moore, J.T., 1972, "A case history of Santa Cruz Harbor, California", Hydraulic Engineering Laboratory, Report HEL-24-14, University of California, Berkeley.

Nordstrom, C.E. and D.L.Inman, 1975, "Sand level changes on Torrey Pines Beach, California", U.S. Army Corps of Engineers, Coastal Eng. Res. Center, Misc. Paper no. 11-75, 116p.

Orme, A.R., and A.J. Brown, 1983, "Variable sediment flux and beach management, Ventura County, California", Proceedings, Coastal Zone '83, San Diego, June 1983, p. 2328-2342.

Pelnard-Considere, R., 1954, "Essai de Theorie de l'evolution des formes de rivages en plages de sable et de galets", U. S. Army Corps of Engineering Map Service Translation.

Sampson, R.J., 1973, "User's manual for the SURFACE II graphics system", Geological Research Section, Kansas Geological Survey, 144p.

Seymour, R.J., and A.L. Higgins, 1978, "Continuous estimation of longshore sand transport", Coastal Engineering - 1978, A.S.C.E., Hamburg, p. 2308-2318.

Seymour, R.J., G.W. Domurat, and D.M. Pirie, 1980, "A sediment trapping experiment at Santa Cruz, California", Coastal Engineering - 1980, A.S.C.E., Sydney, p. 1416-1435.

Seymour, R.J., D. Castel, R.R. Strange, and R.A. Nathan, 1984, "An historical evaluation of North Pacific storms during the winter of 1983", Coastal Engineering - 1984, A.S.C.E., Houston, in press.

Seymour, R.J., and D. Castel, 1985, "Episodicity in longshore sediment transport", Journal of Waterway, Port, Coastal and Ocean Engineering, A.S.C.E., in press.

Shepard, F.P., 1963, "Submarine geology", Harper and Row, New York, 557p.

U.S. Army Corps of Engineers, Los Angeles District, 1970, "Coast of Southern California, Cooperative Research and Data Collection Program, Three Year Report, 1967-1969", December 1970.

U.S. Army Corps of Engineers, Los Angeles District, 1980, "Ventura County California, Survey Report for Beach Erosion Control", May 1980.

U.S. Army Corps of Engineers, San Francisco District, 1969, "City of Capitola, beach erosion study, Santa Cruz County, California", Detailed Project Report, November 1969.

U.S. Army Corps of Engineers, San Francisco District, 1974, "Environmental statement - maintenance dredging, Santa Cruz, California", Report No. FY-1974.

U.S. Army Corps of Engineers, 1975, "Shore Protection Manual", Coastal Engineering Research Center, Fort Belvoir, Virginia.

U.S. Hydrographic Survey, 1968, "Bathymetric map of Monterey Bay", Charts 121-61-4 and 121-62-3.

Walker, J.R., P.J. Williams, and J.W. Dunham, 1978, "Santa Cruz harbor shoaling study, Santa Cruz Harbor, California", Report prepared for the San Francisco District, U.S. Army Corps of Engineers.

Walker, J.R., and P.J. Williams, 1980, "A phase-dredging program for Santa Cruz Harbor", Coastal Engineering - 1980, A.S.C.E., Sydney, p. 1493-1511.

Water Resources Division, U.S. Geological Survey - Annual Reports, "Water Resources data for California".

Wiegel, R.L., 1959, "Sand by-passing at Santa Barbara, California", Journal of the Waterways and Harbors Division, A.S.C.E., vol. 85, No. WW2, p. 1-30.

White, T.E., and Inman, D.L., 1985, "Measuring longshore transport with tracers", Ch. 13 in Nearshore Sediment Transport Study Monograph, Ed. R.J. Seymour, Scripps Institution of Oceanography, La Jolla, in press.

Wright, L.D., and J.M. Coleman, 1973, "Variations in morphology of major river deltas as functions of ocean wave and river discharge regimes", Bull. A.A.P.G., vol. 57(2), p. 370-398.

Wright, L.D., 1976, "Morphodynamics of a wave-dominant river mouth", Coastal Engineering - 1976, A.S.C.E., Honolulu, p. 1721-1737.

Yancey, T.E., and J. Lee, 1972, "Major heavy mineral assemblages and heavy mineral provinces of the Central California Coast region", G.S.A. Bull., vol. 83, p. 2099.

APPENDIX A : DETAILS OF STUDY AREA

This appendix expands on details of the study area: its wave climate, its littoral sediment budget, and the hydrological and coastal conditions through the study period.

A.1 Wave Climate

The waves arriving at Santa Cruz can be divided into three categories according to origin: Northern Hemisphere swell, Southern Hemisphere swell, and seas generated by local winds (Marine advisors, 1961).

Most of the Northern Hemisphere swell is generated by extra-tropical cyclones that move eastwards across the northern Pacific. These storms are most common and intense during the winter and spring. The swells, arriving from the northwest with heights ranging up to 6 m and periods ranging from 8 to 16 seconds, are strongly refracted around the northern margin of Monterey Bay and enter the Santa Cruz Bight at an angle to the shoreline: they provide the main driving force for the net easterly longshore transport of sand that the coastline experiences. A persistent northwesterly swell often occurs in the summer in response to west-northwesterly winds caused by a pressure gradient associated with the Pacific high pressure cell.

Low-height long-period swells approach from the south-southwest during the summer. They originate from intense austral winter storms in the Southern Hemisphere and from tropical storms off Central America.

Locally generated seas are most severe in December-February. While Santa Cruz is exposed to seas from the east clockwise through west-northwest, most coastal storm energy arrives from the south-southwest quadrant; seas from the east are fetch-limited while seas from the west are reduced by refraction.

A.2 Littoral Sediment Budget

The longshore transport rate at Santa Cruz has been estimated from wave studies, both hindcast and directly measured, and from the accretion rates at the harbor.

Anderson (1971) and Walker et al. (1978) estimated the longshore transport potential using shoreward-refracted hindcast deep-water wave data and an equivalent version of equation (1). They calculated upper-bound net easterly transport rates of 270,000 m^3/yr and 373,000 m^3/yr respectively.

Seymour et al (1980), using directional wave data recorded by a slope array near the harbor entrance and using essentially the same transport formula, calculated a transport of only 47,000 m^3 for 1978. They unfairly compare this value, based on one year of data, with the values obtained by the hindcast methods which were based on data averaged over several years. Some further objections to their results are discussed in Appendix D.

Surveys of Seabright Beach in 1965 showed an impoundment rate of 191,000-230,000 m^3/yr for the two years following the harbor's construction (Moore, 1970; Walker et al, 1978). However, this figure

may overestimate the average longshore transport rate because a 1963 San Lorenzo River flood produced a higher than average sand input to Seabright Beach. After 1965, Seabright Beach continued to accrete but sand also by-passed the western harbor jetty, some of it entering the entrance channel. Combined figures of beach accretion and harbor dredging for the period 1966-1978, from Walker and Williams, 1980 (see Fig. 2a), yield a minimum average longshore transport rate of 85,000 m^3/yr. This figure excludes sand naturally by-passing the harbor which Walker et al suggest may be double that dredged. Also, the dredging figures (which average 67,000 m^3/yr) are for "pay yardage" which is determined by comparing pre- and post-dredging surveys. The actual amount dredged will exceed this if shoaling proceeds simultaneously with dredging. Walker et al suggest, on the basis of dredging logs, that in some years the actual yardage dredged was close to twice the pay yardage.

Various estimates have been made of the San Lorenzo's average yield of littoral sediment. Griggs and Johnsons' (1976) figure of 50,000-70,000 m^3/yr is derived directly from bedload and suspended sediment sampling over a several year period. Inman's (1976) estimate of 60,000 m^3/yr is based on Langbein and Schumm's (1958) empirical sediment yield formula. These authors assume that all of the sand yield (i.e. sediment coarser than 0.062 mm) remains within the nearshore zone. The USACE, San Francisco District, (1974) figure of 14,000-21,000 m^3/yr assumes some of the fine sand fractions are lost to offshore areas. The best procedure used to estimate the long-term total sand yield is that of Jones-Tillson et al (1979). Their figure, 59,000 m^3/yr, is based on 32 years of flow records and the assumptions that bedload is equivalent

to 10% of the suspended load and that 50% of the suspended load is sand. In section 3 of the text it is shown that probably all sand finer than 0.18 mm is lost from the Santa Cruz nearshore zone, while in Appendix C it is shown that only 22% of the river's suspended load is coarser than this size. Correcting for this, Jones-Tillson's data indicate a mean annual littoral sand yield of 28,000 m^3/yr.

Taking its average beach sand yield to be 30,000 m^3/yr, the San Lorenzo River therefore supplies something like 15% of the littoral drift passing the harbor. The remainder of the littoral sediment must come from the open coast to the north.

Heavy-mineral analyses of sands from the San Lorenzo River bed and from the beaches either side of the river mouth tend to confirm, qualitatively, that the river is an important but not dominant source of littoral sand at Santa Cruz (Griggs and Johnson, 1976). Nothing quantitative can be gleaned from the heavy mineral comparisons since they can be biased by the sample collection schedule. For example, collecting the beach samples during a time of river drought may reduce the apparent importance of the river. Yancey and Lee (1972) show an augite-rich heavy mineral province in beach sands extending some 70 km north from Santa Cruz. These sands, and so the bulk of the littoral drift arriving at Santa Cruz, can be traced to the eroding sandstone seacliffs and small streams along this stretch of coast.

A.3 Hydrological and Coastal Conditions During Study Period

The central coast of California experienced prolonged and intense precipitation during January 3 and 4, 1982. Features of this storm are reported by Griggs (1983). Rainfall figures were extreme over the whole San Lorenzo basin: most recordings exceeded the projected 100-year 24-hour storm. Antecedent precipitation had also been high. As a result, the rain fell on mostly saturated ground and turned quickly to runoff. The peak riverflow at the Big Trees gaging station on 4 January, estimated by the slope-area technique, was 841 m^3/sec and represented a 30-year flood event. The last flood of similar magnitude occurred in 1955. Overbank flooding took place along much of the San Lorenzo River and its tributaries. In Santa Cruz, the peak flow was barely contained by the flood control levees that were originally designed to contain the 100-year flow. Surface velocities reached 4.2 m/sec in the floodplain channel. Bridge damage and considerable bed scour occurred, particularly in the last 1 km of channel upstream of the mouth. A large subaqueous delta was deposited several hundred meters off the river mouth. Three subsequent high-flow events that winter were of a much smaller scale.

Through the 1982-83 winter, the San Lorenzo basin suffered frequent and prolonged rainfalls. The catchment again became saturated early in the season, and many high-flow events followed. The peak flow at the Big Trees gage was about 425 m^3/sec on 19 January 1983, and represented an 8-year event. While this peak was only half the magnitude of that on 4 January 1982, the 1983 winter total runoff was 31% higher than the 1982 winter total runoff.

The most severe coastal storm of the 1982 winter accompanied the intense hydrological storm of 3-4 January. It produced a peak significant wave height of 3.2 m at the harbor gage. However, these peak waves occurred around an ebb tide and on a lower mean sea level than those of the following winter. As a result, the Santa Cruz beaches away from the river mouth retained much of their bermed summer-profile characteristics.

The winter period of January-March 1983 was one of exceptional storminess in the north Pacific and the California coast was subject to very large waves. Seymour et al (1984) note that the waves of these storms were much higher, and of longer period, than in typical winter storms. Strong winds accompanied many of the high wave events, inducing wind setup of the order of 30 cm. During the entire winter, the El Nino climatic anomaly resulted in a slowing of the California current and a general rise in the coastal sea level of about 20 cm. During the storms of late January, the astronomical tides were very large, with ranges greater than 3 m.

These various setup effects combined with the high waves to inflict substantial coastal erosion and property damage. The Santa Cruz coastline suffered in general with the rest of the California coast. The maximum significant wave height recorded at the harbor gage was 3.2 m on 28 January. Twin Lakes Beach, east of the harbor, was essentially stripped of sand to bedrock by late January and destruction of private property and shorefront roads ensued. However, no damage occurred west of the harbor. The beaches there were sufficiently wide and there were

sufficient quantities of old and fresh sand available about the river mouth to form wave-dissipating bars.

APPENDIX B : NEARSHORE TOPOGRAPHIC SURVEYS

This appendix contains further details of the nearshore topographic surveys. It covers field methods, analysis procedures, estimates of the uncertainties in bottom elevation measurements and volume change computations, and the method of estimating the topography at the river mouth before the January 1982 flood.

B.1 Field Methods

The locations of the 9 rangelines surveyed are shown in Fig 8. Except for Rangeline 7, which extended diagonally seaward from the harbor's west jetty, all rangelines began at a temporary benchmark located at the back of the beach and were continued seaward to a nominal depth of 8 m below mean sea level. Benchmark elevations were fixed with respect to the NGVD (mean sea level) datum. Benchmark locations were fixed with respect to reference points of known location using a single-second theodolite and triangulation. Distances were checked by using a subtense bar and also by scaling from enlarged rectified aerial photographs. The benchmark locations are given in Table IV, in terms of the California Coordinate System. They are considered accurate to within 1 m. Table IV also lists the rangeline trends, given as a bearing east from true north.

The rangeline surveys themselves combined onshore and offshore segments. The survey techniques are illustrated in Fig. 31: they follow those of Inman and Rusnak (1956) and Nordstrom and Inman (1975) except that offshore reference rods were not used. At low tide, the beach profile was surveyed from benchmark to wading depth using rod, level,

Table IV. Coordinates of rangeline benchmarks (in terms of the 1,000 foot grid California Coordinate System) and rangeline orientations (east of north).

Rangeline	Benchmark+ Easting	Benchmark+ Westing	Rangeline* Bearing
1	1557.274	172.646	172
2	1558.198	172.770	203
3	1558.171	172.758	175
4	1559.031	172.583	178
5	1559.798	172.457	178
6	1560.690	172.221	178
7	1561.429	171.255	127
8	1562.419	171.933	192
9	1562.991	171.749	209

\+ Benchmark coordinates are in thousands of feet in terms of the 1000-foot grid California Coordinate System; accuracy is +/- 3 feet.

* Rangeline bearing is in degrees east of north; accuracy is +/- 1 degree.

Figure 31. Procedure for onshore and offshore surveys. (Modified from Nordstrom and Inman, 1975.)

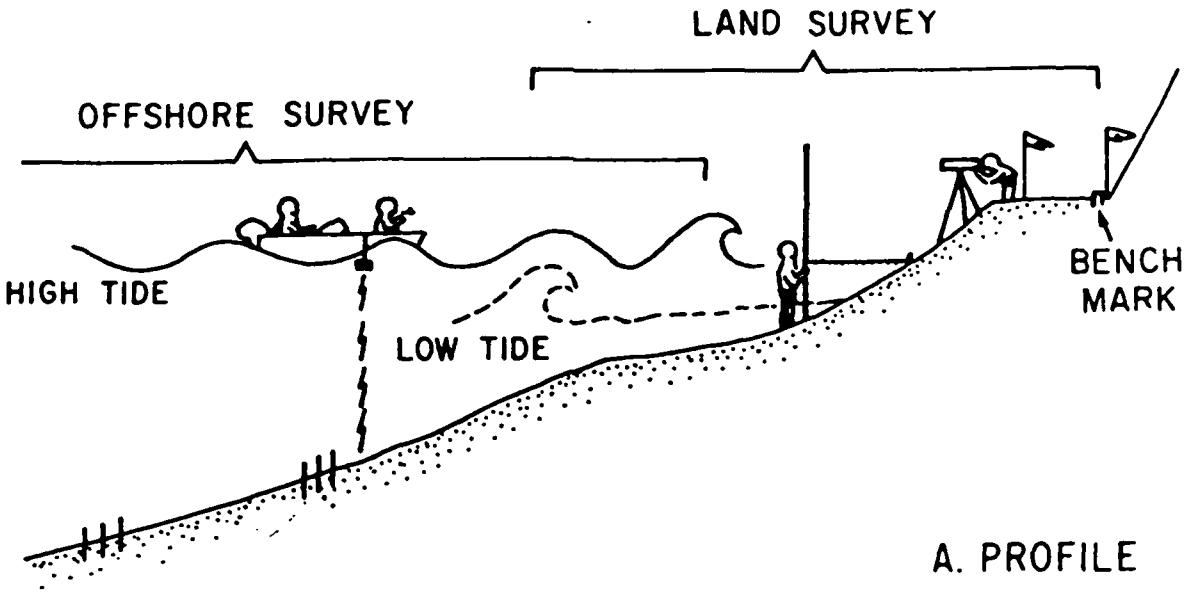
LAND SURVEY
OFFSHORE SURVEY
HIGH TIDE
LOW TIDE
BENCH MARK
A. PROFILE

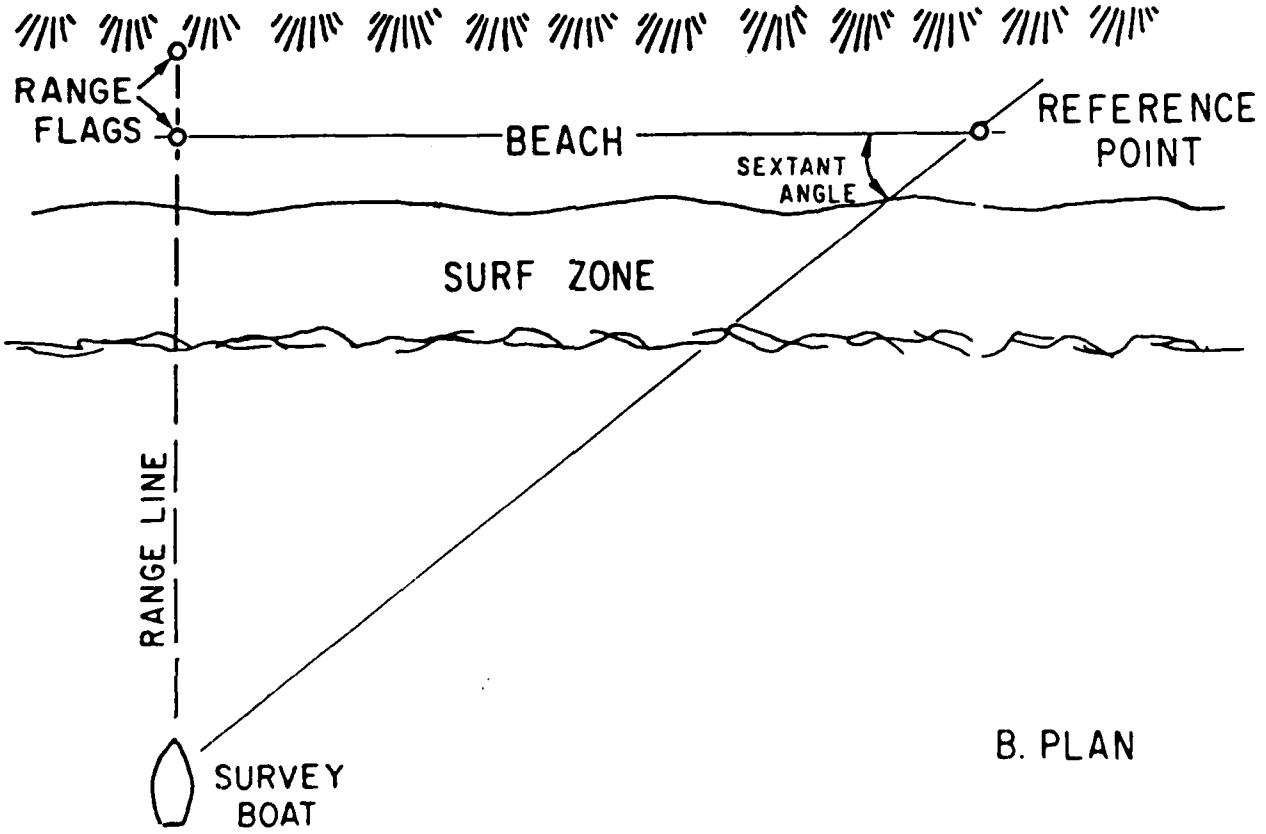
RANGE FLAGS
BEACH
REFERENCE POINT
SEXTANT ANGLE
SURF ZONE
RANGE LINE
SURVEY BOAT
B. PLAN

and 200 m tagline. This technique allows vertical and horizontal accuracies of 1 cm and 10 cm respectively. The offshore segment was surveyed by boat on either the preceding or following high tide. Each line was run from about 8 m depth as close into the surfzone as safety permitted. Overlap with the waded part of the profile was obtained about 50% of the time. A Raytheon Model DE719 survey fathometer recorded continuously bottom elevation with respect to water level. Position fixes were obtained on average every 20 m along the rangeline using a sextant to sight the angle subtended by the rangeline and the line of sight to a reference point along the shore. The position fixes were correlated with time marks on the fathometer chart. Before each survey, the fathometer was calibrated by noting the depth read to a target weight hung at known depths below the transducer.

The fathometer charts were smoothed by hand to remove the gravity-wave record. It was impossible to filter-out any infragravity-period seiching which occurs often in Monterey Bay. The Coastal Data Information Program Reports (CDIP, 1982-83) show that infragravity seiching, typically at periods greater than 4 minutes, did occur at survey times, but that the root-mean-square amplitude was usually only 2 cm and never exceeded 4 cm.

The bottom elevation below mean sea level was derived from the smoothed water depths by subtracting the tide. Tide levels were recorded throughout the offshore surveys, usually at 30 minute intervals, in the harbor at the Murray Street bridge. At this location, midway up the harbor, any harbor seiching is minimized since it is a nodal point. As a precaution against seiching, however, each tide

water-level measurement was "eye-averaged" over several minutes. A calculated tidal curve was superimposed on the measured tide levels to provide a continuous tide-level record.

At the time of each survey, the beaches were photographed, and sand samples were collected from the beach face at each rangeline. Often, additional samples were collected from several points down the beach profile.

B.2 Analysis Procedures

The survey data were initially plotted as beach cross-section profiles. The data were also transferred to 1:8,000 scale maps and contoured at 0.5 m elevation intervals. Aerial and ground-level photographs were used to interpolate the topography between rangelines on the subaerial beach. Approximately concurrent surveys made by the Santa Cruz Harbor Board were used to increase the detail of the bathymetry around the harbor jetties. Additional cross-sectional data were digitized from the contour maps to fill in the gaps between the surveyed cross-sections. The complete set of digitized profile data, surveyed and interpolated, was then input to a series of computer programs.

The elevation changes between consecutive surveys at fixed intervals along each rangeline were computed, plotted in map form, and contoured. The resultant isopach maps locate sites undergoing net erosion or accretion between surveys.

AD-A154 352 SAND DISPERSION FROM AN EPHEMERAL RIVER DELTA ON THE WAVE-DOMINATED CENTRAL CALIFORNIA COAST(U) CALIFORNIA UNIV SANTA CRUZ D M HICKS MAR 85 N00014-80-C-0440 3/3

UNCLASSIFIED F/G 8/3 NL

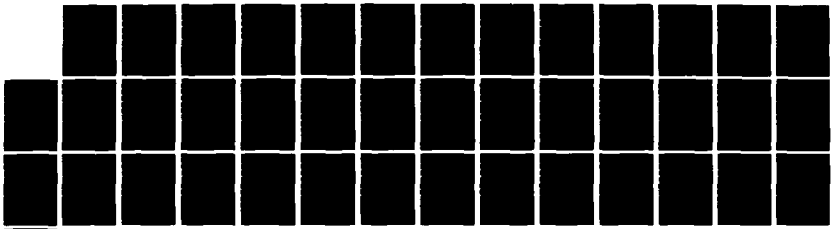

END

FILMED

DTIC

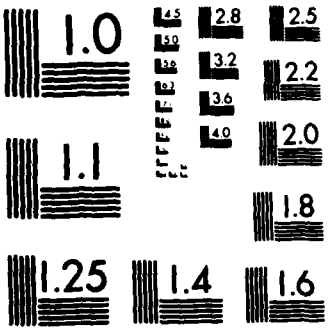

Integrating elevation changes across each profile gave the net volume change per unit length of shore. The cumulative net volume changes per unit shore length since the first baseline survey were then plotted on an x-t diagram. This shows the longshore distribution of sand volume through the study period. A similar x-t diagram was prepared showing the volume changes only as far seaward as the mean lower low water line (-0.88 m MSL). This was done to contrast the longshore volume changes on the visible beach with those of the whole nearshore zone.

Finally, volume changes between surveys for the whole control cell shoreline, and segments of it, were estimated by considering each profile to be representative of a finite length of beach. Again, this was done for the whole cell area and for the visible beach area landward of the mean lower low water line.

B.3 Uncertainties

The uncertainties in this analysis arise from inaccuracies in spot measurements of bottom elevation and in interpolating the elevation between measurement points. Uncertainties in bottom elevation measurements were greater by far on the offshore leg of each rangeline. They arose from the methods of position fixing, wave smoothing, tide level prediction, and fathometer calibration, and from bay-seiching (surge).

An estimate of the accuracy of the fathometer survey method can be obtained from the precision, or reproducibility, of measurements. An estimate of the precision on any given survey day can be obtained from

repeat measurements at the same station. This was possible where rangelines crossed. The root-mean-square error for all same-day comparisons at rangeline intersection points was +/- 6 cm; the maximum error was 13 cm.

Estimates of the precision over periods longer than a day, which ideally should provide a better approximation of the true accuracy, are made uncertain by possible changes in the bed level. This uncertainty is minimized in the area southwest of the harbor where the bottom is largely an exposed bedrock platform (U.S. Hydrographic Survey, 1968). Fig. 32 shows all 10 surveyed profiles across the outer segment of Rangeline 7, which enters this area. The range in elevation is of the order of 24 cm, suggesting an accuracy in the fathometer measurements of +/- 12 cm.

This concurs with the findings of Inman and Rusnak (1956) who made a more rigorous test of the accuracy of fathometer surveys. They compared bottom elevation changes measured by fathometer with the changes relative to reference rods embedded in the bottom. They concluded that fathometer soundings were accurate to +/- 15 cm, although the reproducibility of soundings during any one day was significantly better than this. They suggest that the poorer reproducibility over periods longer than a day may be due to differences in personnel, sea state, and subtle instrument characteristics.

In summary, the uncertainty in the estimate of bottom elevation in this study is taken as +/- 12 cm. This means that the uncertainty in elevation changes between surveys is +/- 24 cm. For this reason, only

Figure 32. Variations in bottom elevation measured along the probably-stable offshore segment of Rangeline 7 during the 20-month study period.

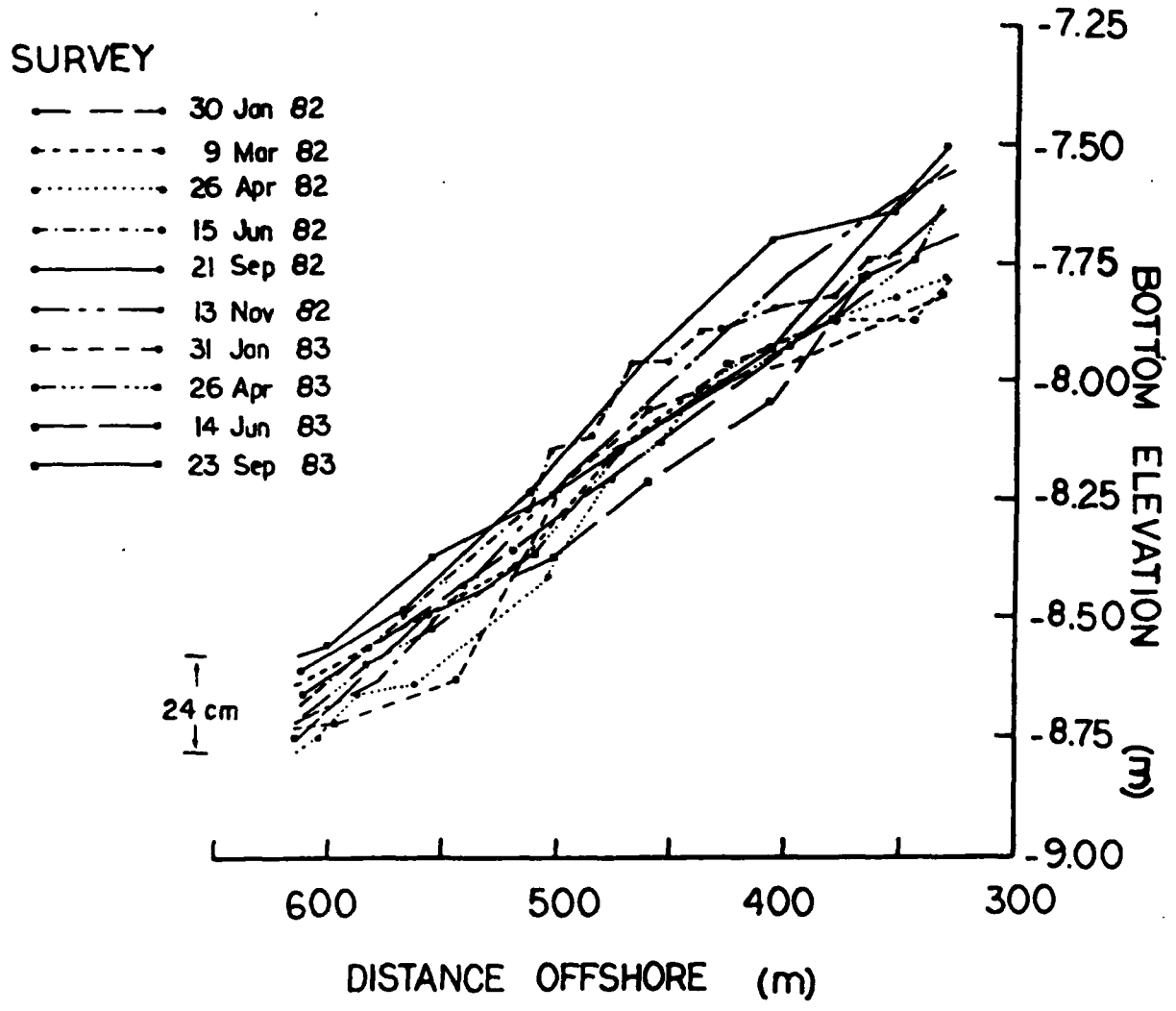
SURVEY
30 Jan 82
9 Mar 82
26 Apr 82
15 Jun 82
21 Sep 82
13 Nov 82
31 Jan 83
26 Apr 83
14 Jun 83
23 Sep 83
24 cm
-7.25
-7.50
-7.75
-8.00
-8.25
-8.50
-8.75
-9.00
BOTTOM ELEVATION (m)
600
500
400
300
DISTANCE OFFSHORE (m)

elevation changes greater than 25 cm were considered significant and plotted on the isopach maps.

Much of the uncertainty in bottom elevation is "pseudo-random" over the time and length scales associated with running a profile. This is the case with the error in the method of smoothing the surface gravity-wave signal, and with positioning errors arising from sextant reading and slight deviations from the rangeline. Such pseudo-random errors wil tend to cancel when integrated over rangeline length scales; they will therefore induce comparatively little uncertainty in the estimate of the total volume under a profile. The residual elevation errors, arising from fathometer calibration and infragravity water level variations (i.e. tides and seiching), are systematic over the run time of a rangeline and should not cancel. They are estimated at +/- 6 cm. This figure incorporates a +/- 3 cm average error due to seiching and a +/- 2 cm error in the tide level measurement.

Thus a reasonable estimate of the uncertainty in volume change under a profile is +/- 0.12 m^3 per m beach length times the length of the offshore segment of the profile. The average offshore segment extends 350 m; therefore, the average uncertainty in volume change per meter of beach is +/- 42 m^3. This figure should probably be doubled to account for errors induced by interpolating alongshore between rangelines. The uncertainty of the estimate of total volume change, integrated along the 1825 m length of the control cell, then becomes +/- 150,000 m^3.

These error estimates justify the boundaries established for the control cell. The offshore terminations of the survey lines and control

cell near the 8 m isobath are justified by observing that the elevation changes to seaward of this line were almost always less than the uncertainty. Clearly, continuing the control volume further seaward would be pointless, since the volume change would remain unaltered but the uncertainty would grow. The longshore length of the cell is such that the total gain in cell volume due to the river input remained significant over the study period.

B.4 Pre-flood Topography

Since the project was initiated after the flood of 4 January 1982, it was necessary to estimate the nearshore topography immediately before this flood. This estimate was based on the late January 1982 survey, aerial and ground photographs taken in late 1981, and older bathymetric surveys of the river mouth area.

It was assumed that before the flood the contours ran essentially straight across the river mouth between Cowell and Seabright beaches. Specifically, this "no-delta" assumption was based on aerial photographs taken in late 1981 that showed no refraction of waves off the river mouth, and on the relatively low sediment yield of the San Lorenzo River over the past several years (c.f. Fig. 1c).

It was also assumed that through January 1982 a small amount of sand accreted on the berms on either side of the river mouth. This was suggested by the profiles of Rangelines 1, 4, 5, and 6 surveyed on 30 January 1982 (Figs 17a and 17d). With this exception, the pre-flood topography beyond the river mouth area was assumed to be the same as that in the first survey on 30 January 1982.

This "pre-January 1982 survey" was taken as the baseline for comparison with subsequent surveys. A conservative estimate of the uncertainty for the pre-flood volume of sand at the river mouth is +/- 50,000 m^3: this represents an average bottom elevation uncertainty of +/- 20 cm over a 300 m x 800 m area opposite the river mouth.

APPENDIX C : LITTORAL SEDIMENT YIELD OF SAN LORENZO RIVER

This appendix outlines the data sources and methods used to estimate the littoral sediment yield of the San Lorenzo River at the Big Trees gaging site and from its floodplain channel. The procedure involved estimating the total sediment yield, then determining the proportion of this that was coarser than the littoral cut-off size.

C.1 Sediment Yield at Big Trees Gaging Site

The sediment yield of the San Lorenzo River past the Big Trees gaging site for the period January through September 1982 was obtained from the USGS, Water Resources Division, estimates of suspended load and bedload (Water Resources Division, 1984). To derive the suspended load yield, the USGS combine time series records of suspended sediment concentration and water discharge. The concentration record is based on depth-integrated samplings which are often made daily or more frequently. The concentration between sampling times is derived from a suspended sediment rating curve. The resultant estimate of suspended sediment yield is quite accurate provided sufficient samples are collected during high flows and the rating is adequately established. Unfortunately, no samples were collected throughout the flood of 4 January 1982. While this flood peaked at 850 m^3/sec, the sediment rating was established only up to a flow of 340 m^3/sec and had to be extrapolated, "based on experience", to the higher flows. Without an independent estimate of the suspended sediment yield of the January flood, it is difficult to assess the error that this extrapolation might induce. However, a 50% error is not unlikely.

The USGS estimate of "bedload", which is actually the unmeasured bed material load (i.e. all sediment of bed-material size moving in the 0.075 m high region above the bed that is not traversed by suspended sediment samplers), is based on a bedload versus water discharge rating. This rating was established over the low flow range (i.e. flows less than 85 m^3/sec) with a Helley-Smith bedload sampler. At higher flows, it was computed by the Modified Einstein procedure.

Because of funding cuts, the USGS sediment record at Big Trees was terminated in October 1982. From then until September 1983, suspended load and bedload yields were estimated using ratings of daily sediment load to daily mean water discharge, in combination with the record of daily mean flow. These ratings, plotted on Figs 33 and 34, were derived from values of daily suspended load, bedload, and mean discharge found in the Water Resources Division data report for the 1982 water year (Water Resources Division, 1984). This method was checked by using it to predict the sediment yield for January-September 1982 for comparison with the USGS estimates. Over that period, the daily-rating method underestimated the bedload by 3% and overestimated the suspended load by 10%.

C.2 Size Distribution at Big Trees

The total sediment yield is obtained by summing the bedload and suspended load yields (as listed in Table II). To find the littoral sediment yield, we need to determine the proportion of the total load coarser than the cut-off size, 0.18 mm. Particle size analyses of Helley-Smith sampled bedload, reported by the USGS, show that

Figure 33. Rating curve of daily suspended sediment load versus daily mean water discharge at Big Trees gaging site, San Lorenzo River. (Data from USGS, Water Resources Division, 1982.)

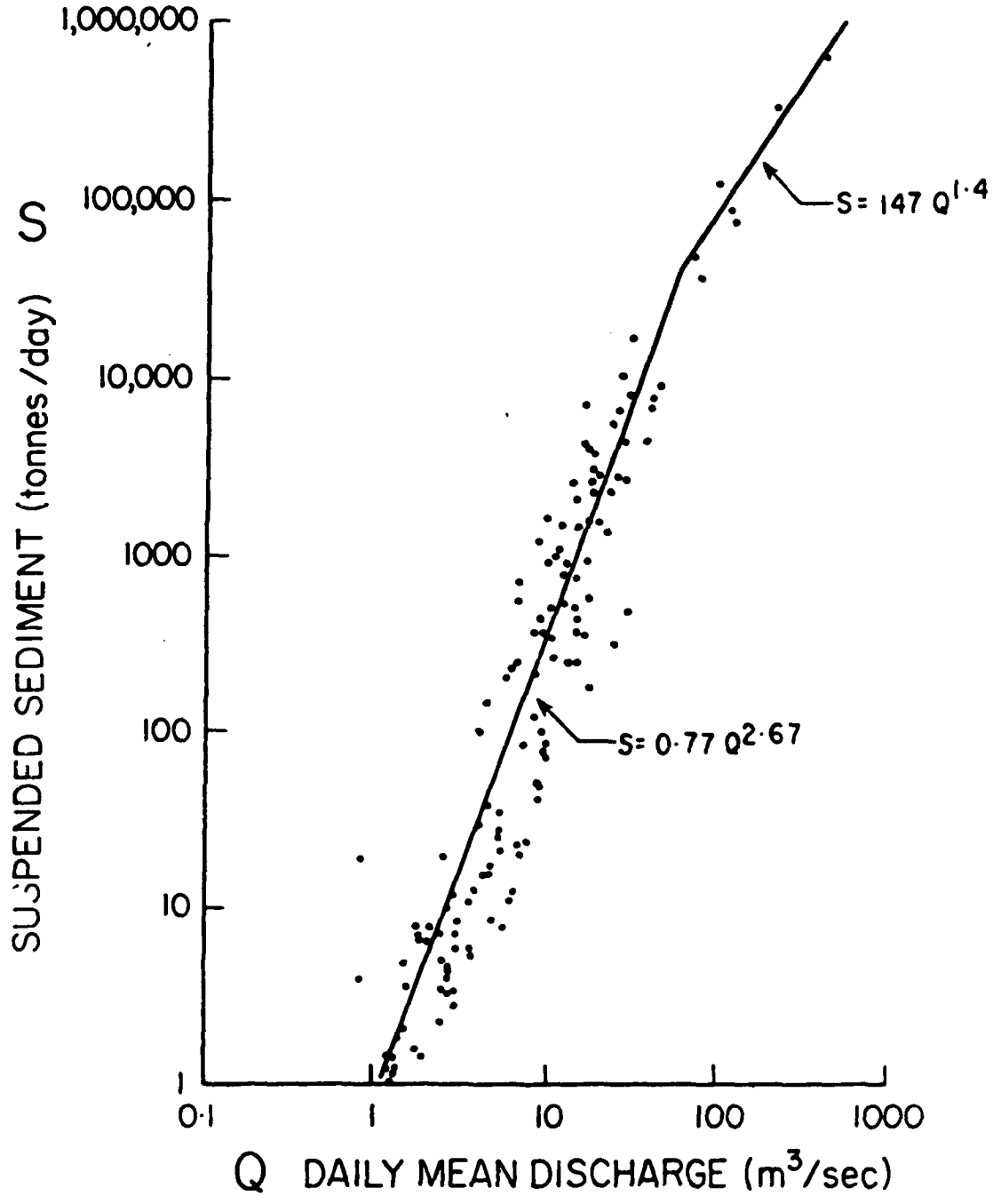
1,000,000
100,000
10,000
1000
100
10
1
SUSPENDED SEDIMENT (tonnes/day) S
S= 147 Q^1·4
S= 0·77 Q^2·67
0·1
1
10
100
1000
Q DAILY MEAN DISCHARGE (m³/sec)

Figure 34. Rating curve of daily bedload versus daily mean water discharge at Big Trees gaging site, San Lorenzo River. (Data from USGS, Water Resources Division, 1982.)

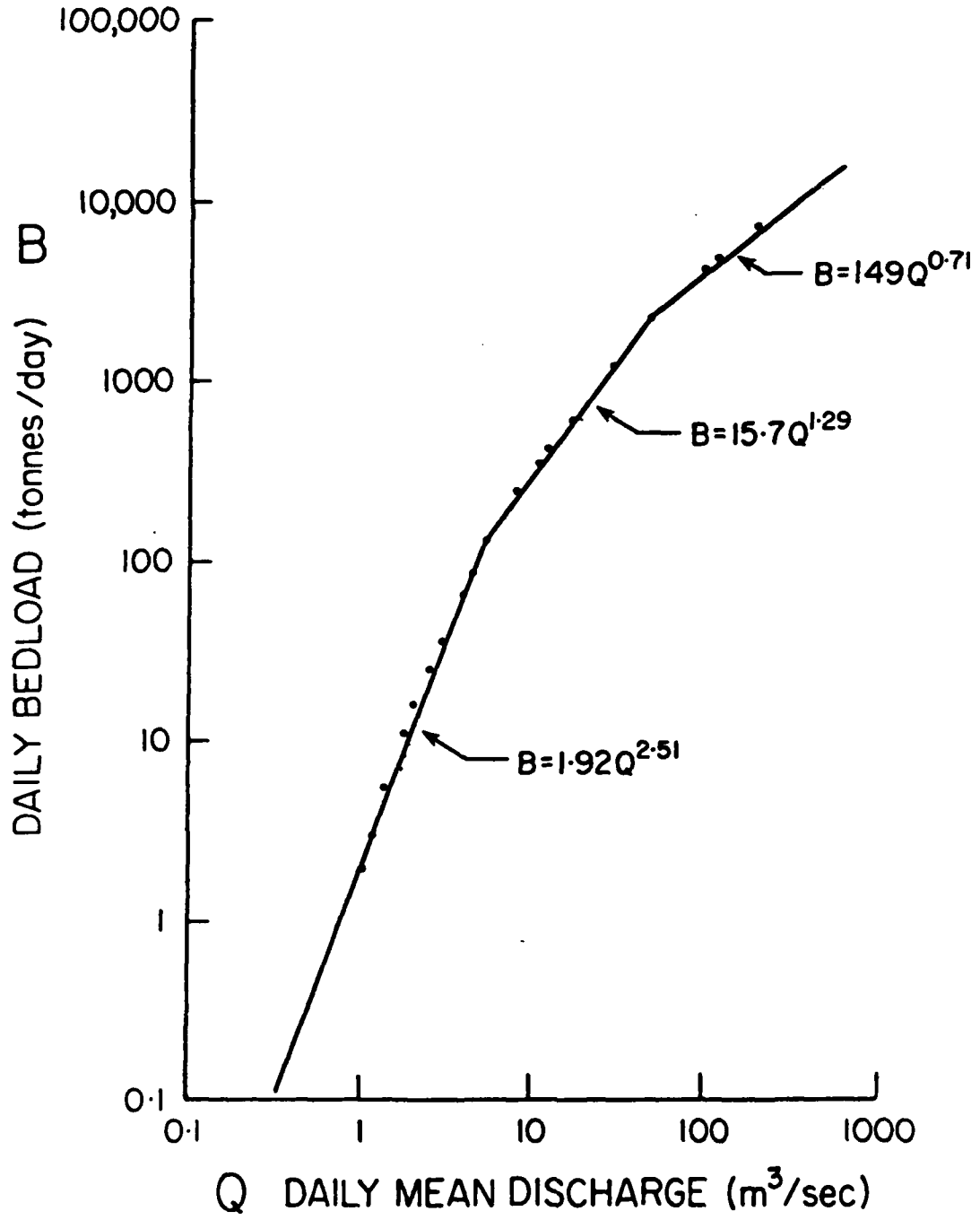
100,000
10,000
1000
100
10
1
0·1
B
DAILY BEDLOAD (tonnes/day)
B=149Q^0·71
B=15·7Q^1·29
B=1·92Q^2·51
0·1
1
10
100
1000
Q DAILY MEAN DISCHARGE (m³/sec)

essentially all (96% on average) of the bedload is coarser than this size. Therefore, we need only be concerned with obtaining a representative size distribution of the suspended load.

The suspended sediment size distributions reported by the USGS are highly variable. Fig. 35, a plot of percent coarser than 0.18 mm versus water discharge at the time of sampling for all reported analyses, is essentially a scatter diagram. The only trend apparent is that the scatter decreases for very low and very high flows. The average per cent coarser than 0.18 mm, for all values through the range of flows sampled, is 15%. However, this simple average takes no account of the significance of each discharge value to the suspended yield totalled over a period of time.

Fig. 36 shows the percentage of the suspended load transported by all flows less than a given flow. This plot was obtained by combining the flow-duration table, based on over 30 years of record, and the suspended sediment rating given by Jones-Tillson (1979). It shows that over the record period, 90% of the suspended load was moved by flows exceeding 23 m^3/sec and that this load was spread fairly equally over these flows. Therefore, a better estimate of the percent coarser than 0.18 mm is obtained by averaging only the data in Fig. 35 at flows exceeding 23 m^3/sec. This results in a time-averaged load-weighted value of 21%.

Thus the littoral sediment yield of the San Lorenzo River at Big Trees is taken as the sum of the bedload and 21% of the suspended load.

Figure 35. Percentage of suspended sediment of San Lorenzo River at Big Trees coarser than 0.18 mm versus water discharge when sampled. (Data from USGS, Water Resources Division, annual data reports, 1973-1980.)

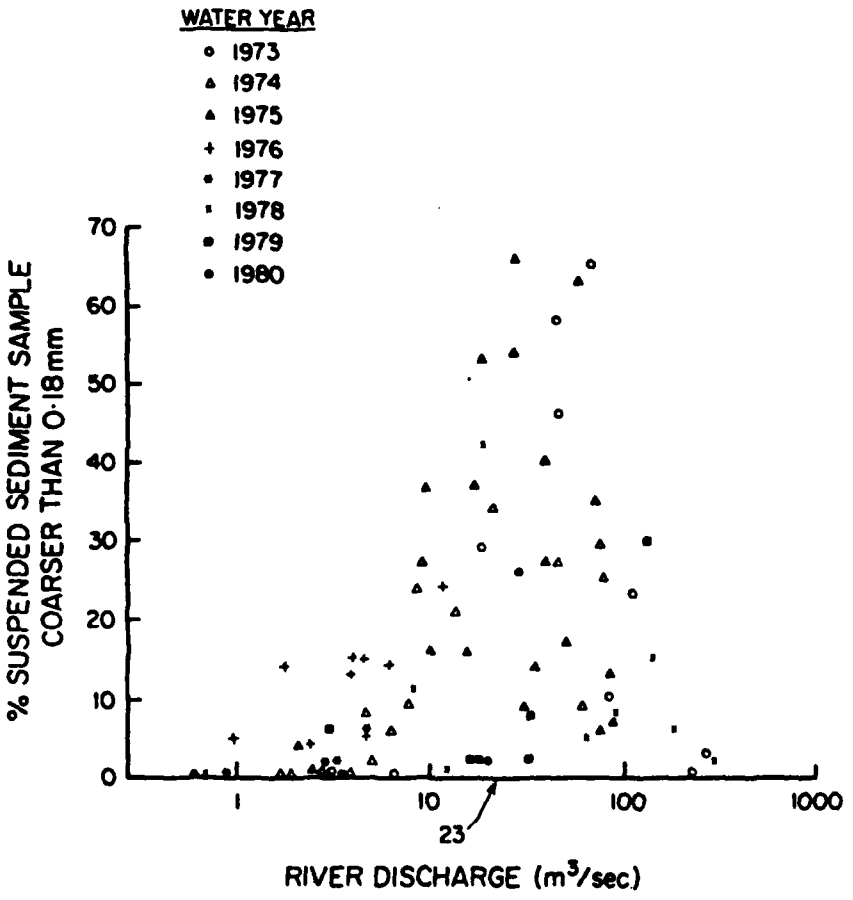
WATER YEAR
1973
1974
1975
1976
1977
1978
1979
1980
% SUSPENDED SEDIMENT SAMPLE COARSER THAN 0·18 mm
70
60
50
40
30
20
10
0
1
10
100
1000
23
RIVER DISCHARGE (m³/sec)

Figure 36. Percentage of the suspended sediment load of the San Lorenzo River at Big Trees transported by discharges less than a given discharge. (Data from Jones-Tillson and Associates, 1979.)

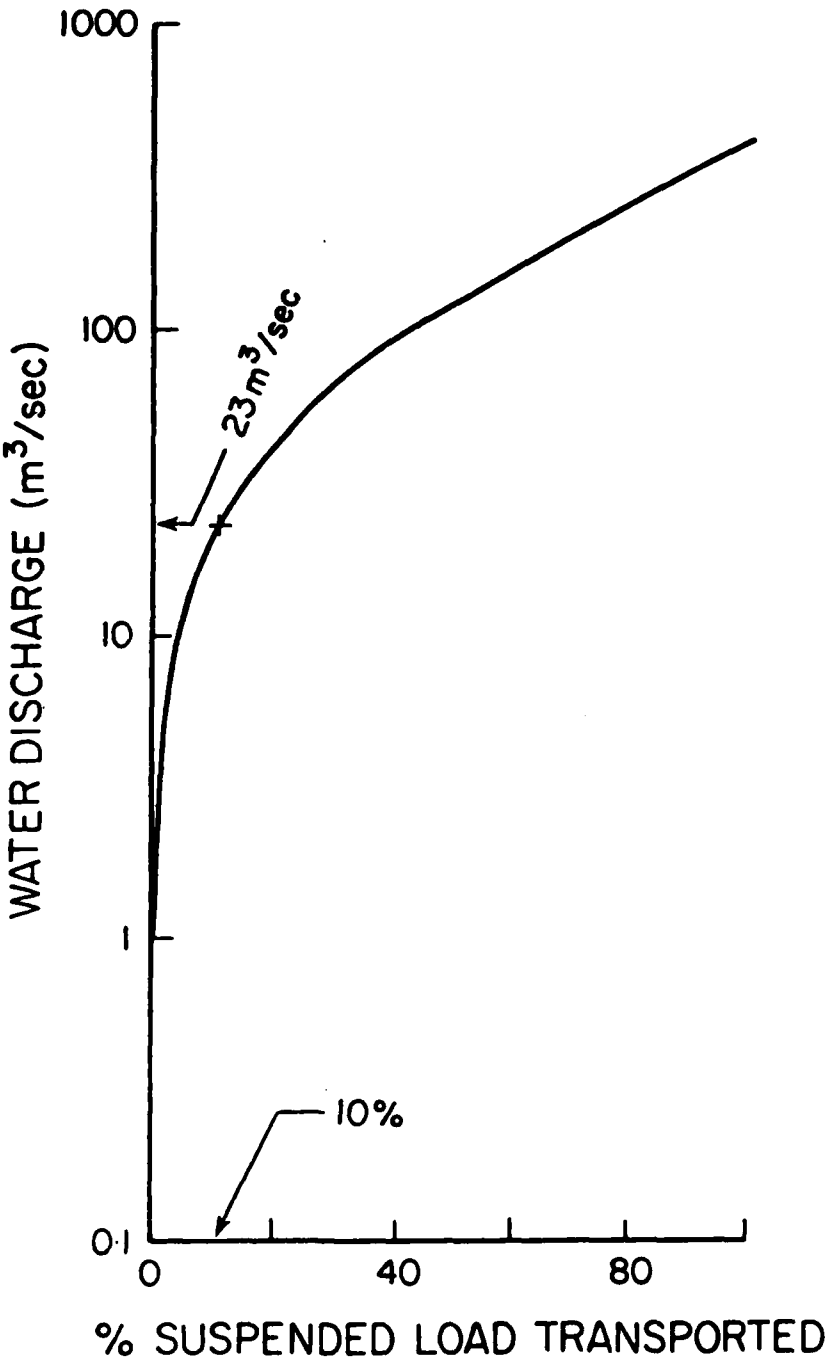
1000
100
10
1
0·1
WATER DISCHARGE (m³/sec)
23m³/sec
10%
0
40
80
% SUSPENDED LOAD TRANSPORTED

C.3 Sediment Yield from Floodplain

The scour/fill record of the San Lorenzo floodplain channel through the study period was estimated from four cross-sectional surveys undertaken by the City of Santa Cruz. The surveys included fourteen cross sections located along the length of the floodplain between the Highway 1 bridge and the river mouth. Volume changes were calculated by the end-area method. Table V shows the net scour/fill along this reach between the surveys of interest.

The last survey prior to the flood of 4 January 1982 was done in June 1980. However, this 1980 channel is considered reasonably representative of the immediately pre-flood channel. This conclusion is based on personal observation (G. Griggs, pers. comm.) and is supported by the low bedload transport capacity predicted by the USGS through the period June 1980 to December 1981 at the Big Trees gaging site (about 7,000 m^3). It was therefore assumed that virtually all of the 144,000 m^3 of scour between the June 1980 and January 1982 surveys occurred during the flood of 4 January 1982.

It was also assumed that after the flood of 4 January 1982 the channel generally accreted at a rate proportional to the bedload supply from upstream. This assumption allowed the floodplain volume changes between survey dates to be scaled off the bedload yield at the Big Trees site, as shown in Fig. 11. For example, the accretion between the 14 January 1982 and 7 December 1982 surveys was made proportional to the bedload yield from Big Trees over this period.

Table V. Bed-material volume changes totalled along the floodplain reach of the San Lorenzo River. Based on surveys by the City of Santa Cruz.

Survey Date	Cumulative Volume Change Since 23 June 1980 (m^3)	Volume Change Between Surveys (m^3)
23 June 1980	0	
		-144,000
14 January 1982	-144,000	
		83,000
7 December 1982	-61,000	
		68,000
12 July 1983	7,000	

Size analyses of bed material in the floodplain reach, shown in Fig. 12, indicate that on average 97% is coarser than 0.18 mm. Thus all sediment scoured from the floodplain channel was assumed to remain in the nearshore zone.

APPENDIX D : COMPUTATION OF LONGSHORE TRANSPORT NEAR WAVE ARRAY

This appendix contains a derivation of the relation used to compute the longshore sand transport potential shoreward of the wave array. Also, it contains discussion on the shortcomings of the transport model and the uncertainties in the input wave data.

D.1 The Transport Relation

The method of Seymour and Higgins (1978) was used to compute the longshore transport potential shoreward of the wave array. Their formula is based on the Scripps/Corps of Engineers relation

$$I_l = K\,(E\ Cn\ \sin\alpha\cos\alpha)_b \qquad (D\text{-}1)$$

where I_l is the immersed-weight longshore transport rate in the surfzone, K is a dimensionless coefficient, evaluated by Komar and Inman (1970) as 0.77, $E = {}^1/_8\,\rho g\,H^2$ is the wave energy per unit surface area, H is the root-mean-square wave height, Cn is the wave group velocity, α is the wave incidence angle with the shoreline, and the subscript b indicates that the parameters are evaluated at the breaker line.

Equation (D-1) can be rewritten as

$$Q_l = K'\,(C\ S_{xy})_b \qquad (D\text{-}2)$$

where Q_l is the "at rest" volume transport rate of sand, C is the wave celerity, here taken as equal to $(gh)^{0.5}$ in shallow water, h is the water depth, S_{xy} is the longshore component of the radiation stress (more specifically, the onshore flux of longshore directed wave momentum), and K' is a dimensional coefficient equal to 7.9×10^{-5}

m^3/N when Q_l is in m^3/sec, S_{xy} is in N/m, and assuming a sand density of 2650 Kg/m^3 and an "at rest" volume concentration of 0.6. As defined by Longuet-Higgins (1970),

$$S_{xy} = En \sin\alpha\cos\alpha \qquad (D-3)$$

where n is 1 for shallow water conditions.

By making two assumptions, (D-2) can be refined to

$$Q_l = K' \; S_{xy}(1.65\, g\, H_s)^{0.5}{}_a \qquad (D-4)$$

where H_s is the significant wave height, approximately equal to $\sqrt{2}\,H$, and the subscript a designates that both H_s and S_{xy} are measured at the array. The two assumptions are: (1), the shore contours are straight and parallel so that S_{xy} is conserved between the array and the breakpoint (after Longuet-Higgins, 1970); and (2), the depth at the breakpoint can be estimated from the significant wave height at the array using Griswold's (1964) empirical predictor

$$h_b = 1.65\,(H_s)_a \qquad (D-5)$$

The latter assumption is justified since the computed transport rate is relatively insensitive to small errors in the estimated breaker depth.

Finally, by expressing S_{xy} and H_s in the units reported by the Coastal Data Information Program, we obtain

$$Q_l[m^3/yr] = 983\,(S_{xy}[cm^2]\;(H_s[cm])^{0.5})_a \qquad (D-6)$$

The dimensional coefficient, 983, in equation (D-5) is approximately 4 times that used by Seymour and Higgins. Half of this discrepancy can be

explained by their direct use of the coefficient recommended by the Coastal Engineering Research Center (USACE, 1975). In terms of equation (D-1), CERC's coefficient converts to a dimensionless K value of 0.4. However, CERC compute wave "energy" as $E = {}^1/_8 \rho g H_s^2$ using the significant wave height. Their K value should be doubled if the energy is computed (correctly) using the root-mean-square wave height, as is the case for the Santa Cruz data. Apart from this, Seymour and Higgins appear to have made an unnecessary division by 2.

Incidently, this discovery, in large part, reconciles the discrepancy reported by Seymour et al (1980) between their computation of annual transport at the harbor, based on the array data and Seymour and Higgin's formula, and Walker et al's (1978) computation, based on hindcast deepwater wave data. While Seymour et al found good agreement between their prediction of transport rate and the accretion rate in the harbor during 1978, this agreement depended on the unlikely assumption that no sand by-passed the harbor entrance.

D.2 Shortcomings of the Transport Relation

The transport relation given by equation (D-1) is very simplistic. Inman and Komar (1970) show that it is really a special case of the more general model of Inman and Bagnold (1963)

$$I_l = K'' (E\ Cn)_b \cos\alpha_b\ v_l/u_m \qquad (D\text{-}7)$$

where v_l is the mean longshore current velocity in the surfzone, u_m is the maximum orbital velocity under the breaking wave, and K" is a dimensionless coefficient. This equation says that the amount of

sediment entrained by the breaking waves is proportional to the total incident energy flux per unit length of shore; any net superimposed longshore current then advects the wave-dispersed sediment alongshore at a mean velocity proportional to v_l. In general, v_l may reflect tidal currents, wind-driven currents, currents due to nearshore cell circulation, and currents due to oblique wave approach. For the latter case only, Komar and Inman show that

$$v_l = K''' u_m \sin\alpha_b \qquad (D\text{-}8)$$

where the dimensionless coefficient $K''' = K/K''$, and so obtain equation (D-1) from equation (D-7).

Therefore, equation (D-1) ignores the role of all longshore current forcing mechanisms but oblique wave approach. Furthermore, the S_{xy} formulation in (D-2) is generally inconsistent with equation (D-7) because total S_{xy} is derived by summing only the "longshore-energy components" of frequencies arriving oblique to the shore; S_{xy} does not represent wave energy arriving normal to the shore. For example, consider a day when 99% of the total energy is contained in 14-second swells that arrive normal to the shore, while the remaining 1% of the energy arrives obliquely to the shore as 6-second seas. Equation (D-2) ignores completely the contribution made by the high energy swell waves in dispersing sediment into the weak, S_{xy}-driven, longshore current.

Dean et al (1982) show that, as reported in the literature, the value of K in equation (D-1) varies considerably - between 0.1 and 2.2. Much of this variation must lie in the relative importance of suspended load and bedload, which, intuitively, should relate to grainsize and

breaker-type. As a corollary, the experimentally-determined values of K reported in the literature should also reflect any bias in the experimental methods towards measuring bedload, suspended load, or total load. For example, bed-material tracer experiments, like those of Komar (1969), principally estimate the bedload transport; direct sampling techniques, like those of Fairchild (1972), are biased towards the suspended load; while volumetric surveys of total littoral drift traps, like those of Dean et al (1982), undoubtedly give the total load.

Recent attempts have been made to relate K to grainsize, breaker-type, and beach slope. Dean (1978) suggests, on a graphical relation, that K should increase as the sandsize decreases. Inman and Jenkins (1983) and White and Inman (1985) relate K to breaker-type and beach slope through the "surf similarity parameter", or reflection coefficient, c_{rb}. They define this parameter as

$$c_{rb} = L_\infty \tan^2\beta \; / \; \pi H_b \qquad (D\text{-}9)$$

where L_∞ is the deep-water wavelength, $\tan\beta$ is the beach slope, and H_b is the breaker height. White and Inman show that K increases with increasing c_{rb} according to the empirical relation

$$K = 2.16 \; c_{rb}^{0.5} \qquad (D\text{-}10)$$

for $0.02 < c_{rb} < 0.42$. They suggest that as the beach becomes more reflective with increasing c_{rb}, the breaker type changes from spilling to plunging and more of the wave energy is focussed onto the bed, thus increasing the transport efficiency.

Substituting a grainsize of 0.27 mm, the median size of sand trapped in Santa Cruz Harbor, into Dean's relation yields K = 1.2. Substituting the mean beach face slope of 0.043 for the east end of Seabright Beach into White and Inman's relation yields a range from K = 1.3 for a 20-second, 1 m high, summer swell wave, to K = 0.38 for a 10-second, 3 m high, winter storm wave. On the basis of White and Inman's relation, the time-averaged value of K = 0.77 assumed in this study seems reasonable.

D.3 Uncertainties in Wave Data

The main uncertainty in the wave data and its analysis concerns direction. Apart from errors inherent in the Lonquet-Higgins et al (1963) method of deriving the directional spectrum, which are probably random over time, there are systematic errors in fixing the orientation of the array and the bottom contours. Probably, the wave approach angle with respect to the shoreline cannot be fixed any better than +/- 4°. Therefore, for small angles of incidence, this can induce large errors in the transport magnitude and possibly the wrong direction.

APPENDIX E: PROCEDURE FOR COMPUTING LONGSHORE TRANSPORT DIVERGENCE

This appendix outlines the methods used to predict the longshore variation in wave conditions and longshore transport at Santa Cruz. Some example results are plotted and discussed. Additionally, the inherent assumptions, approximations, and uncertainties of the method are discussed.

In short, for each wave record, a representative wave ray was back-refracted from the array measurement site to deep water. Many parallel rays were then refracted shoreward from deep water. These refractions proceeded in several stages since the bathymetry was input in two differently-scaled blocks: an offshore block with coarse bathymetric detail, and an inshore block, enclosing the study cell, with fine bathymetric detail. The arrival points from the first "shoot" of wave rays were used to direct a high concentration of rays towards the river mouth area in a subsequent "shoot". The longshore transport rates at fixed points spaced evenly along the shoreline were interpolated from the transport rates computed at the ray arrival points. The variation in transport rate between adjacent fixed points determined the transport divergence.

E.1 The Representative Wave

Each 6-hourly record of the energy and directional spectra at the slope array was collapsed into a single wave having representative height, period, and direction. The representative root-mean-square wave height was taken as $1/\sqrt{2}$ times the significant wave height or $2\sqrt{2}$ times the water level variance. The representative or "significant"

Figure 37. Boundaries of the bathymetry blocks used in the back-refraction analysis.

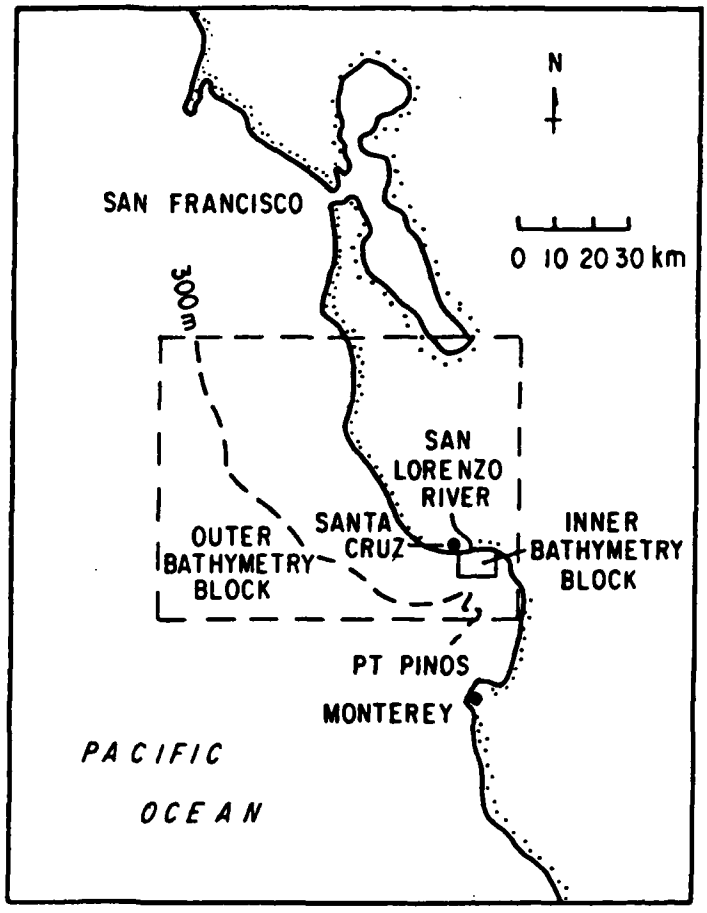
N
SAN FRANCISCO
0 10 20 30 km
300m
SAN
LORENZO
RIVER
SANTA
CRUZ
OUTER
BATHYMETRY
BLOCK
INNER
BATHYMETRY
BLOCK
PT PINOS
MONTEREY
PACIFIC
OCEAN

direction, as defined in the main text, is essentially the energy-weighted direction averaged across all period bands. The representative period is the energy-weighted period averaged across all period bands.

E.2 BATHYMETRY

Because of the physiography of the study area and the large period (20 seconds) of the longest representative waves, it was necessary to digitize the bathymetry over a large area of ocean floor. A 20-second wave begins to refract at a depth of 312 m. This depth is only encountered off the Santa Cruz coastline beyond the continental shelf edge and in Monterey Submarine Canyon. Furthermore, north of Point Santa Cruz, northwest swells arrive at only a slight angle to the shelf contours. Their refraction across the shelf is therefore gradual until they wrap around Point Santa Cruz into Monterey Bay.

The area digitized is shown in Fig. 37: it spans 75 km north-south by 110 km east-west. For practical reasons and to maintain fine bathymetric detail within the 2 km long study cell, it was necessary to break this area up into two blocks: a coarse-scale outer block with comparatively sparse depth fixes; and a fine-scale inner block with much more closely spaced depth fixes, enclosing the study cell. This meant, of course, that the refractions had to be done in two stages going from near shore to deep water and vice-versa. The boundaries of these blocks are shown in Fig. 37. The bathymetry for the outer block was taken from the NOAA National Ocean Survey chart #18680, "Point Sur to San Francisco" (1:210,688 scale), and chart #18685, "Monterey Bay" (1:50,000

scale). The bathymetry of the inner block was taken in part from the "Monterey Bay" chart. The bathymetry inside the study cell, of much greater detail, was based on the present surveys and was changed periodically in accordance with the surveyed changes. The bathymetry for a "no-delta" shore within the study cell was estimated by straightening the isobaths across the river mouth.

The SURFACE II graphics program (Sampson, 1973) was used to fit a smooth surface to the randomly-located bathymetric data for each block and to represent this surface by a grid of points. The grid divisions were 500 m for the outer block and 50 m for the inner block. The bathymetry was called in this format by the refraction program.

Smoothing the bathymetry onto a uniformly-gridded surface provides several advantages. It allows the refracting wave to change direction smoothly, i.e., the ray proceeds across a continuously changing surface rather than across a mosaic of planar elements. Also, it damps locally-steep bottom slopes. This is important because the refraction theory is only valid for the condition of a "locally-flat bottom", i.e., where the change in bottom elevation encountered over a wavelength is small compared to the wavelength.

In order to improve the performance of the surface-fitting routine near the shoreline, the general slope of the shore was used to generate on-land "bathymetry" for a distance inland corresponding to at least three grid divisions.

E.3 Refraction Procedure

The procedure involved refracting the representative wave rays offshore to deep water and then returning many parallel rays. A numerical refraction routine, modified from that of Dobson (1967), was used. Because of the two scales of bathymetry, the backward and forward refractions had to be done in two stages.

The back-refracted ray was stopped 2 km beyond the point where it first encountered deep-water conditions. Sixty rays were then refracted shoreward from both sides of the stopping point. Each ray had the same period and deep-water direction and height as the stopped back-refracted ray. The forward-refracted rays were terminated on one of three conditions: when the ray reached the boundary of the bathymetry block, when the ray hit the shore, or when the ray passed into a caustic. At the boundary between the outer and inner bathmetry blocks, the height, direction, period, and coordinates of the ray were passed on to the inshore refraction program. Near the shoreline, the shoaling rays were stopped at the assumed breakpoint, i.e., when the height equalled 0.78 times the depth. Caustics, where refracted rays converge, were identified when the wave height exceeded 10 times the height in deep water.

This basic routine was repeated three times for each wave record. The first time, the 60 parallel deep-water rays were shot with a "wide spread" at 30 m spacings. The second time, the rays were shot with a "narrow spread" towards the river mouth. The third time, the "narrow spread" of rays was refracted over the "no-delta" bathymetry off the river mouth.

The starting points and spacings for the rays aimed at the river mouth were found by a subroutine that analysed the shoreline-arrival points of the widely spaced rays. This involved defining a 200 m long zone enclosing the river mouth and identifying the two rays that reached shore closest to either side, but outside, of this zone. The 60 deep water rays were then reshot at equal spacings from between the starting points of these two rays.

The height, direction, and coordinates at the break point of each ray were recorded as input for the longshore transport computation. Month-long blocks of wave data, averaging 120 6-hourly records, were processed at a time. Each run involved refracting some 44,000 individual rays and required about 12 hours of C.P.U. time.

E.4 Computing Longshore Transport and Divergence

The longshore transport rate was computed at the arrival point of each refracted wave ray with the formula

$$Q_l = K'(E\ Cn)_b \sin 2\alpha_b / 2 \qquad (E\text{-}1)$$

where Q_l is the volumetric transport rate in m^3/sec, K' equals 7.9 x 10^{-5} m^3/N, E is the wave energy in Nm, Cn is the wave group velocity in m/sec, α is the angle between wave crest and shoreline, and the subscript b signifies that the parameters were evaluated at the breakpoint.

E is computed from

$$E = {}^1/_8\, \rho g\, H_b^2 \qquad (E\text{-}2)$$

where is the water density in kg/m^3, g is the gravitational acceleration in m/sec^2, and H_b is the root-mean-square breaker height.

Cn is computed as

$$Cn = (g H_b / 0.78)^{0.5} \qquad (E-3)$$

The shoreline orientation opposite the arrival point was determined by a subroutine that called a digitized record of the shoreline position. Since the shore trended almost east-west, the shoreline orientation opposite the arrival point was assumed the same as the orientation of the shoreline segment containing the easting coordinate of the ray arrival point. The "shoreline" was actually represented by the -1.0 m isobath, as defined in the bathymetric surveys, and was digitized at 50 m intervals. It was updated on the same schedule as the nearshore bathymetry was updated in the refraction routines.

Since the ray arrival points differed for each record, it was necessary to interpolate the transport rate at fixed points along the shore in order to compile a meaningful time history of the longshore variation in transport rate. Generally, the fixed stations were spaced 50 m apart along an E-W baseline. Around the river mouth, they were spaced 30 m apart. The transport rate computations were repeated for the three refraction situations and were totalled over a month of data. The results from the "wide spread" and "narrow spread" refractings were merged; the "no delta" result was kept separate. The transport divergence along the E-W baseline between the fixed stations was computed by dividing the change in transport rate between adjacent fixed stations by the station spacing.

E.5 Example Results

Fig. 38 shows a refraction diagram for typical northwest swell and also plots the resultant patterns of longshore sand transport and transport divergence along the study shoreline. The refracted waves in this example had a 13 second period, a deep-water direction of N47°W, and a deep-water significant height of 1 m. On Fig. 38a, the wave rays from the first "wide shoot" are shown passing through the inner bathymetry block. For clarity, only every third ray is plotted. The inset box at the river mouth shows the paths of the subsequent "narrow shoot" of closely-spaced rays. Again, for clarity, only every second ray is plotted. The ray paths show how wave energy is concentrated on Point Santa Cruz, spread across the Santa Cruz Bight, and locally reconcentrated at the river delta apex. The longshore variations in wave height and breaker angle result in the longshore transport pattern shown in Fig. 38b. Note that eastward transport is positive. The longshore gradient, or divergence, in longshore transport, dQ_l/dl, is shown in Fig. 38c. On this plot, positive values of dQ_l/dl give rates of potential erosion, while negative values indicate potential accretion.

For the given wave conditions, the predicted transport is generally directed eastward along the study shoreline. The eastward transport is largest on the eastern side of the river delta and off the harbor jetty. Short segments of shoreline, on either side of the delta and at each end of the study shoreline, are subject to westward transport. These transport direction reversals create four isolated littoral sub-cells. Significant accretion is predicted in the transport convergence zones on

Figure 38. (a) Wave refraction diagram for 13 second waves having a significant height in deep water of 1 m and arriving in deep water from N47°W. The inset box shows the refraction paths of closely-spaced wave rays aimed directly at the river mouth. (b) Variation in longshore transport potential along the study shoreline predicted for the above wave conditions. Transport is positive to the east.
(c) Variation in longshore-transport divergence along the study shoreline for the same wave conditions. Positive divergence induces erosion; negative divergence induces accretion.

a. REFRACTION DIAGRAM

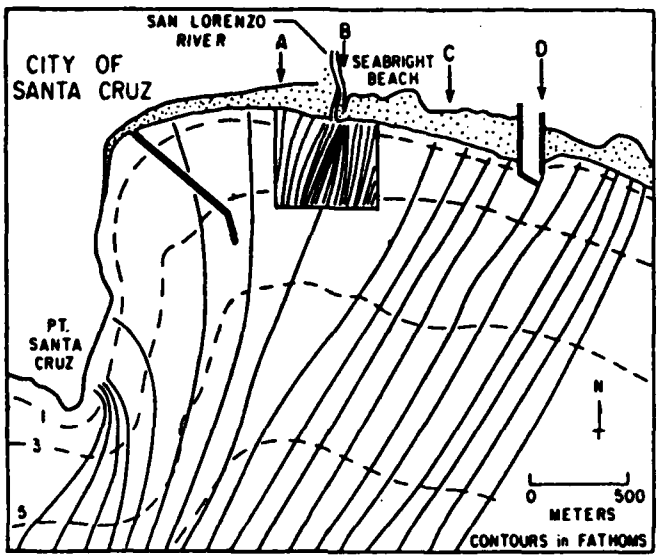

T = 13 sec
$H_{s\infty}$ = 1.0 m

b. LONGSHORE TRANSPORT POTENTIAL

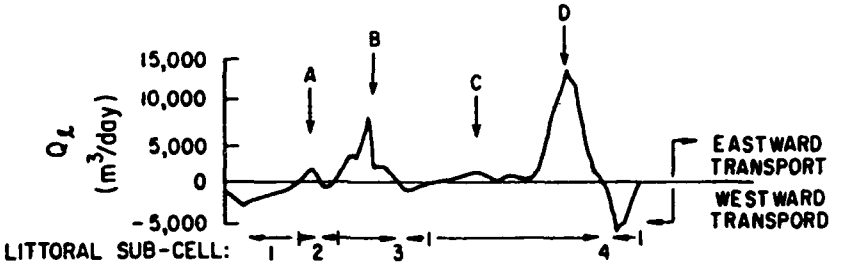

c. DIVERGENCE OF THE TRANSPORT

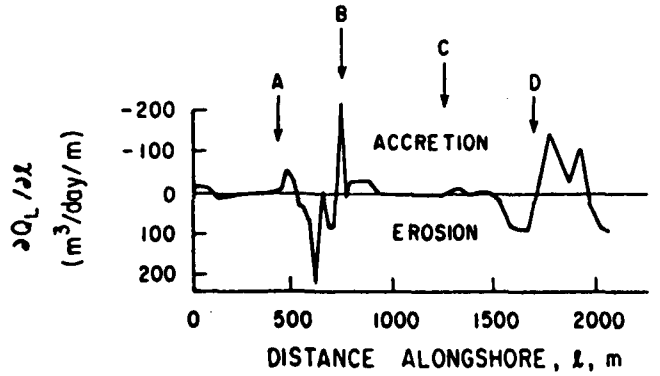

each flank of the delta and east of the harbor. Significant erosion is predicted at the delta apex and off the western harbor jetty. It should be noted that accretion does not require convergence of transport from opposite directions, as occurs in each sub-cell. For example, the accretion predicted near the east end of Seabright Beach results simply from an eastwards decrease in the easterly transport. Similarly, erosion need not result from divergence of transport in opposite directions.

E.6 Assumptions, Approximations, and Uncertainties

The following assumptions and approximations were made:

- waves broke when their height was 0.78 times their depth
- refraction was induced only by changes in bathymetry, and not by currents
- the effect of tides on altering the nearshore water depth could be ignored; sea level was assumed constant at its mean level
- the nearshore bathymetry and shoreline remained constant for 1-2 month periods about each survey time
- the shoreline orientation could be represented by that of the -1.0 m isobath, the assumed average depth of the breaking waves
- the wave directional and energy spectra at the array could be collapsed into a single wave with representative height, period, and direction
- wave diffraction and boundary friction could be ignored
- linear wave theory could be applied to the breakpoint.

The "no-tide" assumption can be justified since high and low tide effects probably average-out over time. Similarly, short-term changes in the representative nearshore bathymetry and shoreline orientation probably average-out over time. Neglecting boundary friction can be justified since friction has already influenced the wave height measured close to the shore at the array. Diffraction cannot be ignored in the close vicinity of the harbor jetties, particularly on the eastern, lee, side: the results there cannot be considered reliable.

The greatest potential inaccuracy lies with refracting only a representative wave instead of the whole directional-frequency range. (Pursuing the latter course, refracting each frequency band in each direction for every 6-hourly record, would have increased the computational time by at least two orders of magnitude - the program would have run continuously for two years.) This technique is valid only as long as the directional and energy spectra are unimodal and narrow - a rare condition with real ocean wave spectra. For example, the representative wave from a bimodal spectra is fictitious and can give a completely wrong estimate of S_{xy} at points alongshore from the measurement site.

The use of linear wave theory and the simple breaking criterion are all that are justified given the other assumptions. Part of the uncertainty induced by these assumptions and approximations can be checked by comparing the longshore transport rates near the array computed by the back-refraction procedure and by the probably-more-accurate S_{xy} method of Seymour and Higgins (1978). This comparison is reported on in section 4.2.1 of the text.

END

FILMED

7-85

DTIC